CENTRO DE INVESTIGACIÓN Y DE ESTUDIOS AVANZADOS DEL INSTITUTO POLITÉCNICO NACIONAL

UNIDAD ZACATENCO

DEPARATAMENTO DE GENÉTICA Y BIOLOGÍA MOLECULAR

“miR-143/145 funcionan como supresores de tumor en cultivos 2D y 3D al regular el citoesqueleto de actomiosina y son expresados durante la estratificación de los queratinocitos”

Tesis que presenta:

M. en C. ALEJANDRO GONZÁLEZ TORRES

Para obtener el grado de:
DOCTOR EN CIENCIAS

EN LA ESPECIALIDAD DE
GENÉTICA Y BIOLOGÍA MOLECULAR

Directores de la Tesis:
Dr. Luis Marat Alvarez Salas

Dr. Xavier Gidrol

Ciudad de México Enero, 2019

CENTRO DE INVESTIGACIÓN Y DE ESTUDIOS AVANZADOS DEL INSTITUTO POLITÉCNICO NACIONAL

UNIDAD ZACATENCO

DEPARTAMENTO DE GENÉTICA Y BIOLOGÍA MOLECULAR

Doctoral Thesis

"miR-143/145 function as tumor suppressors in 2D and 3D cultures by regulating the actomyosin cytoskeleton and are expressed during keratinocyte stratification"

Presented by:

ALEJANDRO GONZÁLEZ TORRES, M.Sc.

IN THE SPECIALTY OF GENETICS AND MOLECULAR BIOLOGY

Tesis Directors

Luis Marat Alvarez Salas, Ph.D.

Xavier Gidrol, Ph.D.

Mexico City January, 2019

Este trabajo se desarrolló en el Laboratorio de Terapia Génica dirigido por el Dr. Luis Marat Alvarez Salas en el departamento de Genética y Biología Molecular del CINVESTAV-IPN, siendo el M. en C. Alejandro González Torres becario del Consejo Nacional de Ciencia y Tecnología (CONACyT) bajo el número de registro 482566.

Además, parte del trabajo se desarrolló en el Laboratorio Biomics de la Unidad Mixta de Investigación 1038 Inserm/CEA/Université Grenoble Alpes, como parte de una estancia de movilidad que contó con el apoyo del CONACyT y de la Comisión de Energía Atómica (CEA) del gobierno francés. Dicha estancia fue dirigida por el Dr. Xavier Gidrol.

INDEX

RESUMEN

Los microRNAs (miRNAs) son RNAs pequeños no codificantes que regulan la expresión de mRNAs que poseen secuencias complementarias. Alteraciones en la función de los miRNAs han sido ampliamente reportadas en cáncer, incluyendo a los cánceres cérvico-uterino y de próstata, dos de los tumores más comunes a nivel mundial. Se ha observado que la expresión del grupo miR-143/145 se encuentra disminuida en tumores de cérvix y próstata, lo que sugiere que tales miRNAs funcionan como supresores de tumor al regular transcritos asociados a procesos celulares tales como viabilidad, proliferación, migración, invasión y diferenciación. El propósito de este trabajo fue evaluar la función de miR-143/145 como genes supresores de tumor en dos contextos opuestos y complementarios: cáncer y diferenciación. Primeramente, el efecto de mimetizadores de miRNAs fue evaluado en cultivos monocapa y esferoides tridimensionales de líneas celulares de cáncer cervical y de próstata. Se observó una disminución en la viabilidad, proliferación, migración e invasión en células transfectadas con miR-143/145, resaltando que el efecto supresor más fuerte fue generado por miR-145. Además, se validó que miR-145 disminuye los niveles de pMLC al regular MYPT1. El silenciamiento de MYPT1 reprodujo los efectos de miR-145, sugiriendo que miR-145 actúa como supresor de tumor mediante la regulación de MYPT1. Por otra parte, la expresión de miR-145 fue analizada en la diferenciación del queratinocito. La expresión de miR-145 fue detectada sólo en queratinocitos estratificados de muestras de prepucio y cultivo tipo órgano, contrario a cultivos monocapa, mostrando la relevancia de los cultivos 3D. Además, la expresión de miR-145 fue responsiva a la irradiación con luz UVC, aumentando tanto en epidermis como en fibroblastos, implicando que miR-145 es necesario para la homeostasis de la proliferación-diferenciación epitelial, un proceso que se encuentra alterado en células de cáncer. En conclusión, miR-143/145 actúan como supresores de tumor en cáncer de cérvix y próstata, siendo miR-145 el efector más fuerte y cuya expresión está relacionada con la diferenciación epitelial.

ABSTRACT

MicroRNAs (miRNAs) are small non-coding RNAs which regulate the expression of mRNAs containing complementary sequences. Disruption of miRNA function has been widely reported in cancer, including cervical and prostate cancer, two of the most common tumors worldwide. The miR-143/145 cluster has been found down-regulated in cervical and prostate tumor cells, suggesting an active cooperation to specifically target gene transcripts associated with cellular processes such as viability, proliferation, migration, invasion and differentiation. The aim of the present work was to evaluate the function of miR-143/145 as tumor suppressor genes in two opposite and complementary contexts: cancer and differentiation. Monolayer and tridimensional spheroid cell cultures were performed to observe the effect of miRNA mimics in cervical and prostate cancer cell lines. We observed that miR-143/145 decreased the viability, proliferation, migration and invasion, showing that miR-145 has the most potent suppressive effect. Furthermore, we found that miR-145 regulates the pMLC levels by targeting MYPT1. The MYPT1 silencing reproduced the miR-145 effects, suggesting that miR-145 acts as tumor suppressor through MYPT1 regulation. Additionally, the expression of miR-145 was analyzed in keratinocyte differentiation. MiR-145 was detectable only in stratified keratinocytes from foreskin samples and organotypic cultures, contrary to monolayer cell cultures, showing the relevance of 3D cultures. Moreover, miR-145 expression was responsive to UVC irradiation both in epidermis and in fibroblasts, implying that miR-145 is needed for epithelial proliferation-differentiation homeostasis, a process disrupted in cancer cells. In conclusion, miR-143/145 act as tumor suppressors in cervical and prostate cancer cells, with miR-145 as the strongest effector and whose expression is related to epithelial differentiation.

INTRODUCTION

MicroRNAs

MicroRNAs (miRNAs) constitute a group of conserved, small non-coding RNAs (ncRNA) of 18-25 nucleotides in length mainly involved in posttranscriptional gene silencing. Nowadays, it is evident that a proper miRNA activity is essential for normal cellular physiology. MiRNAs comprise 1–2% of all genes in worms, flies, and mammals [1], and because each miRNA is predicted to regulate hundreds of target genes, the majority of protein coding genes is thought to be under their control [2]. In practice, this means that virtually every biological process is subject to miRNA-dependent regulation [3]. This new paradigm of gene regulation was established in 1993 when *lin-4* (lineage-deficient-4), was identified as a ncRNA responsible for the silencing of *lin-14*, an essential gene for development of the nematode *Caenorhabditis elegans* [4]. Since then, the number of miRNAs is growing rapidly, and the latest database release (v22, March 2018) described 38,589 loci from 271 species, processed to produce 48,885 mature miRNA products (Sanger miRBase). The functional mature miRNAs are the result of a complex biogenesis process that takes place both in the nucleus and the cytoplasm.

The biogenesis of miRNAs starts in the cell nucleus, similarly to protein-coding genes (Figure 1). Typically, a miRNA gene only expresses an individual miRNA; however, some groups of miRNAs are frequently transcribed as a single polycistronic transcript when they are clustered together [5]. Most miRNAs are transcribed by the RNA polymerase II (Pol II) into primary transcripts called primary miRNAs or pri-miRNAs, although Pol III has also been demonstrated to carry out miRNA transcription [6]. The pri-miRNAs form one or more imperfect stem-loops, have 5′ and 3′ unstructured single-stranded fragments and are capped with 7-methylguanosine at the 5′ terminus and polyadenylated at the 3′ terminus [7]. After their transcription, the pri-miRNAs are cleaved by a type III RNase called *Drosha* and its double-stranded RNA-binding protein co-factor named DGCR8 (DiGeorge syndrome critical region gene 8), also called *Pasha* in *C. elegans* and *Drosophila melanogaster*

(together are known as the Microprocessor complex). DGCR8 recognizes the single stranded–double stranded RNA (ssRNA–dsRNA) junction in pri-miRNAs.

Figure 1. The miRNA biogenesis process. Ago, Argonaute protein; miRNA,

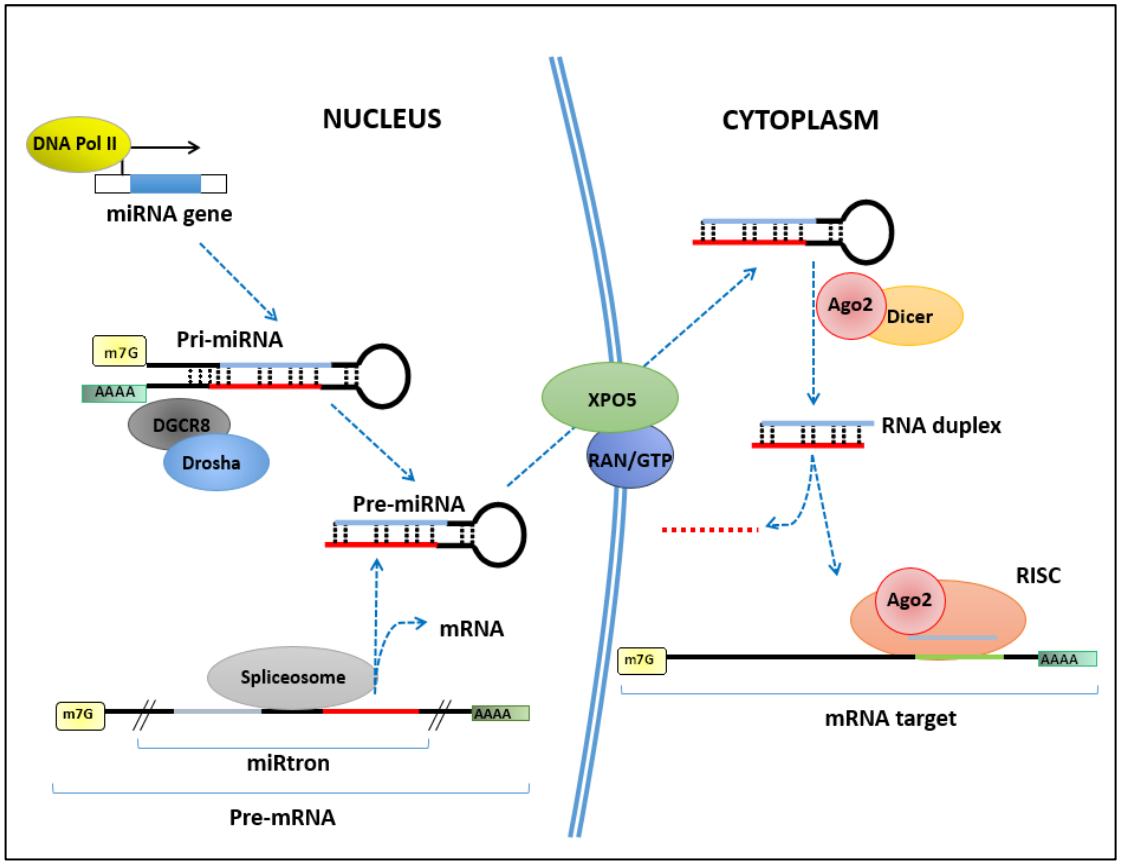

microRNA; ORF, open reading frame; pre-miRNA, precursor miRNA; pri-miRNA, primary miRNA; RISC, RNA induced-silence complex; XPO5, exportin-5 protein.

The cleavage gives rise to the precursor miRNAs, or pre-miRNAs, hairpin-like structures of ~70 nucleotides in length, with a 5′ monophosphate and a 3′ hydroxyl group. A typical feature of pre-miRNAs is a 3′ 2-nucleotide overhang [8]. Alternatively, some intronic miRNAs (called mirtrons) bypass the *Drosha* processing step and, instead, use splicing machinery to generate the pre-miRNA [9]. Then, pre-miRNAs are transported into the cytoplasm for further processing to become mature miRNAs. The transport of the pre-miRNA occurs through nuclear pore complexes, which are large protein channels embedded

in the nuclear membrane [10]. The transport of the pre-miRNA is mediated by the RAN-GTP-dependent nuclear transport receptor exportin-5 (XPO5) [11].

Once the pre-miRNAs are released in the cytoplasm by XPO5, the loop of pre-miRNA is cleaved off by another RNase III called *Dicer*, which is a highly specific enzyme that measures about 22 nt from the pre-existing terminus of the pre-miRNA and cleaves the miRNA strand, resulting in a short RNA duplex with 3′ 2-nucleotide overhangs [12]. The latter reaction is often accompanied with the formation of RISC (RNA-induced silencing complex), which enables silencing of mRNAs. The RISC complex is made up of a strand of the mature miRNA, called guide strand, as well as *Dicer*, TRBP (TAR RNA binding protein), PACT (protein activator of PKR) and *Argonaute* (Ago) proteins [13]. The guide strand functions as an adaptor to specifically recognize target mRNAs, binding to specific binding sites typically, but not exclusively, located in the 3′ untranslated regions (3′ UTRs) of target mRNAs through Watson-Crick base pairing [14]. The degree of miRNA–mRNA complementarity is a major determinant of the regulatory mechanism process. In plants, complementarity between target sites and miRNAs is usually perfect or near-perfect, leading to Ago-catalyzed mRNA cleavage and degradation [15]. However, in animals complementarity between miRNAs and mRNA is not perfect and regulation is mainly through base-pairing interactions with their proximal region (encompassing nucleotides 2–8) called the “seed region” [16], resulting in multiple pathways of regulation. Transcript degradation is the outcome of destabilization due to recruitment of deadenylation factors that remove the poly(A) tail and make the mRNA susceptible to exonucleolytic degradation [17]. Moreover, translation repression by miRNAs is achieved by inhibition of translational initiation or elongation, as well as for directed proteolysis of the peptide that is being synthesized from the target mRNA [18,19].

It has been proposed that mRNA regulation by miRNAs occurs in the P-Bodies. The P-bodies are discrete cytoplasmic foci that co-localize with mRNA-RISC complex and, moreover, they contain many enzymes that participate in mRNA deadenylation, decapping and degradation [20]. This led to consider that the

P-bodies are centers of miRNA regulation, that is to say, where the mRNA translational repression or degradation takes place [21].

Despite their clear importance as a class of regulatory molecules, determining the biological relevance of individual miRNAs has proven challenging. Generally, the physiological functions of specific miRNAs have been inferred from overexpression studies in animals and monolayer cultured cells, or from studies that used antisense molecules as a means of disrupting their pairing to targets [22]. These experiments have attributed critical roles to miRNAs in processes such as cell proliferation, differentiation, and survival, and have implicated them as crucial players during normal development and homeostasis [23–25].

Implications of miRNAs in cancer

In few years miRNAs have been firmly established as key molecular components of the cell in both normal and pathological states. The initial indication that miRNAs play important roles in human disease came from high-throughput and functional studies in cancer cells. A seminal study by Calin and colleagues showed that miR-15a/16-1 cluster is frequently deleted in chronic lymphocytic leukemia, implicating these miRNAs as tumor suppressors [26]. After this discovery, hundreds of studies were published defining a role for miRNAs in the pathogenesis of cancer. When miRNAs are up- or down-regulated in malignant tissues compared to the normal counterpart, they are considered as oncogenes or tumor-suppressors, respectively [27]. In addition, miRNAs have shown to be differentially expressed in cancer cells, in which they formed distinct and unique miRNA expression patterns [28], and these tumor miRNA profiles can define patient survival and treatment response [29,30].

Changes of miRNA expression in tumors are caused by different conditions. Usually, miRNA genes are located in or nearby chromosomal alterations within tumors (amplifications, deletions or linked to regions of loss of heterozygosity) or in common chromosomal-breakpoints that are associated with the

development of cancer [31]. In addition to structural genetic alterations, miRNAs can also be silenced by promoter DNA methylation and loss of histone acetylation [32]. Interestingly, somatic translocations in miRNA target sites can also occur, representing a drastic means of altering miRNA function [33,34]. Single nucleotide polymorphisms (SNPs) and mutations have been identified, as well as deletions of 3′UTRs during mRNA splicing in cancer cells rendering mRNAs insensitive to miRNA regulation [35].

Furthermore, most miRNAs have been found repressed in tumors relative to normal tissue counterparts, as indication of the general loss of differentiation of cancer cells [28]. In agreement with these observations, global depletion of miRNAs by genetic deletion of the miRNA-processing machinery favors cell transformation and tumorigenesis in vivo [36,37]. This highlights that miRNA alteration is not simply an effect of tumorigenesis but plays a causative role in cancer development. Despite the general reduction of miRNAs in tumors, several miRNAs are upregulated, some of which undoubtedly play oncogenic roles [38].

Understanding of the function of miRNAs and how it contributes to cancer development provides new insights on the molecular basis of cancer and, especially, an opportunity for the generation of new strategies for diagnosis and therapy. Restoring miRNAs with tumor-suppressive functions is one of the aims of current cancer therapies [27].

Cervical cancer

Cancer is a generic term for a large group of illnesses that can affect any part of the body. Other terms used are malignant tumors and neoplasms. One defining feature of cancer is the rapid creation of abnormal cells that grow beyond their usual boundaries, and which can then invade adjoining parts of the body and spread to other organs, the latter process is referred to as metastasizing. Metastases are the major cause of death from cancer [39]. Cancers figure among the leading causes of morbidity and mortality worldwide, with approximately 14 million new cases and 8.2 million cancer related deaths

in 2012. Uterine cervix and prostate are among the 5 most common sites of cancer in women and men, respectively [40].

Cervical cancer is a public health issue in Mexico and the World; in fact, it is the second most common cancer in women living in underdeveloped countries with an estimated 445 000 new cases in 2012 (84% of the new cases worldwide) [39]. Epidemiological studies show that infection with the high-risk human papillomavirus (HPV) infections is the major risk factor for the subsequent development of cervical cancer, being the HPV types 16 and 18 the most commonly detected [41].

It is well known that HPV infection and vegetative viral growth are dependent upon a complete program of keratinocyte differentiation (Figure 2a). Viral infection is targeted to the basal keratinocytes, but a high-level viral expression of viral proteins and virion assembly occur only in the spinosum and granulosum strata of squamous epithelia. It is important to recognize that, in the normal infectious cycle, viral gene expression is tightly controlled by the keratinocyte differentiation. However, in pre-cancerous lesions and cervical cancer cell differentiation viral expression is deregulated (Figure 2b) [42].

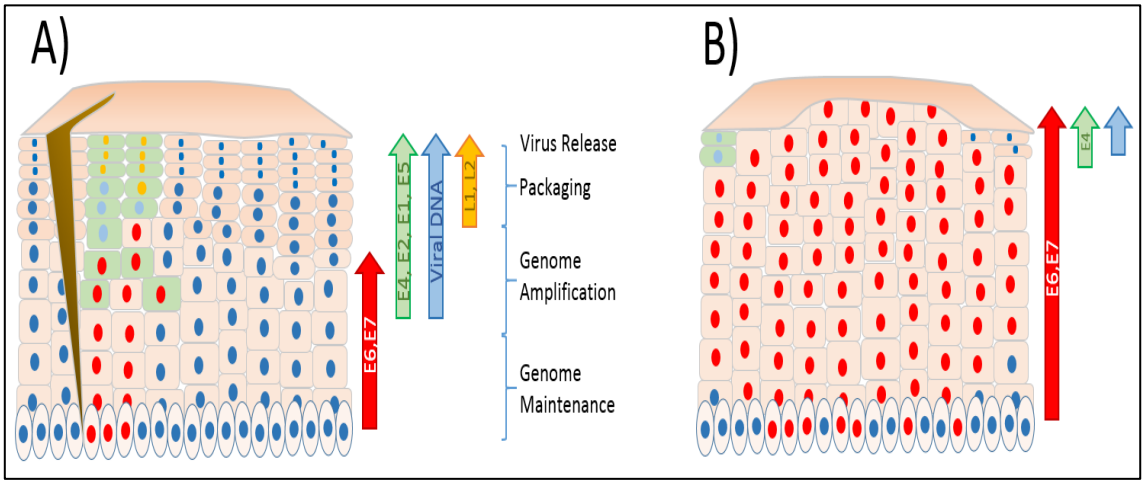

Figure 2. Expression pattern of high-risk HPV genes during the normal life cycle and cervical cancer. A) After infection (i.e. through a wound), the viral genome is maintained as a low copy number episome. During epithelial differentiation E6 and E7 genes are expressed and are necessary for S-phase entry (red). Later in the higher epithelial layers viral replication proteins (E1, E2, E4, and E5) increase in abundance (green), facilitating amplification of viral genomes (blue). Finally, in the upper epithelial layers the viral capsid proteins (yellow)

are found. B) In pre-cancerous neoplasia and cervical cancer, the normal regulation of HPV life cycle is lost and E6/E7 expression is increased [42].

Experimental studies showed that the E6 and E7 genes of the high-risk HPVs encode oncoproteins that deregulate key controls in cell proliferation. E7 most biologically relevant interaction is with pRb protein, effectively blocking the transcriptional repressor function of this protein. E6 enhances the degradation of p53, thus compromising the cell's own ability to arrest growth in response to DNA damage [43,44]. When the E6 and E7 oncogenes of the high-risk HPVs are introduced into primary genital keratinocytes (the target cell for HPV infection), it can result in an escape from senescence and the acquisition of an immortal phenotype [45]. Nevertheless, these immortalized lines, when injected into nude mice, do not produce invasive tumors and the progression to the invasive phenotype by these cell lines is an infrequent event requiring prolonged in vitro passage [46] or additional insults such as the introduction of activated oncogenes [47]. Moreover, genital HPV16 infection, for example, is common in young sexually active women, but relatively few infected women progress to cervical carcinoma [48]. Despite the fact that HPV16 encodes potent oncoproteins, the development of cervical cancer as a consequence of HPV gene expression is, in the real world, a rare event [49]. Thus, HPV infection is required but not enough for cervix neoplasia, and genetic and/or environmental co-factors, such as alterations in miRNAs expression, must contribute to tumor progression.

Prostate cancer

Prostate cancer is the most common cancer among men behind non-melanoma skin cancer and is the second highest cause of cancer death among men of all races [50,51]. Although human prostate cancer displays significant phenotypic heterogeneity, >95% of prostate cancers are classified pathologically as adenocarcinoma, which has a strikingly luminal phenotype [52]. The age (it is predominantly diagnosed in senior adults), family history, diet, and pharmaceutical drugs such as nonsteroidal anti-inflammatory drugs,

lipoxygenase inhibitors, and isoflavones have been associated with this kind of cancer [53,54].

Diagnosis and treatment of prostate cancer is based on a series of clinical states: beginning with localized disease, followed by the non-castrate rising prostate-specific antigen (PSA) state and the non-castrate metastatic state; finally, the castration-resistant states are lethal for most men [55]. The implementation of the highly accessible blood test for PSA almost three decades ago revolutionized the diagnosis and increased prostate cancer awareness [56]. PSA is a kallikrein-related serine protease that is produced in normal prostate secretions but is released into the blood as a consequence of disruption of normal prostate architecture by cancer [57]. Historically, the established cut-off of an abnormal PSA level was greater than 4.0 ng/mL [58], but more contemporary studies have shown that any level of PSA incorporated within a prostate cancer risk calculator may be a better method of evaluating the indication for a prostate biopsy [59,60]. Furthermore, there is recent evidence that patients with a normal PSA level (<4.0 ng/mL) have a high prevalence of prostate cancer [61], showing that PSA test could fail for a good prostate cancer diagnosis. To improve upon the accuracy, age, ethnicity, family history of prostate cancer, PSA velocity, and previous prostate biopsy information were incorporated into a predictive model among these men [60].

If prostate cancer is diagnosed, conventional treatment regimens include surgical excision of the prostate (radical prostatectomy), or irradiation through external beam therapy or implantation of radioactive ‘‘seeds’’ (brachytherapy). In the case of advanced cancer, these regimens are usually followed or substituted with androgen deprivation therapy, which initially will reduce tumor burden and/or circulating PSA to low or undetectable levels, but ultimately the disease will recur in most cases [52]. In the case of bone metastases (this organ has an unusually high propensity for being metastasized [62]), most current treatments have only palliative effects, with little effect on long-term survival [63].

At present, there are several major clinical challenges associated with prostate cancer diagnosis and treatment. The miRNAs could be useful for a better understanding of the mechanisms by which prostate cancer develops and metastasizes and at the same time, produce new potential biomarkers for diagnostic as well as new therapeutic targets. Between all miRNAs reported to date, the miR-143/145 cluster is a couple of promising miRNAs for cancer diagnostic and therapy.

The miR-143/145 cluster as tumor suppressor genes

The miR-143 and miR-145 genes are closely located in a 1.6 kb region on chromosome 5q33.1. These miRNAs, highly conserved in vertebrates, are transcribed as a bicistronic precursor (Figure 3) and frequently display a coordinated expression profile.

The miR-143/145 cluster has been related to several cellular processes, mainly differentiation. In adipocytes, miR-143 showed to promote the differentiation targeting ERK5 [64]. Moreover, miR-145 and miR-143 are tightly integrated into a core transcriptional network involved in smooth muscle differentiation and proliferation, and miR-145 functions as a critical switch in promoting smooth muscle differentiation. Also, they are transcribed as a bicistronic unit and therefore share common regulatory elements that control their expression resulting in that miR-143 is co-expressed in virtually all samples where miR-145 is detected [65,66]. Regarding stem cells, miR-145 acts to silence multiple pluripotency factors (SOX2, OCT4 and KLF4) during the switch from self-renewal to lineage commitment [67].

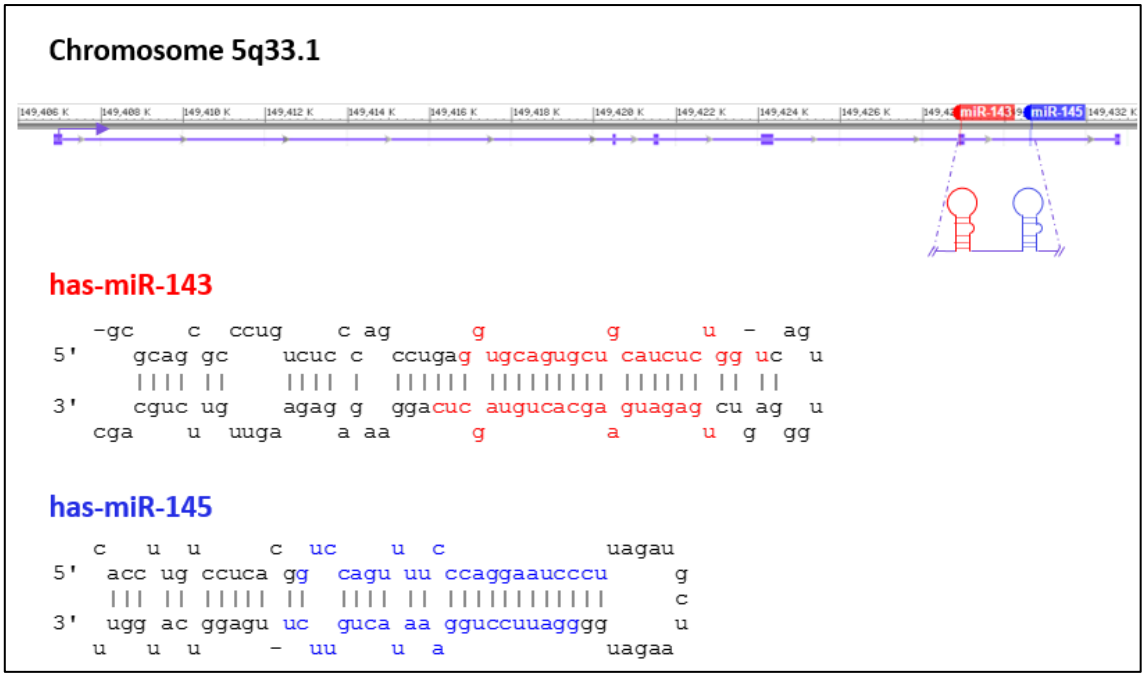

Figure 3. Upper panel, genomic organization and major primary transcript structure of the miR-143/145 cluster (edited from NCBI Graphical Sequence Viewer). Lower panel, secondary structures of pre-miR-143 and pre-miR-145, highlighting in red and blue the mature miRNA sequences for miR-143 and miR-145, respectively (obtained from miRBase web site).

The initial discovery of miR-143 and miR-145 in humans came in 2003 from the report of Michael *et al*. in which both transcripts were identified in colonic adenocarcinoma tissue and demonstrated a reduced level compared to normal colon mucosa. Cloned and sequenced small RNAs were homologous to known murine miRNA sequences for miR-143 and miR-145, and these were found at lower levels in neoplastic tissue compared to the matched normal tissue [68]. This differential expression between normal colon and colorectal cancer was confirmed by Akao *et al*., who also found that overexpression of this cluster decreased proliferation of colorectal cancer cell lines [69].

This general approach of comparing either tumor tissue/cell lines to normal tissue was performed for a variety of other malignancies, such as gastric cancer [70], chronic lymphocytic leukemia and B cell lymphoma [71], bladder cancer [72,73], nasopharyngeal carcinoma [74], cervical [75] and prostate cancer [76]. Thus, a broad sense of miR-143/145 loss in cancer was established and

suggested a potential role as tumor suppressor. In addition, several tumor-related genes have been validated as target of miR-143/145 (Table 1), reinforcing the idea that this miRNA cluster act as tumor suppressors and provide an important clue in the study of the mechanism of tumor initiation and progression.

Table 1. Validated miR-143/145 targets related to cancer

Gene	Targeted by	Process	Reference
KRAS	miR-143	Proliferation	(Chen et al., 2009b)
ELK1	miR-143	Proliferation	(Cordes et al., 2009)
ERK5	miR-143	Proliferation	(Esau et al., 2004)
c-MYC	miR-145	Proliferation	(Sachdeva et al., 2009)
BCL2	miR-143	Apoptosis	(Zhang et al., 2010)
HK2	miR-143	Glycolysis	(Fang et al., 2012)
OCT4	miR-145	Pluripotency	(Xu et al., 2009)
KLF4	miR-145	Pluripotency	(Xu et al., 2009)
SOX2	miR-145	Pluripotency	(Xu et al., 2009)
MYO6	miR-143	Migration	(Szczyrba et al., 2010)
MMP-13	miR-143	Migration	(Osaki et al., 2011)
ADAM-17	miR-145	Migration	(Doberstein et al., 2013)

Normally, mature miR-143 and miR-145 show a high expression in human normal tissue like the cervix, uterus and prostate [75,77].

On one hand, numerous studies have associated the cervical cancer with changes in miRNA expression. In a meta-analysis performed by Li et al., they identified that down-regulation of miR-143 and miR-145 were the most consistently reported (seven and six studies respectively), suggesting that these miRNAs are potential biomarkers of cervical cancer. In addition, HPV is able to modulate expression of host miRNAs to control its own life cycle, like miR-145, which is repressed to allow viral replication by targeting viral sequences and by acting on cellular factors, such as KLF-4 [78]. When primary human vaginal keratinocytes are infected with HPV-18 and cultured in stratified and differentiated raft tissues, miR-143/145 is downregulated, suggesting that

the virus regulates this miRNA cluster to control its life cycle which is differentiation-dependent. In the same study, both miR-143 and miR-145 were found suppressive to HeLa cell growth, thus these data suggest that miR-143/145 probably need to be downregulated in cervical cells for tumor progression [75]. In addition, in our preliminary work, we showed that miR-143 is not expressed in cervical cancer cell lines nor immortalized keratinocytes.

On the other hand, studies have shown that miR-143 is considerably decreased in prostate cancer, and its expression is further decreased during cancer progression [79]. K-RAS, a key molecule of MAPK signaling pathway, is a viral oncogene homolog involved in cell proliferation and migration in response to growth factors. The MAPK pathway also works at another level through its effect on androgen receptors (AR), where it increases AR in response to low androgen, and this is considered a main process in androgen derivation therapy relapse. K-RAS is a potential target for miR-143 [2], thereby lower levels of miR-143 in prostate cancer cells may be involved in carcinogenesis due to the lack of its inhibitory effect on K-RAS and MAPK pathway. Moreover, Xu et al. [80] showed that miR-143 regulates K-RAS, p-ERK1/2, and cyclin D1 and plays a role in cell proliferation, migration, and chemosensitivity in prostate cancer. They also showed that miR-143 over-expression in prostate cancer cells represses proliferation and migration, thereby augmenting sensitivity to docetaxel by affecting the EGFR/RAS/MAPK pathway. Exploring the correlation between the levels of miR-143/145 and the pathological features of prostate cancer showed that down-regulation of miRNAs-143 and -145 was negatively associated with bone metastasis and the levels of free PSA in primary prostate cancer patients [2]. Over-expression of miR-143/145 by retrovirus transfection decreased the ability of migration and invasion *in vitro*, and tumor development and bone invasion *in vivo* of PC-3 cells (a human prostate cancer cell line originated from bone metastatic prostate cancer). Their upregulation also enhanced E-cadherin expression and decreased fibronectin expression in PC-3 cells with features of a less invasive morphologic pattern [2]. Emerging evidence showed that cancer stem cell

(CSCs) are the critical drivers of tumor progression and metastasis. Overexpression of miR-143/145 inhibits CSC properties in PC-3 cells suppressing tumor sphere formation and expression of CSC markers and 'stemness' factors including CD133, CD44, Oct4, c-Myc and Klf4. Furthermore, miR-143/145 inhibits bone invasion and tumorigenicity in PC-3 cells *in vivo* [81]. The information above suggests that miR-143 and 145 are related to bone metastasis of prostate cancer and may play a biological role in this process.

Therefore, the miR-143/145 cluster is a potential biomarker and probably a tumor suppressor miRNA that could be useful to understand tumor progression in cervical and prostate cancer.

Moreover, the miR-143/145 cluster has been previously reported as a regulator of cytoskeleton dynamics in vascular injury conditions [82]. Because cytoskeleton remodeling is crucial for processes related to cancer, such as cell division and migration, miR-143/145 may affect tumor growth, progression and metastasis.

Relevance of the actomyosin cytoskeleton in cancer

Several chemotherapeutic drugs have cytoskeletal proteins as target. Although the main target is tubulin [83], actin-binding drugs have a great potential as novel chemotherapeutic agents [84].

Actin is a globular protein that polymerizes into semi-flexible filaments that form a network that is crucial for the cytoskeleton structure. These filaments are organized in different types, such as branched and crosslinked networks, parallel bundles, and anti-parallel contractile structures. These different architectures are actively interconnected to act as biochemical and mechanical elements to drive cell shape changes and motility [85]. Furthermore, actin filaments are dynamically reorganized during mitosis due to a tight regulatory interaction with mitotic events [86]. Nevertheless, for proper function actin filaments should work in conjunction with the myosin molecular motor.

The myosin superfamily is represented by 15 isoforms. Myosin II is the conventional two-headed myosin first identified in muscle. Much of our

understanding of the regulation of non-muscle myosin II is by analogy with smooth muscle myosin II. Myosin II is composed of a pair of heavy chains, a pair of essential light chains and a pair of regulatory light chains (RLC) also named as myosin light chain (MLC) [87]. The phosphorylation of non-muscle myosin II on Ser19 of the MLC regulates both its motor activity and filament assembly [88–90]. These mechanical forces driven by myosin activity have a key role in the regulation of cell proliferation, apoptosis, adhesion and migration [91,92]. The phosphorylation of MLC is carried out by two groups of enzymes: one consists of several kinases that phosphorylate MLC (including ROCK, MLCK, citron kinase, PAK, among others) and the opposing reaction reflects only the activity of myosin phosphatase (MLCP) that dephosphorylates MLC [93].

The MLCP holoenzyme contains three subunits: the type 1 protein phosphatase catalytic subunit (PP1), the myosin phosphatase target subunit (MYPT1, also termed myosin binding subunit) and a small subunit of unknown function [94]. The MLCP activity is inhibited by phosphorylation of MYPT1 at Thr695 by different kinases including ROCK, ZIP kinase, PAK, among others [95–97]. In addition, ROCK phosphorylates MYPT1 at Thr850, which induces myosin dissociation from MLPC [98].

MLCP can modulate cell cycle and motility, two events which are upregulated in prostate cells and tumors, breast and bone cancer [99,100]. Indeed, MLCP inhibition by a small antagonist resulted in decreased growth rate, reduced DNA synthesis and G2/M arrest in prostate cancer cells [99]. Several cancer cell lines present low pMLC levels due to MLCP overexpression and MLCK downregulation, resulting in cytokinesis failures due to mitotic defects such as multinucleation and multipolar spindles [101]. In addition, membrane blebbing, apoptotic body formation and nuclear disintegration during apoptosis are dependent on MLC phosphorylation and thereby of the actomyosin contractile activity [102–104].

The contractility of cells highly responds to environment features such as biochemical composition and stiffness, subsequently dictating the assembly

and dynamics of cytoskeleton networks [105]. Cells in tissues are embedded into a highly structured microenvironment. Nonetheless, the properties of the cell microenvironment are lost in standard cell culture. Micropatterning methods, a technique to create culture substrates with microscopic features that provide a defined cell adhesion pattern, allow cells to precisely adapt their cytoskeleton architecture to the geometry of their environment [106], allowing comparison cytoskeleton changes through different conditions and thus facilitating the understanding of the cell physiology. Besides micropatterning methods, three dimensional (3D) cultures represent a relevant *in vitro* model to mimic physiological cell conditions and reveal the miRNA function.

3D cultures

Cell culture is an important tool for biological research. Two-dimensional cell culture has been traditionally used by several decades [107], but growing cells in flat layers on plastic surfaces does not accurately reproduce the *in vivo* physiology, resulting in an 95% ineffectiveness of translation of in vitro experimental data into clinical trials [108]. 3D cultures represent a more relevant alternative to monolayer cell cultures because they recreate physiological features in tissue such as cell-cell and cell-matrix interactions, complex transport dynamics for nutrients and cells, spatial organization, cell polarization, greater stability and longer lifespan, among others. 3D cultures show improvements in several studies of basic biological mechanisms, like: cell number monitoring, viability, morphology, proliferation, differentiation, response to stimuli, cell-cell communication, migration and invasion of tumor cells into surrounding tissues, angiogenesis stimulation and immune system evasion, drug metabolism, gene expression and protein synthesis, general cell function and *in vivo* relevance [109]. Recently, contrary to monolayer cultures, 3D cultures recapitulated the molecular signature (mRNA, miRNA and metabolic profiles) of tumors or tissues [110,111]. To date, several 3D cell cultures technologies have been developed based on advances in cell biology, microfabrication techniques and tissue engineering. These include:

multicellular spheroids, organoids, scaffolds, hydrogels, organ-on-a-chip, and 3D bioprinting, each with its own advantages and limitations (Table 2) [112].

Table 2. Advantages and Disadvantages of Different 3D Cell Culture Techniques (reviewed by [112])

Technique	Advantages	Disadvantages
Spheroids in low attachment surfaces	Easy-to-use protocol Scalable to different plate formats Compliant with high-throughput screening (HTS)/high-content screening (HCS) Co-culture ability High reproducibility	Simplified architecture Forced aggregation
Organoids	Patient specific In vivo–like complexity In vivo–like architecture	Can be variable. Less amenable to HTS/HCS Hard to reach in vivo maturity Complicated protocol. Lack vasculature May lack key cell types
Scaffolds/hydrogels	Applicable to microplates Amenable to HTS/HCS High reproducibility Co-culture ability	Simplified architecture Can be variable across lots
Organ-on-a-chip	In vivo–like architecture In vivo–like microenvironment, chemical, physical gradients	Lack vasculature. Difficult HTS adaptability
3D bioprinting	Custom-made architecture Chemical, physical gradients	Lack vasculature

	High-throughput production Co-culture ability	Challenges with cells/materials Difficult HTS adaptability Issues with tissue maturation

Spheroid cultures in low attachment surfaces and organotypic cultures based in scaffold system represent easy and reproducible techniques for drug screening with several advantages compared to 2D monolayer cultures.

Several techniques to growth spheroid cultures have been developed, such as liquid overlay, hanging drop, microwell hanging drop, micropatterned agarose wells, microfluidic, and lately, ultra-low attachment surfaces [113]. The latter, promotes the self-aggregation of cells into spheroids using both an ultra-low attachment polymer coating and a well-defined geometry (e.g. round, tapered or v-shaped bottom) to drive and position a single spheroid per well, enabling high-throughput screening (HTS) or high-content screening (HCS) [112]. In addition, spheroids develop gradients of oxygen, nutrients, metabolites, and soluble signals, thus creating heterogenous cell populations (e.g. hypoxic vs normoxic, quiescent vs proliferating cells, a necrotic center vs replicating outside) (Figure 4) [114]. Commercially available products such as Matrigel® basement membrane matrix or hyaluronic acid are used to mimic the ECM interactions, allowing cells to respond to external stimuli and degrade the ECM proteins for invasion [115].

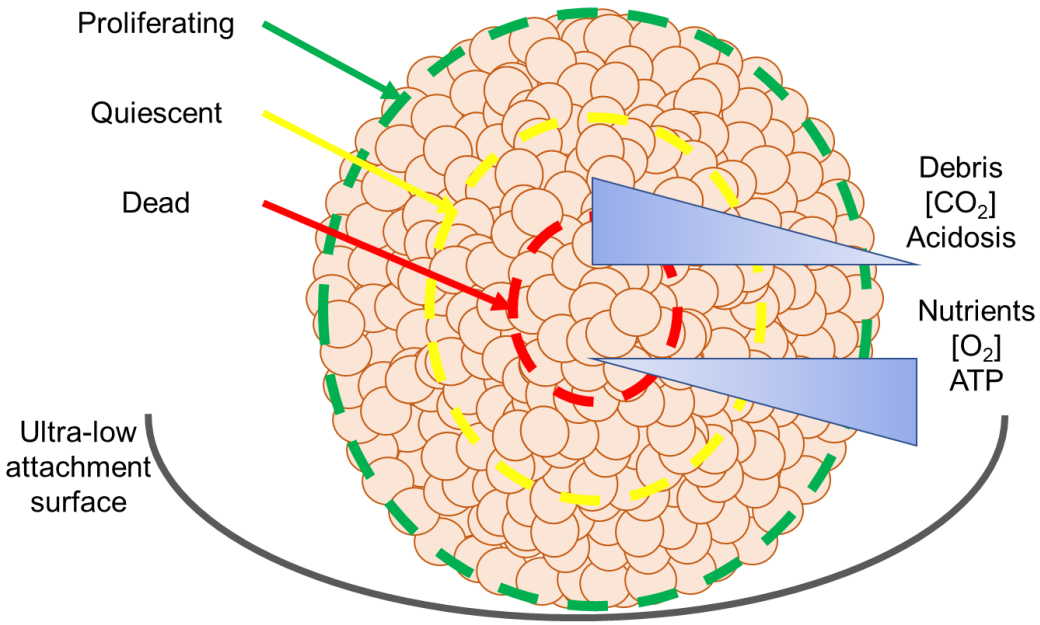

Figure 4. Representation of a spheroid in an ultra-low attachment surface with pathophysiological gradients schematically reported [114].

Although spheroid is a great technique for drug screening in cancer research, it has several disadvantages to study epidermal physiology as spheroids cannot be easily recovered from the matrix where they are embedded and they fail to reproduce all the epidermal layers [116]. Some of these disadvantages are overcome when keratinocytes are cultured in systems based on air-liquid interface exposition [117].

Skin organotypic cultures, traditionally constructed in air-liquid systems, overcome weaknesses observed in differentiation of keratinocytes monolayer cultures, like the lack of caspase-14 expression, a terminal-differentiation epidermal marker [118]. The structure of this model consists in the co-culture of keratinocytes and fibroblasts embedded in a gel matrix, resulting in tissue-like features from epidermal differentiation like morphology and rates of cell division [119]. These cultures start adding fibroblast support cell (called feeders) to vacant scaffolds, ranging from collagen gel to commercial ECM proteins mixtures. When fibroblasts have already populated the scaffold, the keratinocytes are seeded in the top. Stratified differentiation is induced by stablishing a liquid-air interface on the keratinocyte layer (Figure 5) [120].

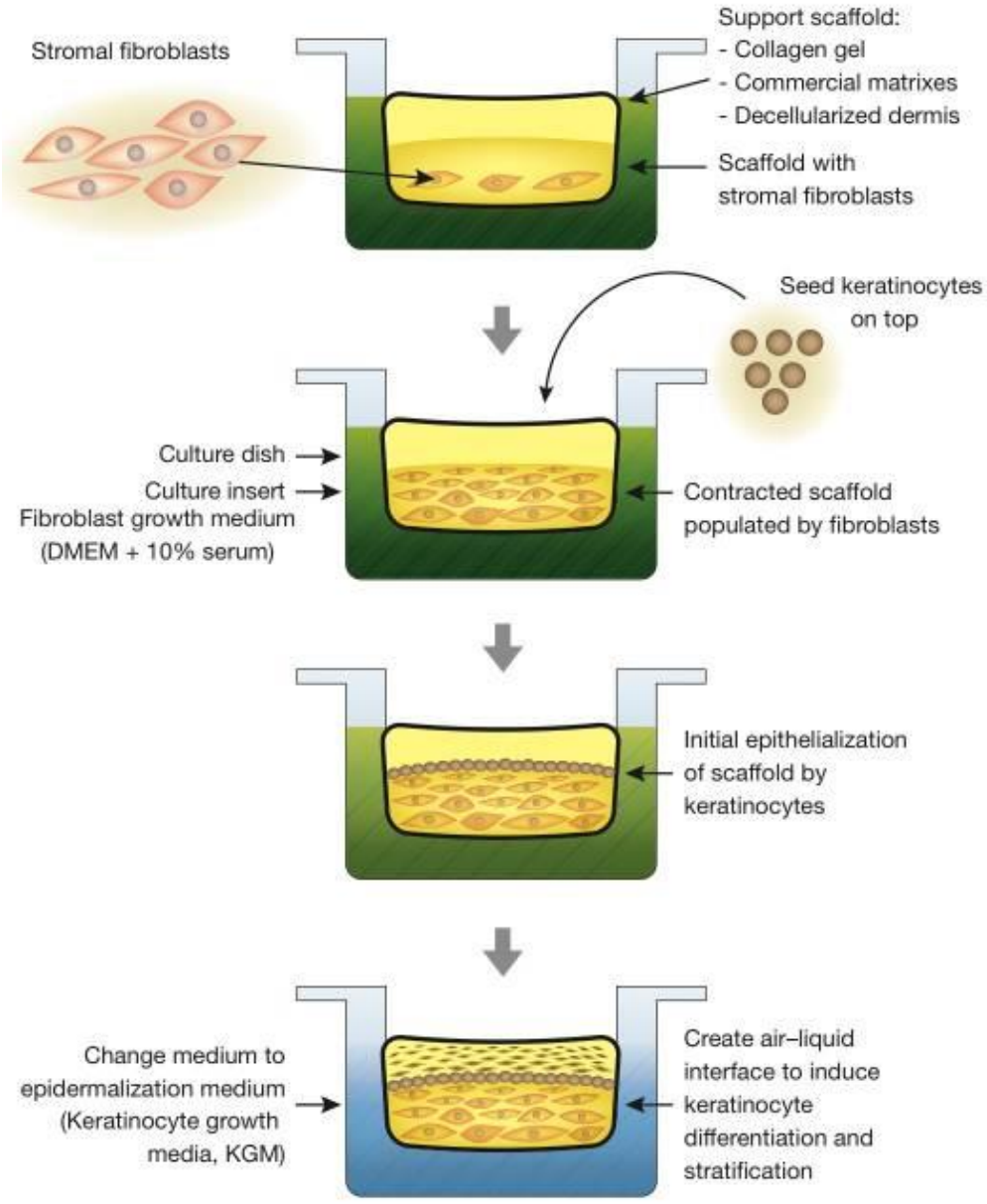

Figure 5. Flowchart of organotypic epidermal culture system [120].

The skin organotypic cultures are useful to study molecular mechanisms that regulate tissue homeostasis and development, and to compare the behavior of human epidermis under a variety of diseases-like scenarios. Moreover, epithelial cells are surrounded by connective tissue, which contains immune cells, blood vessels, fibroblast and ECM-bound signaling molecules. Since these components can regulate epithelial cells and contribute to disease progression, 3D culture systems are appropriate because of they enable the

manipulation of components of the microenvironment and the analysis of how they affect the structure and function of cells or tissue. RNAi, Cre-*lox*-based recombination, lentiviral short hairpin RNA and recently CRISPR-Cas9 genome editing approaches have been adapted to 3D culture, enabling the evaluation of single genes and genome-scale screening [107].

Alternatives based on epidermis attached to a porous substrate in a chemically defined serum-free medium instead of matrix-embedded fibroblasts have been reported [121]. This way, cytokines released by keratinocytes that are not trapped into a dermal compartment can be analyzed in the culture media [122], as well as the easy recovering of not-embedded fibroblast which can be co-cultured below the porous membrane. This kind of reconstructed epidermal culture leads to terminal keratinocyte differentiation just as it has been demonstrated by immunohistochemical localization of several epidermal differentiation markers [123], reproducing every layer of normal stratified epidermis (Figure 6). Additionally, the latter can be achieved following a simple protocol for in-house production [124]. Thus, 3D cultures are the methods of choice to study miRNA expression in a more physiological context.

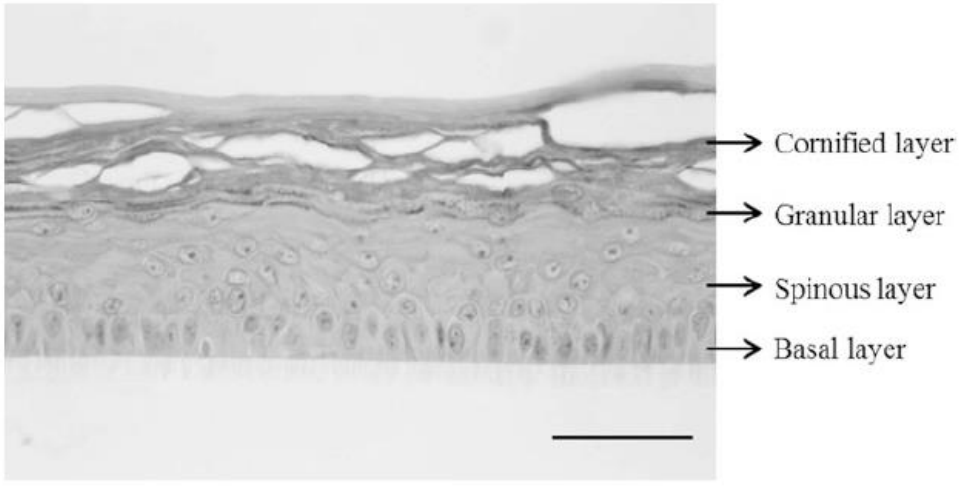

Figure 6. Histology of reconstructed human epidermis (RHE) at day 11. After 11 days of culture, RHE were fixed in acetic formalin and embedded in paraffin. Then histological sections perpendicular to the surface of RHE were prepared and stained with hematoxylin-erythrosine to allow the morphological analysis of RHE (bar: 50 µm) [124].

HYPOTHESIS

Down-regulation of the miR-143/145 cluster has been associated with tumor progression of cervical and prostate cancer cells suggesting an antitumor function. Therefore, if miR-143/145 expression is reestablished in tumor cells, this cluster will cause inhibition of several tumor cell processes such as viability, proliferation, migration and invasion through the targeting of transcript targets associated to such processes. Moreover, inducing cell differentiation (an event opposite to cancer) miR-143/145 expression will increase, thus confirming their role as tumor suppressors.

GOALS

General

Characterization of the putative tumor suppressor role of the miR-143/145 cluster on the viability, migration, invasion and the proliferation-differentiation homeostasis of cervical and prostate cancer cells.

Specific

- Analyze the endogenous expression of miR-143-3p and miR-145-5p in cervical cell lines and HPV-immortalized keratinocytes.
- Overexpress miR-143/145 and determine their effects in viability, proliferation, migration and invasion in 2D monolayer and 3D spheroid cervical and prostate cancer cultures
- Look for and validate miR-143/145 targets related actomyosin cytoskeleton dynamics, focusing on phosphorylation of MLC
- Determine the role of miR-143/145 during the differentiation of keratinocytes in 2D and skin organotypic cultures
- Evaluate the miR-143/145 expression in response to UV irradiation

EXPERIMENTAL STRATEGY

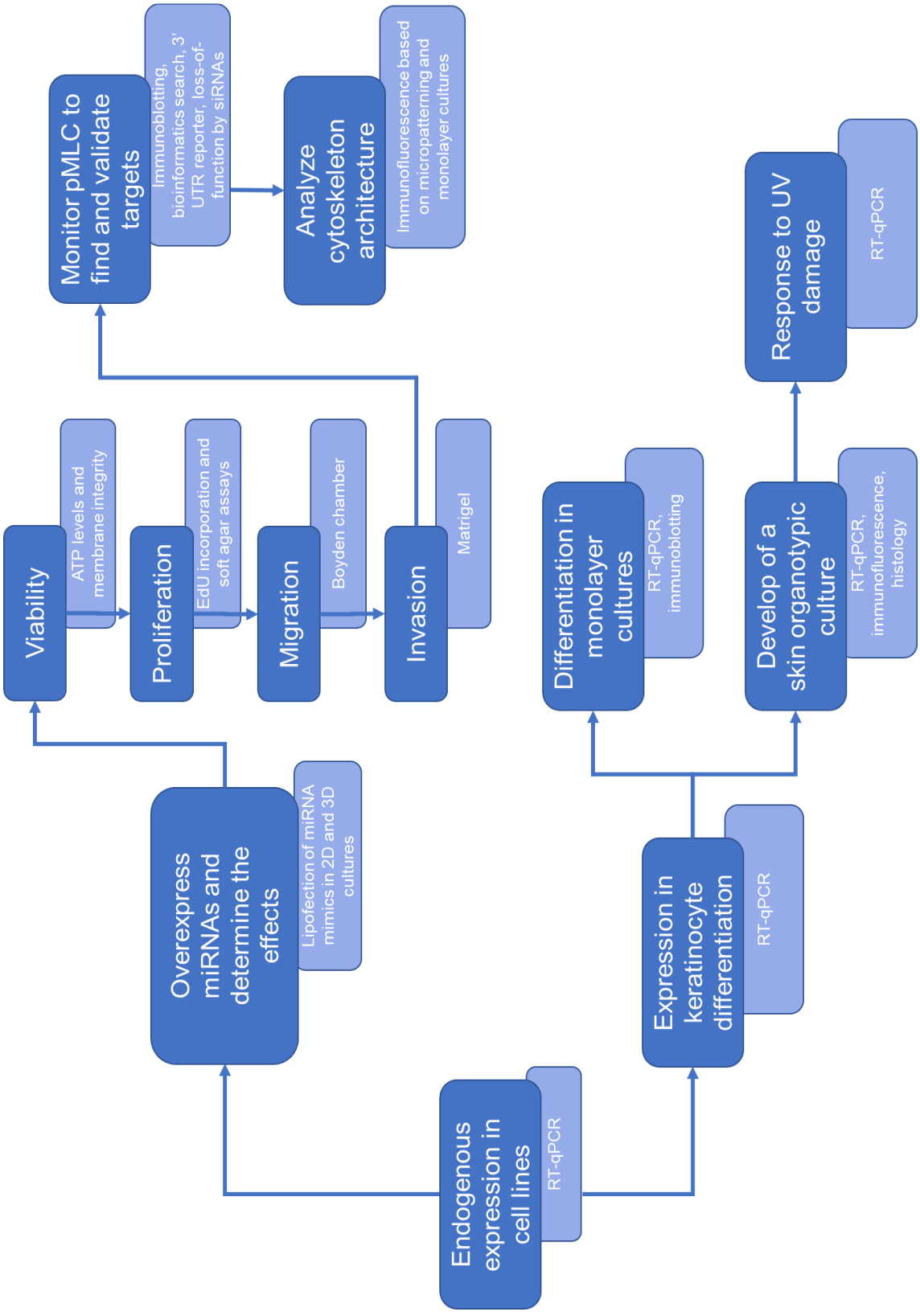

METHODOLOGY

Plasmids and oligonucleotides

All oligodeoxynucleotides were purchased from T4 oligo® (ADN Sintetico S.A.P.I. de C.V., Mexico). The sequences for hsa-miR-143-3p primers were based on previous reports [125]. All RT-qPCR primer sequences are listed below.

Primer	Sequence
miR-143-3p RT	5'GTCGTATCCAGTGCGTGTCGTGGAGTCGGCAATTGCACTGGATACGACTGAGCTA3'
miR-143-3p Forward	5'AGTGCGTGTCGTGGAGT3'
miR-143-3p Reverse	5'GCCTGAGATGAAGCACTGT3'
miR-145-5p RT	5'GTCGTATCCAGTGCAGGGTCCGAGGTATTCGCACTGGATACGACAGGGAT3'
miR-145-5p Forward	5'ACACGCAGTCCAGTTTTCCCAG3'
miR-145-5p Reverse	5'GTGCAGGGTCCGAGG3'
snRNA U6 RT	5'AAAATATGGAACGCTTCACGAATTTG3'
snRNA U6 Forward	5'CTCGCTTCGGCAGCACATATACT3'
snRNA U6 Reverse	5'ACGCTTCACGAATTTGCGTGTC3'
PPP1R12A Forward	5'GAGAGGGGATGAAGATGGCG3'
PPP1R12A Reverse	5'TTCACCTTGGTCTTCTGGCG3'

The wild-type miR-145 target sequence in *ppp1r12* (MYPT1) transcript (5'-CTCGAGGACCATAATTGGCAGTCACTGGAAGCGGCCGC-3') was predicted using the TargetScan.org software [126] and a mutant version with three nucleotide substitutions at the seed sequence (5'-CTCGAGGACCATAATTGGCAGTCACGTCAAGCGGCCGC-3') was designed as a control. Both sequences were cloned into the dual-reporter vector psiCHECK2 (Promega, Madison, WI).

The synthetic miR-143-3p/145-5p mimics and the scrambled miRNA negative control (NC) were purchased from Ambion® (Thermo Fisher Scientific Inc.,

Waltham, MA). MYPT1 and Allstars-Negative Control siRNAs were purchased from Santa Cruz Biotechnology (Dallas, TX) and QIAGEN (Venio, The Netherlands), respectively.

RT-qPCR Assays

The miRNA relative quantification was made by two-step RT-qPCR, as described [127]. Briefly, small RNAs (<200 nucleotides) were column-purified (Zymo Research, Irvine, CA) from monolayer cultures. The miR-143/145 expression was determined by 2-step RT-qPCR. An initial retro-transcription step was performed with SuperScript III (Invitrogen) at 42ºC/30 minutes and finally at 85ºC/5 minutes. Next, the qPCR was carried out using the Maxima SYBR Green/ROX qPCR Master Mix (Thermo Scientific) or a miR-145-specific probe using a Rotor-Gene 3000 thermocycler (Corbett Research, Australia). The program for amplifying the miRNAs was: 95ºC/10 minutes to inactivate the RT enzyme; later, 40 cycles for miRNA or 30 for U6 control gene, each cycle consist in 95ºC/15 seconds and 60ºC/60 seconds. The U6 snRNA was used as reference control. Relative gene quantification was estimated by the $^{\Delta\Delta}$CT [128]. A melting curve was produced to identify the DNA amplicons. In addition, the PCR products were examined through native 8% polyacrylamide gels.

Cell culture

Cervical tumor cells, prostate cancer cells and immortalized keratinocytes used in the present work are listed below.

Cell line	Phenotype	HPV	Origin
HeLa	Tumoral	18 (+)	Cervical cancer
SiHa	Tumoral	16 (+)	Cervical cancer
Caski	Tumoral	16 (+)	Cervical cancer
QGU	Tumoral	16 (+)	Cervical cancer

C33A	Tumoral	(-)	Cervical cancer
HaCaT	Immortal	(-)	Spontaneously transformed human keratinocytes from adult skin
HKC16 E6/E7	Immortal	16 (+)	Foreskin keratinocytes immortalized with E6/E7 from HPV 16
CXT1	Immortal	16 (+)	Cervical cancer
CX16.2	Immortal	16 (+)	Cervix keratinocytes immortalized with the HPV 16 genome
PC-3	Tumoral	(-)	Prostate cancer
DU-145	Tumoral	(-)	Prostate cancer
RPE-1	Immortal	(-)	Retinal epithelial cells h-TERT immortalized

The cervical cancer cell lines HeLa (ATCC® CCL-2™), SiHa (ATCC® HTB-35™), CaSki (ATCC® CRL-1550™) and C-33A (ATCC® HTB-31™) ™) were grown in GIBCO™ DMEM medium (Thermo Fischer Scientific) supplemented with 5% GIBCO™ fetal bovine serum (FBS) (Thermo Fisher Scientific). The spontaneously immortalized keratinocytes HaCaT [129] and the HPV16-immortalized keratinocytes HKc16E6/E7-II [130] and Cx16.2 [131] were cultured in GIBCO® keratinocyte serum-free medium (K-SFM) (Thermo Fisher Scientific). The foreskin primary fibroblasts and RPE1 cells were grown in GIBCO® DMEM/F12 1:1 medium (Life Technologies) supplemented with 5% FBS (Life Technologies). Prostate cancer cell lines PC-3 (ATCC® CRL-1435™) and DU 145 (ATCC® HTB-81™) were cultivated in GIBCO® RPMI 1640 medium (Life Technologies). All media were supplemented with 1% Streptomycin/Penicillin (PAA Laboratories Germany) and 10 µg/mL Gentamicin (Life Technologies) and cultures were maintained in a humidified atmosphere at 5% CO_2 and 37ºC.

RNAi transfection was performed using Invitrogen™ Lipofectamine RNAiMAX reagent (Thermo Fisher Scientific) following the manufacturer instructions, using miRNA mimics or siRNAs at 60nM final concentration for cervical cell lines and 20 nM for prostate cancer cell lines.

Primary culture

Primary keratinocytes and fibroblasts were isolated from neonatal foreskins treated with dispase (Corning) at 25 U/mL in KSFM and maintained at 4 ºC overnight. In the following day, dermis and epidermis were splitted using forceps. Both epidermis and dermis were tripsinized and neutralized with DMEM 5% FBS. The keratinocyte primary cultures were maintained in KSFM while fibroblasts were kept in DMEM/F12 (Thermo Fisher Scientific) until they had at least 4 passages. Culture homogeneity was determined by RT-qPCR of miR-203 and desmin as markers for keratinocytes and fibroblasts, respectively.

3D Spheroid Culture

Three hundred transfected cells per well were seeded in 96-well Corning® U-bottom ultra-low attachment plates (Corning Inc., Corning, NY) and incubated for 7 days changing media every 2 days. Spheroid phase-contrast photographs were taken with a Zeiss Axiovert 25 inverted Microscope (Carl Zeiss GA, Oberkochen, Germany) at 10X magnification. The area of every spheroid was calculated with the FIJI software, a distribution of Image J [132].

Viability Assay in monolayer culture by ATP level

PC-3 cells were cultured in 96-well plates (Corning). Cells were maintained 72h post transfection and viability was analyzed using the ViaLight plus kit (Lonza, Basel, Switzerland) following manufacturer's instructions. The luminescence was measured with a GloMax® 96 Microplate Luminometer (Lonza).

Viability in Spheroid Culture by membrane integrity

Cell viability was determined three days after transfection by adding 100 mM SYTOX Green (Thermo Fisher Scientific) and 1µg/mL Hoechst 33342 (Merck KGaA, Darmstadt Germany) followed by a further 24 h incubation. Live cells fluorescence was calculated by subtracting of SYTOX Green (impermeable)

from Hoechst (permeable) fluorescence staining intensities using a Zeiss Axiovert 25 inverted microscope (Carl Zeiss) with epifluorescence at 10X magnification and FIJI software.

Soft Agar Colony Formation Assay

$1.25x10^3$ transfected cells were embedded in 0.35% agarose and layered on a 0.5% agarose base. Cultures were maintained for 12 days with media change every three days. Five colonies per assay were randomly photographed with an inverted microscope (Carl Zeiss) and the size (area) was determined using FIJI software.

Proliferation Assays by EdU Incorporation

PC-3 cells were cultured in 96-well clear bottom plates (Promega) and the effect was analyzed after 72h transfection. To determine proliferation, cells were fixed and stained with Click-iT® 5-ethynyl-2′-deoxyuridine (EdU) Alexa Fluor 647 HSC assay (Thermo Scientific), according to manufacturer's protocols. Later, the plates were analyzed by CellInsight™ CX5 High Content Screening (HCS) Platform (Thermo Scientific) using HCS Studio and R Software.

Migration Assay

Migration assays were performed essentially as described [133]. Briefly, $1.5x10^4$ transfected cells were seeded into the upper chamber of non-coated polycarbonate Transwell® inserts (8 µm pore) (Corning) and starved by 16 hours in basal media before addition of media supplemented with 10% FBS to the lower chambers followed by further 48 hours incubation. Non-migrating cells were removed from the upper chamber using cotton swabs. Cells were fixed with cold methanol (-20 ^oC) and stained with 2% crystal violet solution for 30 minutes. Membranes were removed from the inserts and analyzed by densitometry with the ImageStudio Software (Li-Cor Biosciences, Lincoln, NE).

Invasion Assay

Spheroids cultures were transfected and grown for four days as described above, before addition of 100 µL of Matrigel® Matrix (Corning) and allowed to solidify by 30 minutes at 37ºC and later overlayered with DMEM medium. The matrix-embedded spheroids were maintained for 48 h and the invasion rate was estimated by measuring the area between the spheroid edge and the leading edge of invasive cells using an inverted microscope (Zeiss) and FIJI software.

Micropatterns

Glass coverslips were first spin coated at 2,000 rpm for 30 s with an adhesion promoter (TI Prime; MicroChemicals, Madhya Pradesh, India) and then with 1% polystyrene dissolved in toluene. The polystyrene layer was further oxidized with an oxygen plasma treatment (FEMTO; Diener Electronics, Germany) for 10 s at 30 W and incubated with 0.1 mg/ml poly-lysine polyethylene-glycol (JenKem Technology, Beijing, China) in 10 mM HEPES, pH 7.4, at room temperature for 45 minutes. Coverslips were then dried by spontaneous dewetting. Polyethylene-glycol–coated slides were placed in contact with an optical mask holding the transparent micropatterns (Toppan Photomasks, Round Rock, Texas) using a home-made vacuum chamber and exposed for 5 min to deep UV light (UVO Cleaner; Jelight Company, Irvine, California). Micropatterned slides were washed once in PBS and finally incubated for 30 min with a solution of 20 µg/ml bovine fibronectin solution (Sigma-Aldrich, St. Louis, Missouri). Before plating cells, patterned coverslips were washed three times with sterile PBS. The circular micropattern has an area of 1000 μm^2. RPE1 cells were transfected for 48 h and then plated on the micropatterns for 2 h [134].

Immunostaining

Cells were pre-permeabilized for 10 seconds with 0.5% Triton X-100 in cytoskeleton buffer pH 6.1 and fixed in 4% paraformaldehyde in cytoskeleton buffer for 15 min at room temperature. They were then rinsed twice with PBS and incubated in 0.1 M ammonium chloride in PBS for 10 min. Cells were then blocked with 3% BSA in PBS Ca^{2+} Mg^{2+} for 30 min. Cell nuclei, pMLC2 and actin were stained with Hoechst 33342, anti-phospho-Myosin Light Chain 2 (Ser19, Cell Signaling Technology) and Phalloidin (Sigma), respectively.
Images were taken with an ApoTome microscope (Zeiss). Fluorescent images of pMLC2 and actin staining are the sum of 15 Z projection of different aligned cells acquired with oil immersion objectives at 100X (NA = 1.4) using the Fiji-ImageJ software.

Western Blot

Protein extracts from transfected cells were prepared in ice-cold RIPA buffer (50 mM Tris-HCl, pH 7.4, 150 mM NaCl, 0.1% SDS, 0.5% Sodium deoxycholate, 1% NP-40, 1mM AEBSF) supplemented with cOmplete™ protease cocktail inhibitor (Roche, Basel, Switzerland), 1 mM PMSF, 2 mM Na_3VO_4, and 20 mM β-glycerophosphate. Lysates were cleared by centrifugation at 1.5 x 10^4 g for 15 min at 4°C. A total of 30 µg of protein were resolved on 4-8% SDS-polyacrylamide gels and transferred onto PVDF membranes (Merck-Millipore, Billerica, MA). Membranes were blocked with 5% BSA or 10% non-fat dry milk for 1h and incubated with primary antibody overnight at 4°C. Membranes were revealed with anti-rabbit horseradish peroxidase-conjugated secondary antibodies (Santa Cruz Biotechnology) and Luminata™ HRP substrates (Merck-Millipore) using a C-Digit Scanner (Li-COR Biosciences). A β-Actin antibody was used as loading control.

Antibody	Origin	Dilution	Blocking
β actin (sc-1616, Santa Cruz Biotechnlogy)	Goat polyclonal	1 :2000	With milk 10%
MYPT1(sc-414261, Santa Cruz Biotechnology)	Mouse monoclonal	1:500	With milk 10%
Phospho-Myosin Light Chain 2 (Ser19) (Cell Signaling Technology)	Rabbit polyclonal	1 :1000	With BSA 5%
Involucrin (Research Diagnostics, Flanders NJ)	Mouse monoclonal	1:500	Without milk
Anti-IG from goat (sc-2020, Santa Cruz Biotechnology)	Donkey	1:2000	1%
Anti-IG from rabbit (sc-2004, Santa Cruz Biotechnology)	Goat	1:2000	1%
Anti-IG from mouse (sc-2314, Santa Cruz Biotechnology)	Donkey	1:1000	1%

Luciferase reporter assay

Cells ($2.7X10^4$) were co-transfected with 20 nM miRNA mimics and 20 ng dual-luciferase reporter using Invitrogen™ Lipofectamine™ RNAiMAX reagent (Thermo Fisher Scientific). After 48 hrs, *Renilla* and Firefly luciferase activities were determined with the Dual-Luciferase Reporter Assay System (Promega) following the manufacturer's instructions, in a Glomax® Multi JR Luminometer (Promega). Luciferase activity was calculated as *Renilla* luciferase (hRluc) activity divided by firefly luciferase (hluc+) activity.

Differentiation assay in monolayer keratinocytes

Differentiation induction in immortalized human keratinocytes was made by addition of $CaCl_2$ (2.5 mM final concentration). Confluent keratinocytes were maintained 10 days in high-calcium medium. The involucrin protein (a late differentiation protein), and miR-203 (a differentiated-keratinocyte specific miRNA), were used as differentiation markers.

Skin organotypic cultures

Epidermis reconstruction was performed following a previously standardized protocol [124] with slight modifications. Briefly, keratinocytes were seeded inside a Transwell insert (Corning) with polycarbonate membrane (0.4 µm pore-size) and fibroblasts were seeded on the outside bottom and incubated overnight in KSFM medium supplemented with 5% of FBS. The following day, the media is changed by DMEM/F12-KSFM high-calcium 1:1 mixture, creating a liquid-air interface on the polycarbonate membrane. The culture is maintained for two weeks changing medium every 2 days the first week and daily the second week. The epidermis was UVC irradiated at 100 J/m^2. The cultures transfected with miRNA mimics followed the lipofection protocol described above. Total RNA was isolated using TRIzol reagent (Thermo Fischer Scientific)

Histology

Polycarbonate membranes were recovered from the inserts using a sterile syringe needle and forceps. Excised membranes were placed on a filter paper to absorb the liquid medium before embedding in Tissue-Tek® O.C.T. Compound (Sakura® Finetek). Cryosections of 8 µm were obtained with a cryostat CM1950 (Leica, Wetzlar, Germany) and were used for both hematoxylin & eosin and immunofluorescence staining.

Statistical analysis

Statistical analyses were performed with the GraphPad Prism 5 software (GraphPad Software, San Diego, CA). A Student's t-test was used for comparison of two groups and one-way ANOVA with Tukey post-hoc tests when comparing three or more experimental groups. Statistical significance was considered at $p<0.05$ (indicated with *). Results were expressed as a bar graph of the mean with standard deviation of at least three different experiments or as a boxplot with whiskers and maximum range (1.5 interquartile) from at least three technical replicates from three different experiments.

RESULTS

Because of the extension, this work was divided in three parts. In the first part, miR-143/145 tumor suppressor function was determined in prostate cancer cells. The second follows a similar flowchart for cervical cancer cells and additionally MYPT1 was validated as target of miR-145. Finally, miR-143/145 expression was determined in the keratinocyte differentiation, a process opposite to cancer.

PROSTATE CANCER

miR-143/145 overexpression decreases PCa cells growth in 2D and 3D cultures

To analyze the effect the miR-143/145 cluster on cell viability in a PCa context, miR-143/145 mimics and LNA miRNA inhibitors were transfected into PC-3 cells, using siRNAs Allstars and CellDeath as negative and positive transfection controls, respectively. To monitor effect on 2D cell growth, the ATP levels were detected using bioluminescence as a measure of cell viability. The cells transfected with the miR-145 mimic showed a significant decrease in cell viability compared to the negative control (siAllStars). Transfection of miR-143 mimic and both LNA inhibitors (LNA-143-3P and LNA-145-5P) did not produce

any significant difference. No additive effect was observed when miR-143 and miR-145 mimics were used in combination (Figure 7A).

Since 3D culture models are more physiologically relevant than monolayer cell cultures, spheroid growth assays were performed to complement the effect of miR-143/145 on PCa cells viability. As described above, both miRNA mimics and LNA inhibitors were transfected into PC-3 cells and analyzed for spheroid growth (Figure 7B). Spheroids transfected with miR-143/145 mimics showed a significant decrease in size compared with the negative control. MiR-145 had the highest effect, even higher than miR-143/145 transfected together. As for monolayer cell cultures, the LNA inhibitors had no significant effect on PC-3 spheroid growth (Figure 7C). Because LNA inhibitors did not induce any apparent effect on cell growth, only miRNA mimics were used for the further assays.

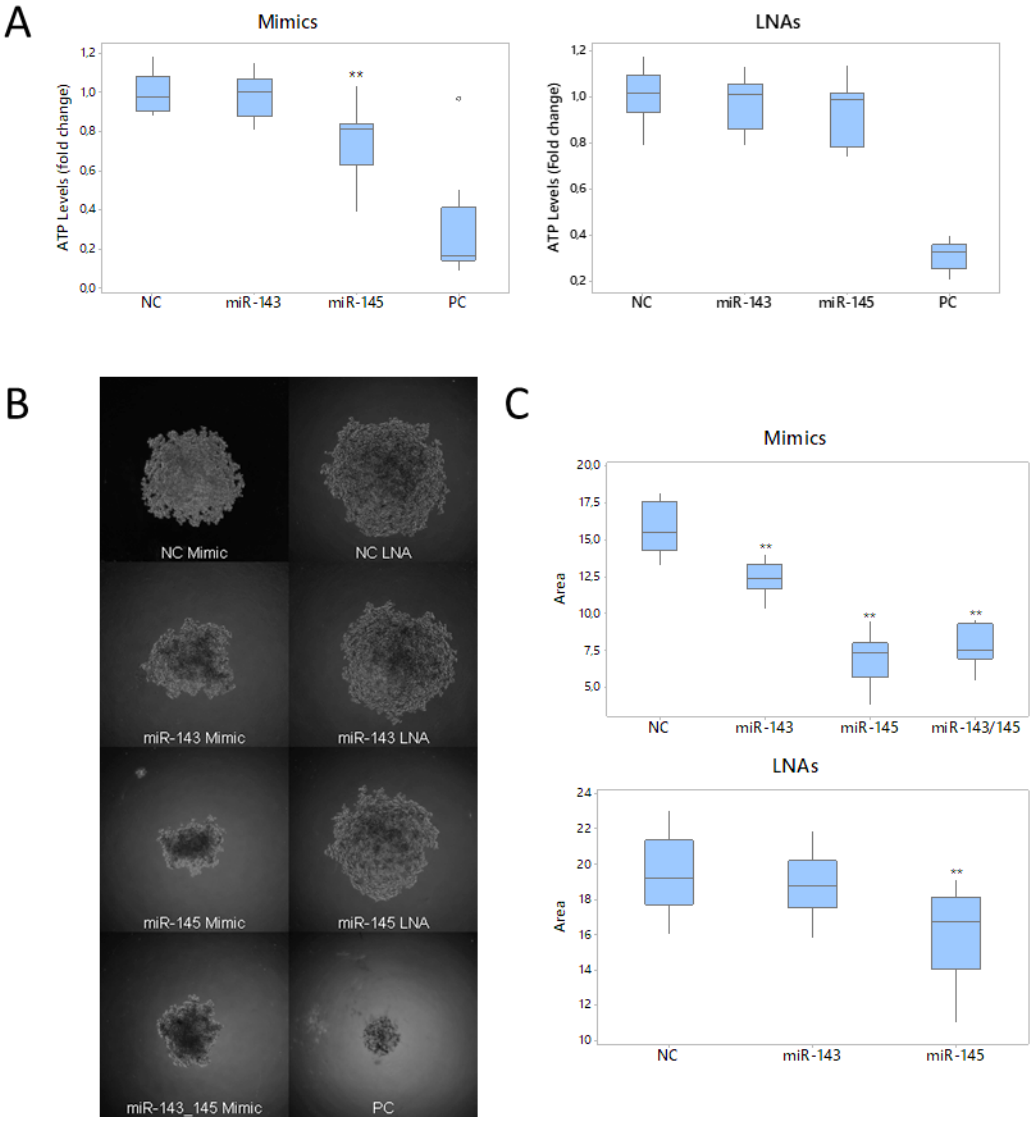

Figure 7. miR-143/145 cluster decrease the viability and growth of spheroid cultures. A) Fold changes in ATP levels as effect on viability after overexpressing miR-143/145 mimics and inhibitors (LNAs). B) Contrast microscopy for spheroid cultures. C) Quantification of spheroid relative area. NC, negative control. PC, positive control. **p<0.005.

The miR-143/145 cluster inhibits proliferation but does not induce apoptosis

Transfection of miR-143 and/or miR-145 mimics clearly affect PCa growth; however, it was not clear if this effect is due to an inhibition of cell proliferation or apoptosis induction. To understand the nature of this effect, high-content

screening approaches were performed to analyze cell proliferation in PC-3 cells transfected with miRNA mimics. EdU incorporation showed a significant proliferation decrease in presence of miR-145 and miR-143 compared to negative control. As previously observed, the strongest inhibitory effect after miR-145 mimic transfection (Figure 8A). Using active Caspase-3/7 for apoptosis detection, cells transfected with miRNA mimics did not show any induction of apoptosis compared to the negative control. Moreover, apoptosis induction decreased in cells transfected with the miRNA mimics, probably because these miRNAs induced cell cycle arrest without apoptosis induction (Figure 8B). Thus, the inhibitory growth effect on 2D and 3D cultures likely resulted from inhibition on cell proliferation instead of apoptosis induction.

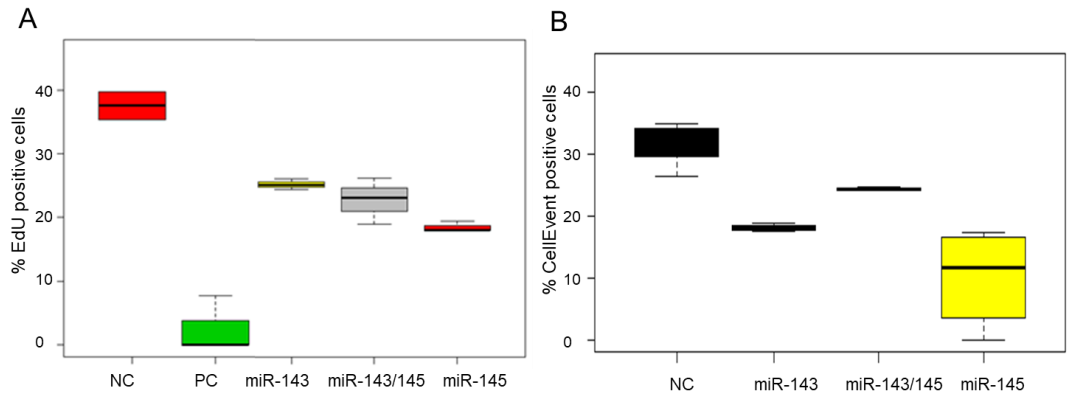

Figure 8. miR-143/145 inhibit proliferation but does not induce apoptosis. A) Percentage of positive cell for EdU incorporation in the proliferation assay after 72 h transfection. B) Percentage of CellEvent positive cells in the caspase 3/7 assay after 72 h transfection. NC, negative control. PC, positive control

Transfection of miR143/15 mimics increase pMLC2 levels

It has been reported that miR-143/145 can regulate cytoskeleton dynamics during muscle injury [82]. Since the actomyosin cytoskeleton activity is crucial for cell division and migration [135,136], the observed inhibitory effects of miR-143/145 were analyzed through the phosphorylation of the Myosin Light Chain (pMLC), a key post-translational modification for actomyosin contractile activity,

and ROCK1, one of the direct kinases that act in MLC. The levels of pMLC on Ser19 were determined by immunoblotting of protein lysates from DU-145, a PCa cell line, and RPE1, a human retinal pigment epithelial cells, one day after cell transfection with either miR-143 or miR-145 mimics. Immunoblot assays showed no effect on ROCK1 level of either miR-143 or miR-145. However, pMLC2 level increased after miR-143/145 mimic transfection, suggesting that miR-143/145 can modulate the phosphorylation and thus the activity of pMLC2 by targeting one or more effector of the pMLC2 pathway (Figure 9).

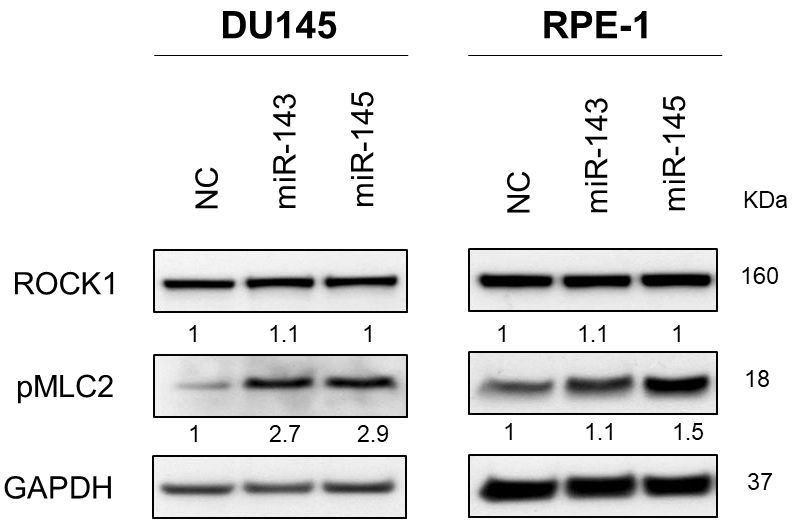

Figure 9. pMLC2 levels changes after miR-143/145 expression, but not ROCK1. Western blotting for prostate cancer cell line DU145 and epithelial immortalized cell line RPE1 after 24 h transfection with miR-143/145 mimics. NC, negative control.

pMLC2 is overexpressed in the cytoskeleton transversal arcs after transfection with miR-143/145

The role of miR-143/145 on actin organization was further investigated by monitoring pMLC2 location on actin fibers. The RPE1 cells, a widely-used cell model in cytoskeleton studies [134], were used on circular fibronectin micropatterns to normalize the cellular shape and actin cytoskeleton architecture. Cells transfected with the miR-145 mimic showed a higher pMLC2

fluorescence on the transversal arcs relative to the negative control. Transfection of miR-143 had a moderate increase on pMLC2 in the transversal arcs relative to miR-145. It was not possible to quantify the signal due to the high fibronectin-fluorescence background (Figure 10).

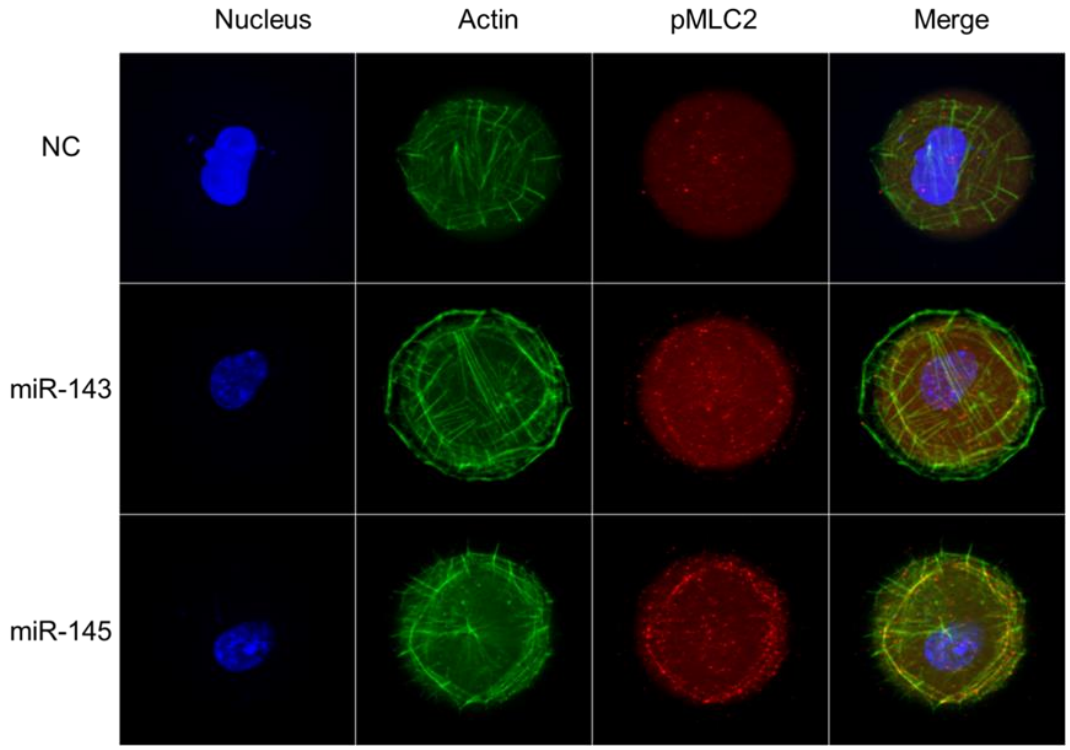

Figure 10. Cell localization of pMLC2 in the actin cytoskeleton. Transfected RPE1 cells were attached to circular fibronectin micropattern slides. Cells were fixed and stained for DNA (blue), F-Actin (green) and pMLC-2 (red). The image is the projection of the sum of each pixel on Z acquisition. MiR-145 transfected cells showed more pMLC2 fluorescence in the transversal arcs compared with the control and miR-143 transfected cells.

CERVICAL CANCER RESULTS

miR-143/145 are not expressed in cervical cancer cell lines and immortalized keratinocytes

As a first approach to further elucidate the role of the miR-143/145 cluster in cervical cancer, miR-143 and miR-145 expression was analyzed by end-point RT-PCR using small RNA (<200 nt) isolated from monolayer cultures of the

cervical cancer cell lines HeLa (HPV18+), CaSki (HPV16+), SiHa (HPV16+) and C-33A (HPV-) and the non-tumorigenic immortal keratinocytes HaCaT (HPV-), CX16.2 (HPV16+) and HKc16E6/E7-II (HPV16+), using normal foreskin RNA as positive control for miR-143/145 expression. The U6 snRNA was used as load control. No expression of either miR-143 or miR-145 was detected in any of the cell lines tested although both miRNAs were expressed in RNA extracted from neonatal foreskins, suggesting that the miR-143/145 cluster is not constitutively expressed in the cell lines used in this study (Figure 11A). Expression of miR-143 and miR-145 was restored in HeLa cells by transfection of miRNA mimics to test their function on a cervical cancer cell line able to form 3D spheroids [137], a cell culture technique that provides a more physiological model to mimic *in vivo* tumor conditions. Both miRNA mimics showed efficient transfection although miR-143 was detected with 5-fold higher intensity than miR-145 (Figure 11B).

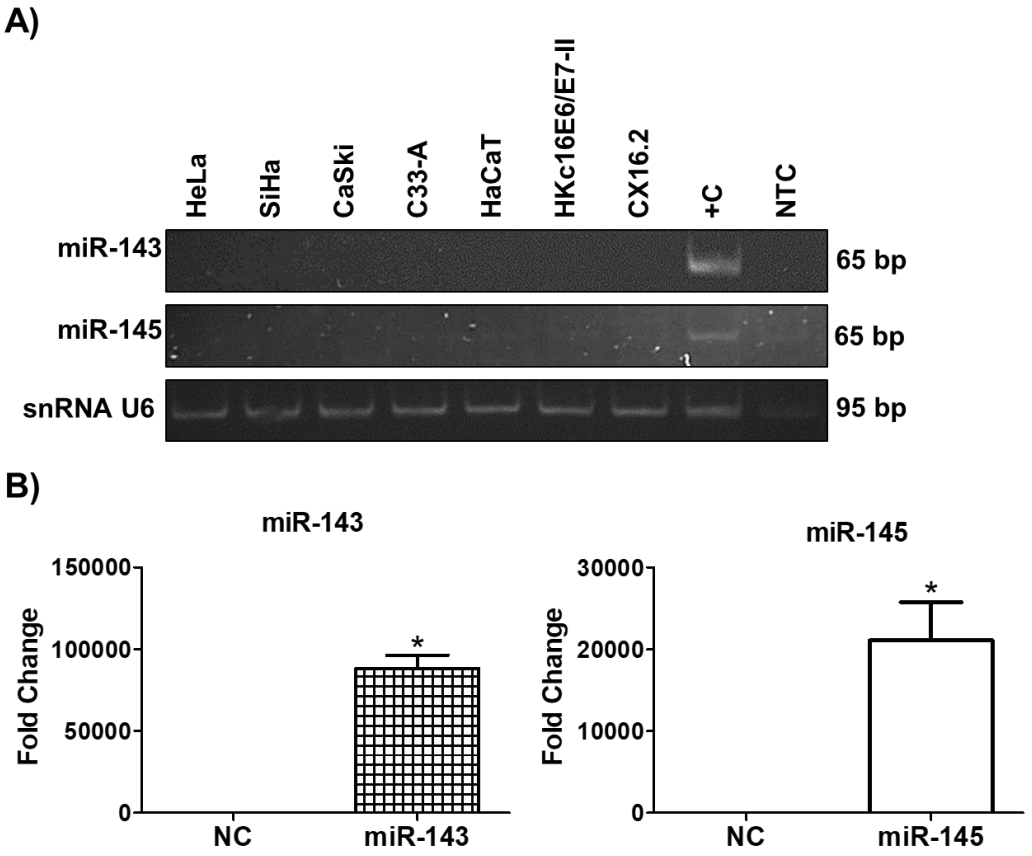

Figure 11. miR-143/145 is not expressed in cervical cancer cell lines and immortalized keratinocytes. A) Endogenous levels of miR-143/145 were determined RT-PCR in different cervical cancer cell lines (HeLa, SiHa, CaSki, C33-A) and immortalized keratinocytes (HaCaT, HKc16 E6/E7 II, CX16.2). Rat lung RNA worked as positive control and small nuclear U6 was used as reference gene. NTC, non-template control; bp, base pairs. B) HeLa cells were transfected with miR-143 and miR-145 mimic respectively and the expression was determined by RT-qPCR. *p<0.05

Overexpression of miR-143/145 decreases spheroid culture viability and impairs anchorage-independent growth

Because 3D cell cultures provide a more relevant model to mimic physiological tumor conditions, miR-143 or miR-145 mimics were transfected in 3D spheroid cultures of HeLa cells to evaluate the effect of the miR-143/145 cluster in 3D growth. A scrambled miRNA mimic was used as negative control (NC). Transfection with miR-145 mimic severely affected spheroid size (35% smaller

than NC) and morphology suggesting cell death, although miR-143 mimic transfection produced no statistically significant effect (Figure 12A).

To evaluate cell death, viability assays based on membrane integrity were performed with SYTOX Green/Hoechst 33342 on HeLa spheroid cultures transfected with miRNA mimics. Both miR-143 and miR-145 mimics produced a significant decrease in viability (30 and 60% less than NC, respectively) further suggesting that the miR-143/145 cluster expression may induce cell death with miR-145 producing the strongest effect (Figure 12B).

In addition to cell death, inhibition of proliferation can also affect 3D growth. Soft agar colony formation assays were performed to further explore the ability of miR143/145-transfected single cells to proliferate and form anchorage-independent colonies relative to the NC. Only HeLa cells transfected with the miR-145 mimic showed a significant reduction of 60% in colony size compared with the NC. No morphological difference was noticed in these assays as the mechanical restraint produced by the soft agar limits colony shape. Transfection of the miR-143 mimic did not produce a statistically significant effect on the colony size of HeLa cells (Figure 12C). These results suggest that although both miR-143 and miR-145 affect cell viability on 3D cultures, they follow different regulatory pathways with miR-145 producing a strong inhibitory effect on 3D cell proliferation and viability.

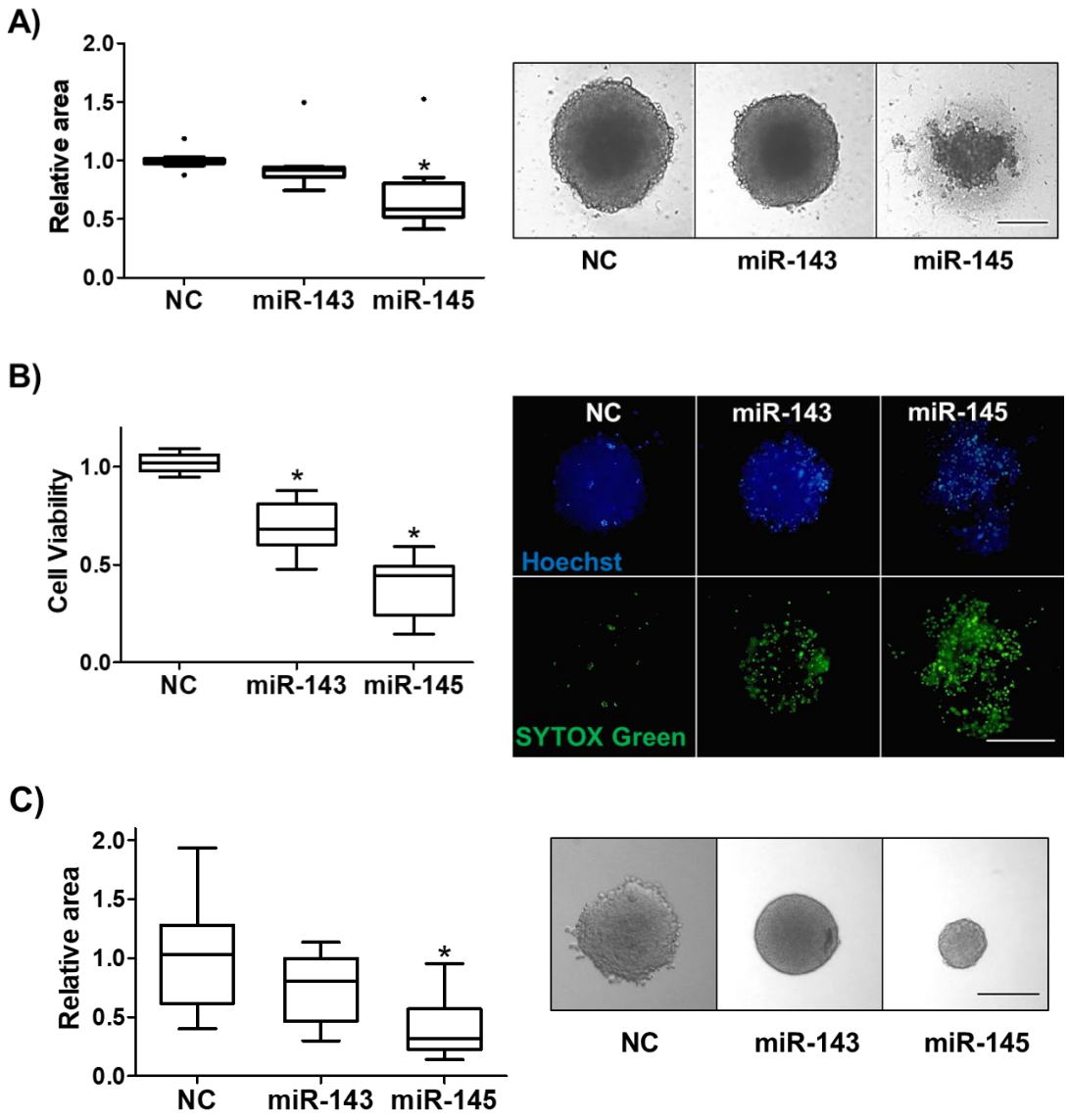

Figure 12. The miR-143/145 cluster decreases viability in 3D spheroid cultures and impairs colony formation. A) Left panel, HeLa cells were transfected with NC, miR-143 or miR-145 mimics. Spheroid cultures were grown by 7 days before size quantification. Data are represented as a boxplot of at least three technical replicates of three different experiments (*p<0.05). Outliers are depicted as points beyond whiskers. Right panel, a representative image of HeLa spheroids after transfection with NC, miR-143 or miR-145 mimics. Scale bar= 500 µm. B) The viability of HeLa spheroids after transfection with NC, miR-143 or miR-145 mimics. Right panel, transfected spheroids were stained with SYTOX Green (green) and Hoechst 33342 (blue) to quantify cell viability. Left panel, the box plot represents the quartiles distribution of the difference between blue cells minus green cells (Cell viability) from three independent experiments (*p<0.05). Scale bar= 500 µm. C) Soft

agar colony formation inhibition by miR-145. Hela cells transfected with NC, miR-143 or miR-145 mimics were grown in soft agar for 12 days. Left panel, the box plot represents quartiles distribution of the relative colony area of at least five colonies of three independent experiments (*p<0.05). Right panel, a representative brightfield image of HeLa colonies transfected with the NC, miR-143 or miR-145 mimics. Scale bar=500 µm**.**

Selective inhibition of cell migration and invasion by the miR-143/145 cluster

The effect of miR-143 and miR-145 on cell migration was analyzed by stimulation of cell movement through porous membranes in transwell inserts. Hela cells transfected with the miR-145 mimic exhibited a significant inhibition of 35% on cell migration relative to the NC, while transfection with the miR-143 mimic showed no significant effect (Figure 13A). Furthermore, invasion assays using HeLa spheroids transfected with miR-143 or miR-145 mimics presented a significant decrease (>50%) on invasion area compared to the NC, suggesting that the miR-143/145 cluster may play a role in the control of cell migration and invasion (Figure 13B).

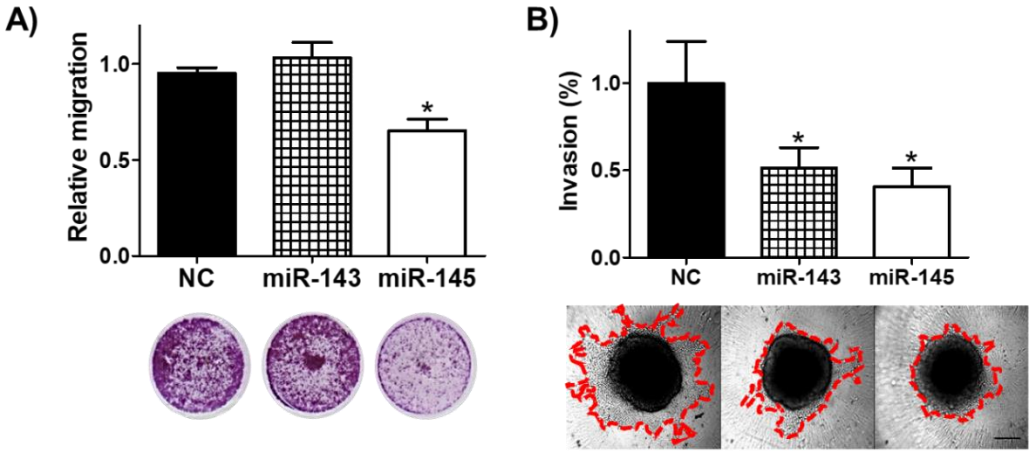

Figure 13. Selective inhibition of cell migration and invasion by the miR-143/145 cluster. A) Transwell migration assays were performed using HeLa cells transfected with NC, miR-143 or miR-145 mimics. The plot represents the mean and standard deviation of the relative migration from three independent experiments. The inset below shows an image of the bottom side of the insert from a representative migration assay stained with crystal violet. B) HeLa spheroids cell invasion assays. 3D spheroids transfected with NC, miR-143 or

miR-145 mimics were embedded in Matrigel and allowed to invade for 48 hrs. The plot shows the mean invasion area (dashed lines on the insets) and standard deviation of three independent experiments (*p<0.05). The inset shows a brightfield image of a representative experiment. Scale bar= 500 µm.

pMLC levels are increased by miR-145

It has been reported that miR-143/145 can regulate cytoskeleton dynamics during muscle injury [82]. Since the actomyosin cytoskeleton activity is crucial for cell division and migration [135,136], the observed inhibitory effects of miR-143/145 on cell viability, migration and invasion were analyzed through the phosphorylation of the Myosin Light Chain (pMLC), a key post-translational modification for actomyosin contractile activity. The levels of pMLC on Ser19 were determined by immunoblotting of protein lysates from HeLa cells one day after cell transfection with either miR-143 or miR-145 mimics. Transfection of miR-145 produced a significant 2-fold increase of pMLC levels compared to the NC. On the contrary, no significant difference was observed between miR-143 transfected cells and the NC (Figure 14A). The increase in pMLC levels was further corroborated by immunofluorescence, where miR-145 transfected cells showed higher fluorescence signal for pMLC as well as thicker actin bundles (white arrows, Figure 14B). The increase of pMLC in response to miR-145 could be explained due to the silencing of a negative regulator (i.e. a phosphatase or a kinase inhibitor).

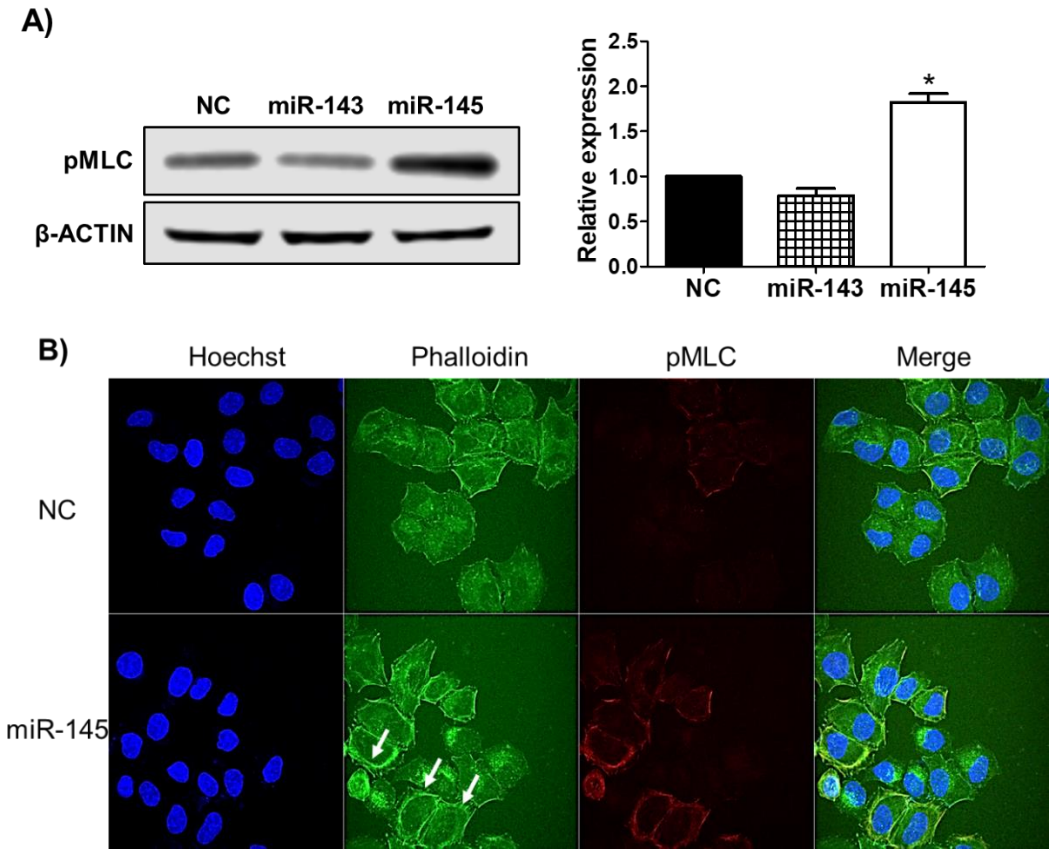

Figure 14. Phospho-Myosin light chain (pMLC) levels are increased by miR-145 but not by miR-143. A) Left panel: immunoblot for pMLC with protein extracts from HeLa cells transfected with NC, miR-143 or miR-145 mimics. β-actin was used as a load control. Right panel: densitometric analysis of pMLC immunoblots of HeLa cells transfected with NC, miR-143 or miR-145 mimics. The plot represents the mean pMLC expression relative to β-actin from three independent experiments. (*p<0.05). B) Immunofluorescence for actin (green) and pMLC (red) in transfected HeLa cells.

Myosin Phosphatase is a target of miR-145

To elucidate the role of miR-145 on pMLC up-regulation, a TargetScan search for miR-145 target sequences (http://www.targetscan.org/vert_71/) was performed to select transcripts involved in MLC phosphorylation. Although gene transcripts such as ROCK1, PAK1 and MYLK3 had putative target sites for miR-145, these kinase mRNAs wound not explain the observed increase in pMLC by miR-145 inhibitory regulation, contrary to the MYPT1 transcript, a

subunit of the phosphatase involved in the negative regulation of MLC, that contains also a potential miR-145 target site within the 3'-UTR.

Dual-luciferase reporters containing the wild-type or an inactive miR-145 mutant target site in MYPT1 were produced and co-transfected in HeLa monolayer cultures with NC or miR-145 mimics (Figure 15A). Co-transfection with miR-145 produced a significant inhibition of 30% in luciferase activity in the reporter containing the wild-type target sequence compared with the NC, suggesting a direct regulation of MYPT1 by miR-145 (Figure 15B). This inhibition was completely abolished by mutation of the miR-145 target sequence (Figure 15B), confirming the seed sequence specificity of this inhibition.

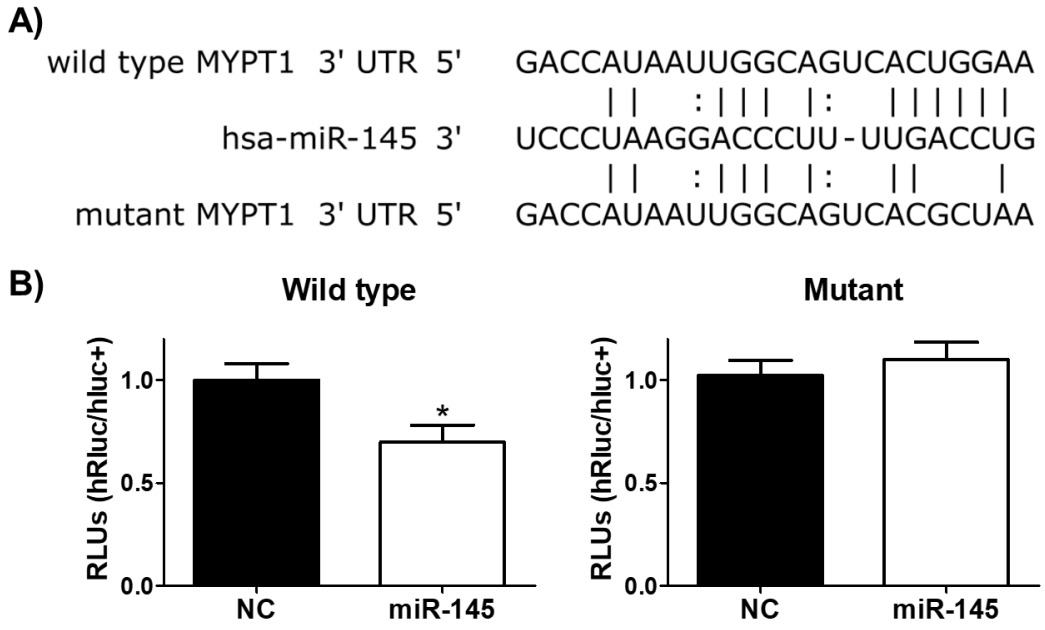

Figure 15. Myosin phosphatase target subunit 1 (MYPT1) is targeted by miR-145. A) The target sequence for miR-145 within the MYPT1 3'-UTR (upper sequence). A three-base mutation (mutant MYPT1) on the MYPT1 miR-145 target site was produced as a negative control (lower sequence). Lines indicate Watson Crick pairings of miR-145 (middle sequence) with the MYPT1 target site. Dotted lines represent non-Watson Crick pairing. B) HeLa cells were co-transfected with NC or miR-145 mimics and a dual-Luciferase expression vector containing either the wild-type or mutant miR-145 site on MYPT1. RLUs, Relative Lights Units of three independent experiments.

Moreover, transfection of the miR-145 mimic downregulated MYPT1 protein levels relative to the NC, although it did not affect the MYPT1 mRNA content (Figure 16A), suggesting that miR-145 may mediate MYPT1 translational repression but not RNA degradation.

MYPT1 knockdown increases pMLC levels and reduces viability and cell migration

Further support for the miR-145 suppressive effects through MYPT1 downregulation was obtained by reproducing MYPT1 silencing by siRNAs. HeLa cells transfected with a MYPT1-specific siRNA (siMYPT1) significantly decreased over 80% MYPT1 protein levels compared to cells transfected with a scrambled siRNA negative control (siControl) (Figure 16B, left panel). In addition, as with miR-145, cells transfected with siMYPT increased 2.4-fold pMLC levels relative to siControl, thus confirming the regulatory pathway miR-145-MYPT-pMLC (Figure 16B, right panel).

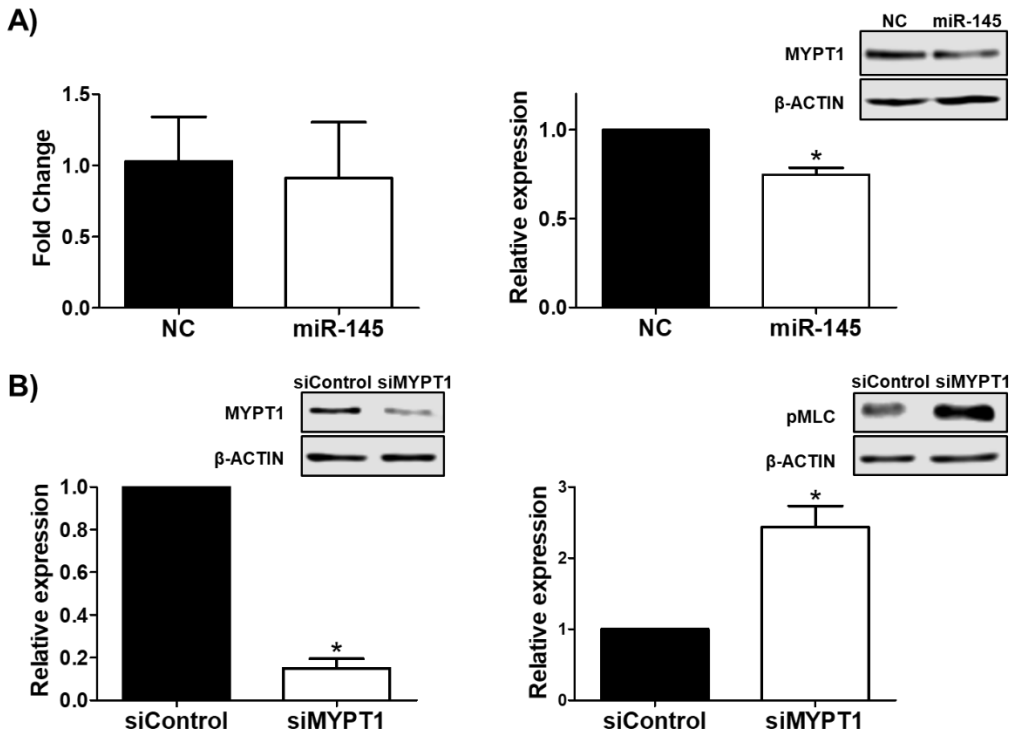

Figure 16. MYPT1 silencing increases pMLC expression. A) Transfection of miR-145 decreases MYPT1 protein levels but not mRNA levels. Monolayer cultures of HeLa cells were transfected with NC or miR-145 mimics. MYPT1 expression levels were determined by RT-qPCR (left panel) and

immunoblotting (right panel). U6 snRNA and β-actin were used as load controls for RNA and protein assays, respectively. The inset is a representative immunoblot of the MYPT1 content in miR-145-transfected HeLa cells. The plots represent the mean and standard deviation of three independent experiments. B) The siRNA-mediated silencing of MYPT1 increases pMLC expression. HeLa cells were transfected with a MYPT1 siRNA (siMYPT1) or a scrambled siRNA negative control (siControl). The levels of MYPT1 (left panel) or pMLC (right panel) were determined by immunoblotting. β-actin was used as loading control. The insets are representative immunoblots of the MYPT1 or pMLC content. The plots represent the mean and standard deviation of three independent experiments.

Evaluation of the cell response to MYPT1 silencing by siRNAs on HeLa cells produced similar results to those observed for miR-145. Transfection of siMYPT (but not siControl) significantly decreased spheroid viability (Figure 17A) and inhibited cell migration and invasion (Figure 17B). Additionally, cells transfected with siMYPT had high levels of pMLC and, as miR-145 transfected cells, thicker actin bundles (white arrows, Figure 17C). Therefore, downregulation of MYPT1 by miR-145 increased pMLC levels negatively affecting cell viability/migration/invasion, suggesting a regulatory role on pMLC levels of miR-145 by directly targeting of MYPT1.

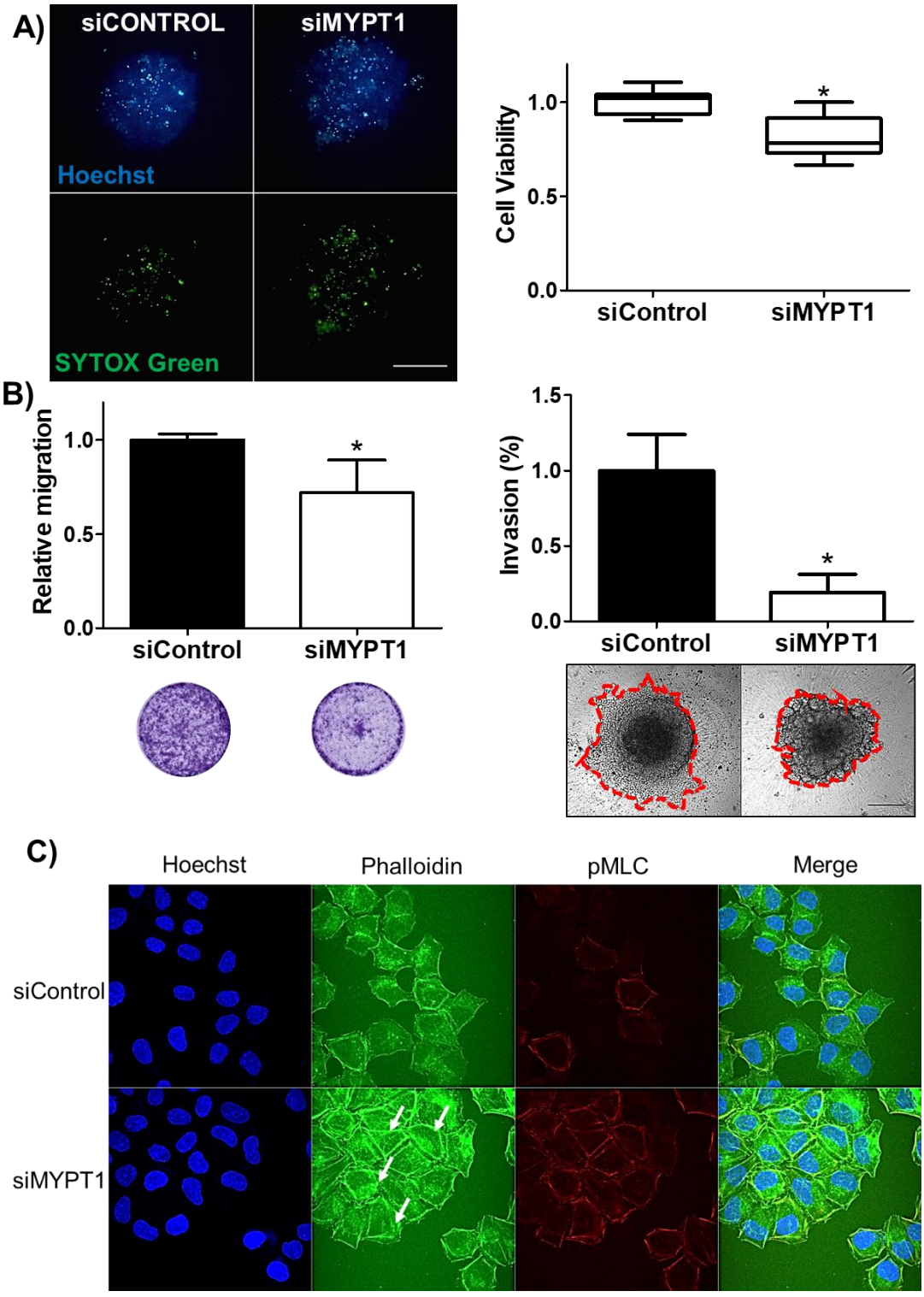

Figure 17. The siRNA-mediated silencing of MYPT1 reproduces miR-145 effects. HeLa cells were transfected with siControl or siMYPT1 siRNAs. A) Spheroid cultures were grown by 7 days and stained with SYTOX Green (green) and Hoechst 33342S (blue) to quantify cell viability (Left panel). Scale bar= 500 µm. Fluorescence quantification is represented as a distribution of

quartiles of the cell viability from three independent experiments (*p<0.05) (Right panel). B) HeLa cells were transfected with siControl or siMYPT1 siRNAs and used for transwell migration assays (Left panel) or 3D spheroid cell invasion assays (Right panel). The plots show the mean relative migration or invasion area and standard deviation of three independent experiments (*p<0.05), respectively. The inset below shows an image from a representative migration assay stained with crystal violet (left) and a brightfield micrograph of a representative invasion experiment (right). Scale bar= 500 µm. C) Actin and pMLC2 immunofluorescence of HeLa cells transfected with siControl or siMYPT.

EXPRESSION OF MIR-143/145 IN KERATINOCYTE DIFFERENTIATION

The miR-143/145 cluster is not expressed in monolayer differentiated keratinocytes

Previously, we observed that miR-143/145 is not expressed in non-differentiated immortalized keratinocytes. Since the miR-143/145 cluster has been implicated in differentiation [65,66], the expression of these miRNAs in keratinocyte differentiation was further investigated. After 10 days of differentiation induction by calcium, the keratinocytes showed a flattened morphology, a characteristic of differentiated keratinocytes (Figure 18A). In addition, involucrin (a keratinocyte late differentiation marker [138]), was strongly expressed in calcium differentiated keratinocytes in contrast with non-differentiated cells (Figure 18B), thus confirming that HaCaT and HKc16E6/E7-II immortal keratinocytes were terminally differentiated. No miR-143/145 expression was detected by RT-qPCR in both non-differentiated and differentiated keratinocytes although miR-203 (a keratinocyte differentiation miRNA marker [139]) was clearly detected in keratinocyte samples.

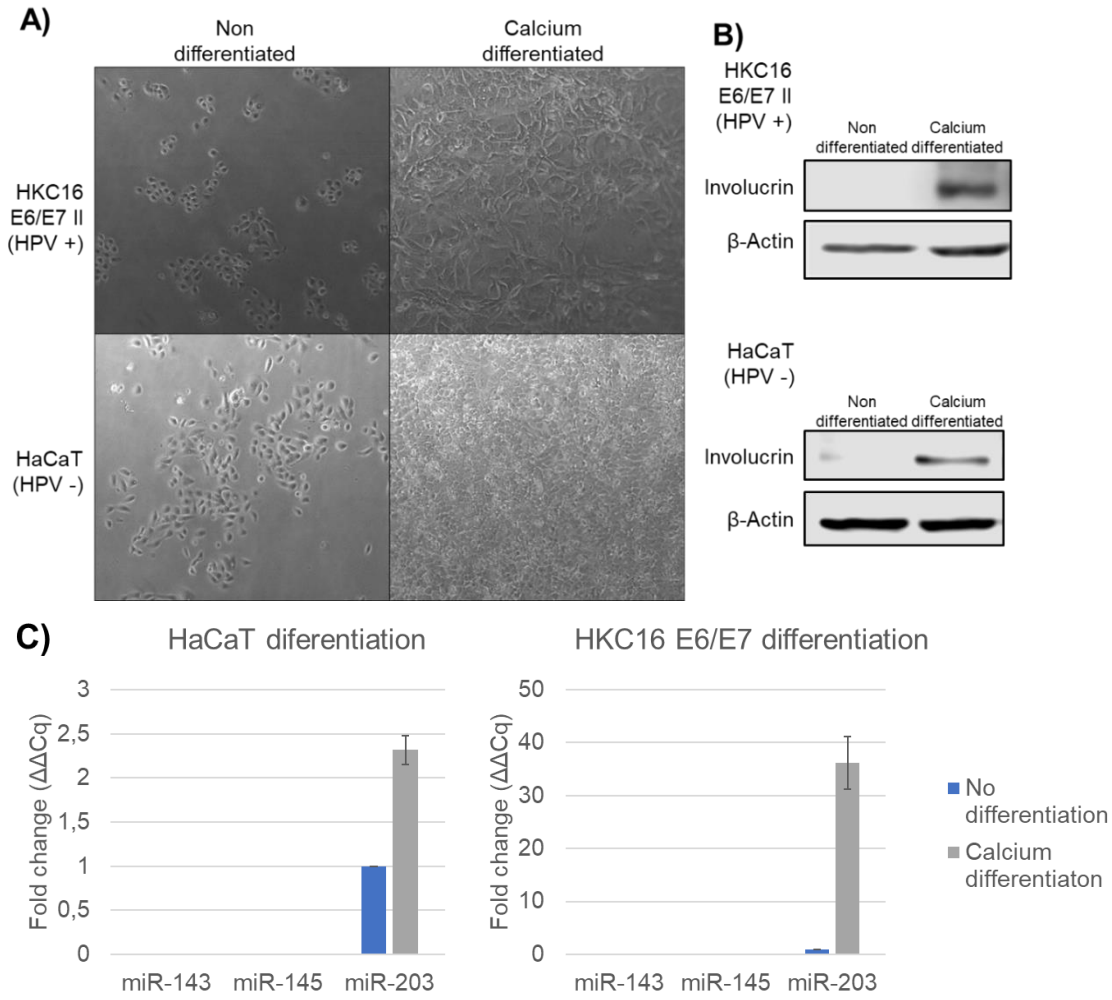

Figure 18. miR-13/145 is not expressed in differentiated immortalized keratinocytes. HaCaT and HKc16E6/E7-II keratinocytes were differentiated by 2.5 mM calcium chloride. A) Phase-contrast micrograph of immortalized keratinocytes before and after calcium-induced differentiation. B) Representative immunoblot for involucrin, a late differentiation marker for keratinocytes. C) Relative expression for miR-143 and miR-145 in non-differentiated and differentiated immortalized keratinocytes. miR-203 was used as keratinocyte differentiation miRNA marker. RNU6 was used as reference gene.

miR-143/145 are expressed in epidermis but the expression is lost in primary monolayer keratinocytes cultures

Although miR-143/145 expression has been reported in stratified epithelia like skin or cervix [140], the lack of expression in immortalized keratinocytes could be explained by two possibilities: miR-143/145 is expressed only in stromal

tissue like in intestine [141] or miR-143/145 is under regulation by cellular factors (i.e. native p53) which is mutated in HaCat cells [142] or inhibited by HPV proteins in HKc16E6/E7-II [143]. To elucidate this, foreskin samples were parted in dermis, (fibroblast-enriched) and epidermis (keratinocyte-enriched) portions, and miR-143/145 levels were determined by RT-qPCR. Both foreskin portions expressed miR-143/145, suggesting that these miRNAs are expressed both in fibroblasts and keratinocytes (Figure 19A). However, miR-143/145 was not detected in isolated primary human foreskin keratinocytes (HFK), showing again that HFK do not express miR-143/145 even if differentiated (Figure 19B). In contrast, primary human foreskin fibroblasts (HFF) expressed both miR-143 and miR-145 (Figure 19C). The differential miR-143/145 expression pattern between foreskin epidermis and HFK suggested that keratinocytes may require further stimuli to express miR-143/145.

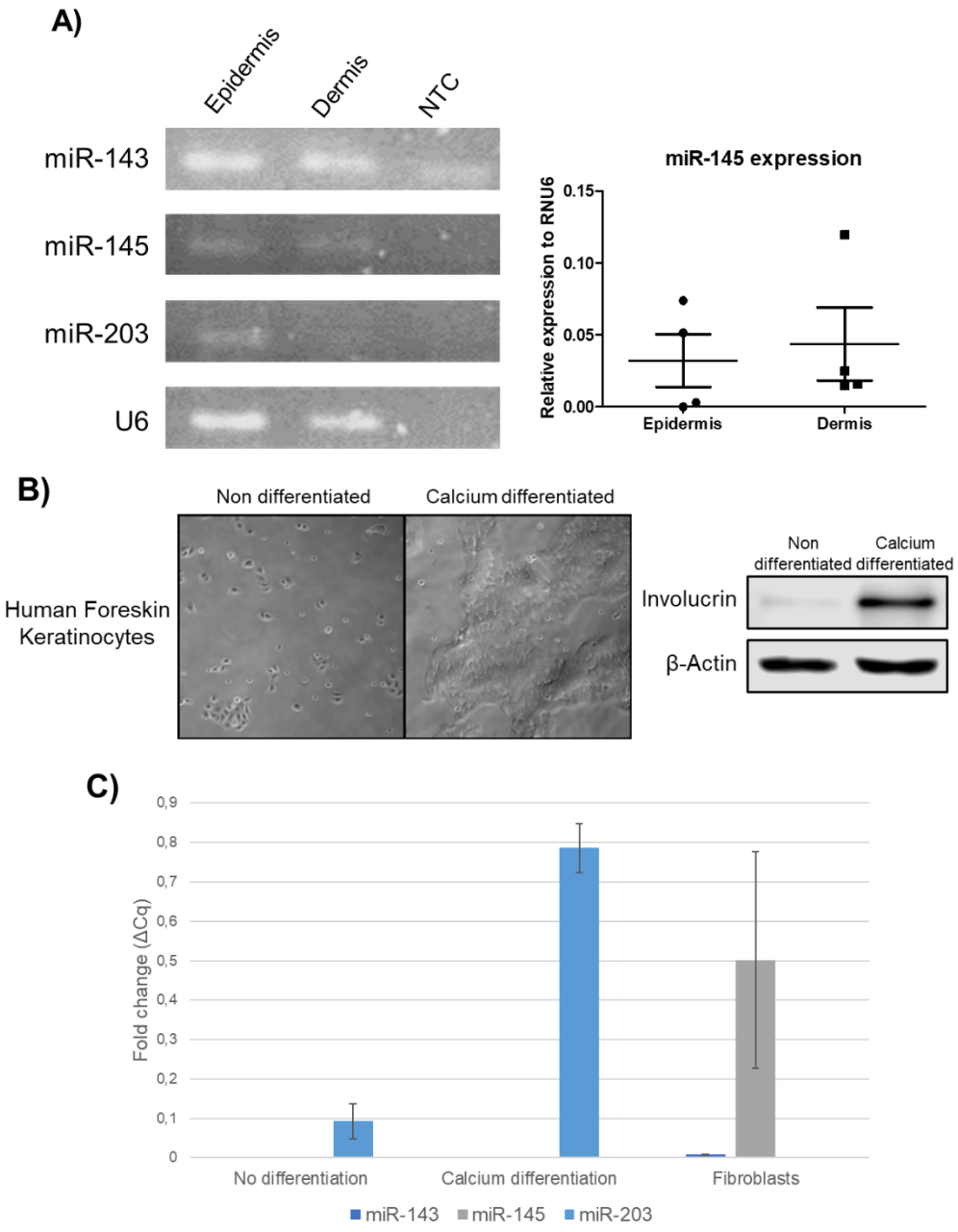

Figure 19. miR-143/145 are expressed in both dermis and epidermis but no in primary keratinocytes. A) Neonatal foreskin samples were separated using dispase. Expression of miR-143/145 was determined by RT-qPCR (right) and the products were observed in native PAGEs (left). B) Contrast photography of primary human foreskin keratinocytes before and after of calcium-induced differentiation (left). Immunoblots for involucrin confirmed terminal differentiation (right). C) Expression of miR-143 and miR-145 in non-differentiated and differentiated primary keratinocytes and fibroblasts. miR-203

was used as keratinocyte differentiation marker. RNU6 was used as reference gene.

miR-143/145 are expressed in 3D stratified keratinocytes cultures

To determine if stratified keratinocytes express miR-143/145, co-cultures of HaCaT Reconstructed Epidermis (HRE) and HFF we performed, obtaining a skin organotypic culture. Following De Vuyst modified protocol [124], stratified HRE were H&E stained to confirm stratification (Figure 20A) and subjected to cytokeratin K10 and involucrin immunofluorescence established differentiation (Figure 20B). Expression of miR-143/145 was later determined in HRE and HFF by end-point RT-PCR, showing that keratinocytes express both miRNAs when they are stratified (Figure 20C).

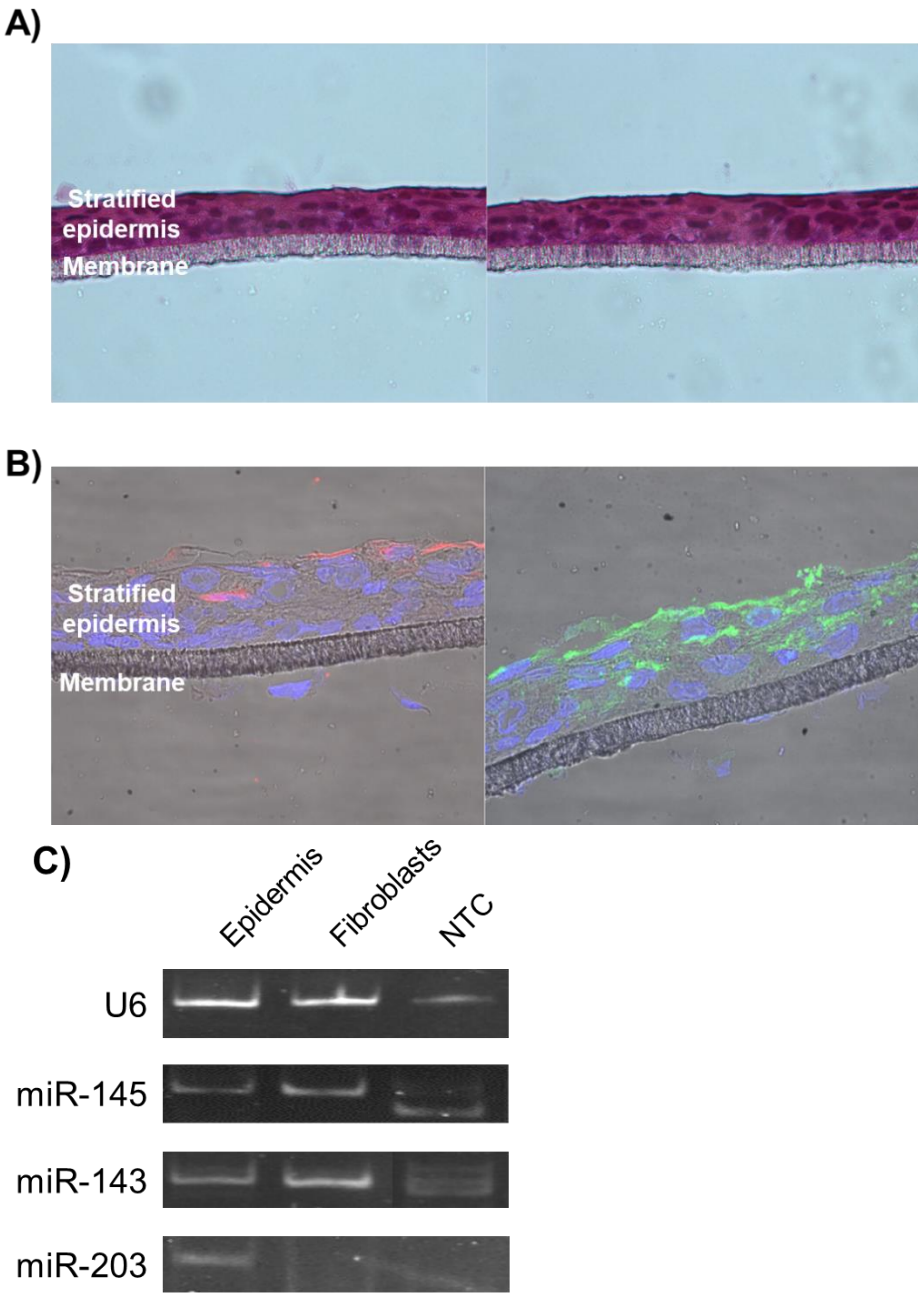

Figure 20. miR-143/145 expression in 3D stratified keratinocytes. HaCaT cells were co-cultured with primary fibroblasts in organotypic 3D cultures. A) Micrograph of H&E staining for HaCaT epidermis. 40X Magnification. B) Immunostaining for cytokeratin K10 (red) and involucrin (green). Nuclei were stained with Hoechst 33342 (blue). 60X Magnification. C) miR-143/145 expression in 3D epidermis and fibroblast by end-point RT-PCR. miR-203 was used as keratinocyte-specific miRNA marker and RNU6 was used as reference gene. NTC, non-template control.

miR-145 expression is responsive to UV irradiation in 3D stratified keratinocytes cultures (Preliminary Results)

Additionally, miR-143/145 has been implicated in wound healing in epithelial tissues like intestine [141]. We focused on miR-145 expression because it has a stronger tumor suppressor activity compared to miR-143 (see above). To create a wound-like in skin organotypic cultures and evaluate miR-145 expression in both epidermis and dermal fibroblasts, skin organotypic cultures were transfected with miRNA negative control (NC), miR-145 mimic or miR-145 inhibitor and HREs were irradiated with 100J/m^2 of UVC light (an irradiation level that leads to sunburn in human skin [144]), to simulate a wound healing process. In all transfections, UVC-irradiated HREs expressed higher miR-145 levels than non-irradiated cultures (Figure 21A). However, HREs transfected with miR-145 enhanced expression after being UVC irradiated. Expression of miR-145 in co-cultured fibroblasts was also determined, observing a similar effect than in HREs, where fibroblasts co-cultured with irradiated HRE showed higher miR-145 expression. Fibroblasts transfected with miR-145 inhibitors did not recover expression even when they were co-cultured with irradiated HRE (Figure 22B). Furthermore, miR-145 expression in response to UVC irradiation was time-lapse evaluated in HRE and fibroblasts. The first expression peak was observed in HRE 12 h after irradiation and subsequently fibroblasts showed an expression peak 24 h after irradiation (Figure 23B), indicating that miR-145 is expressed in time-dependent manner after irradiation in a wound healing process.

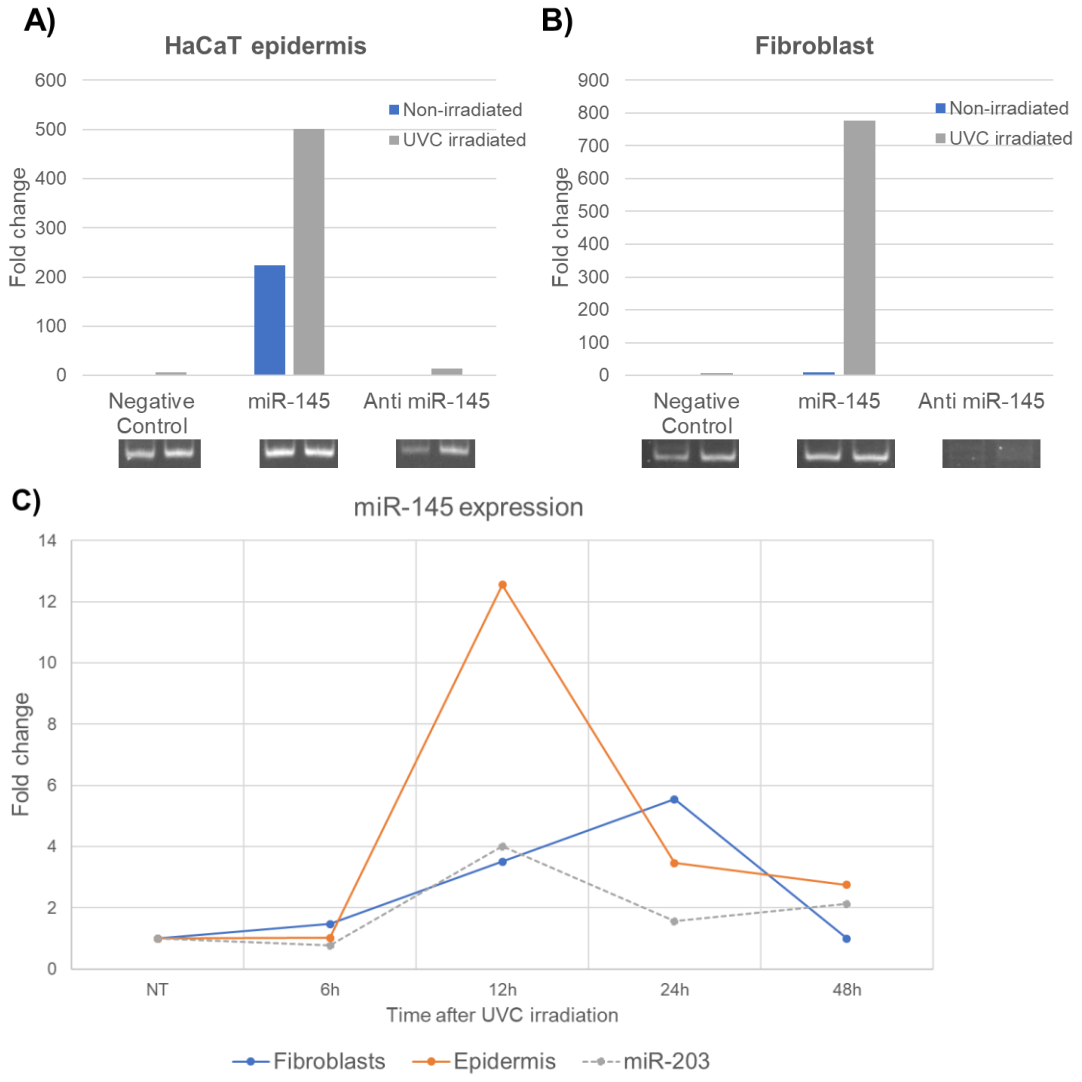

Figure 21. miR-145 expression in epidermis and fibroblast after UVC irradiation. 3D skin equivalent were transfected with NC, miR-145 mimic or miR-145 inhibitor and subsequently were irradiated with UVC light. A) miR-145 expression in epidermis (A) and fibroblasts (B) was determined 24 h after by RT-qPCR, using RNU6 as reference gene. C) Kinetic of miR-145 expression in epidermis and fibroblast co-cultured in 3D skin equivalent after being UVC irradiated.

DISCUSSION

Prostate Cancer

Dysregulation of the miR-143/145 cluster is involved in many pathologies including cancer, where it can modulate tumor progression. Downregulation of miR-143/145 has been recently reported in PCa tissue samples and cell lines, suggesting a tumor suppressor role [145–148]. In this report, miR-143/145 significantly decreased cell growth of PCa cells in a 2D cell model. This effect was not limited to 2D growth but also showed a strong effect on 3D spheroid growth resulted from transfection of miR-143 and miR-145 mimics. Although transfection of miR-143 or miR-145 mimics alone showed significant spheroid growth inhibition, co-transfection of the combined miR-143/145 mimics did not prove additive nor synergic effect in our PCa model, in contrast to previous reports in bladder and breast cancer [149,150]. Inhibition on 2D and 3D growth may be related to proliferation inhibition rather than apoptosis activation as shown by the DNA synthesis inhibition experiments without apoptosis induction. Moreover, miR-143/145 prevented apoptosis probably because most cells were arrested in G1-G0 [80]. In addition, it has been reported that miR-143 can increase cell death without affecting apoptosis rate [79], suggesting that a different cell death pathway could be induced by miR-143/145, such as necrosis or autophagy.

To date, miR-143/145 has been shown to affect processes such proliferation and migration of PCa cells through targets such as ERK5, KRAS, FSCN1 and GLOM1 [79,80,151,152]. Here, the miR-143/145 cluster increased pMLC2 levels at serine 19. This phosphorylation is important for processes such as cell cycle and motility, crucial events for tumor progression. For example, it has been demonstrated that a pMLC2 deficiency in wide range of cancer cells causes cytokinesis failure leading to multinucleation and multipolar mitosis [101]. Furthermore, pMLC2 is increased in PCa cells due to MLC phosphatase (MLCP) inhibition, reducing growth rate and DNA synthesis with an induction of G2/M cell cycle arrest and chemotaxis inhibition [99].

After miR-143/145 overexpression, pMLC2 accumulated at the actin transversal arcs, the main stress fiber responsible of the contractile force [153]. Moreover, pMLC activation in the transversal arcs is critically important for the assembly and integrity of the all actin system [89]. Therefore, it is possible that disruption of the pMLC turnover could affect processes related to the cytoskeleton function, such as cell division and motility. Indeed, MLC activity is regulated in a spatiotemporal fashion by multiple kinases and a single phosphatase. Several molecules of this network (ROCK; MLCK; PAK; MYPT1 and PP1) contain at least a putative target site for miR-143/145 according to a previous search using mirWalk 2.0 database [154]. Although previous reports describe ROCK1 as a miR-145 target in hepatocellular carcinoma, osteosarcoma and breast cancer (Ding et al., 2015; Lei et al., 2014; Zheng, Sun, Li, & Zuo, 2015), no changes in ROCK1 levels were observed in miR-143/145 expressing PCa cells. It is not clear if this difference could be due to the different cellular context. MLCP is overexpressed in PCa [99] and MLCP inhibition blocks turnover of focal adhesion decreasing cell migration [159] and during the cytokinesis. Additionally, MLCP depletion avoids the contractile ring disassembly leading to an increase in multinuclear cells [94]. Further experiments are needed to validate all the targets implicated in the pMLC2 increase.

In summary, the present work reports the growth suppressor role of miR-143/145 tumor suppressor role in a PCa 3D spheroid model. This miRNA cluster decreased spheroid growth affecting cell proliferation without apoptosis induction. Moreover, miR-143/145 overexpression can increase the levels of the cytoskeleton regulator pMLC2, affecting its dynamic state between phosphorylation and dephosphorylation, a crucial modulation for processes such as proliferation.

Cervical cancer

The miR-143/145 cluster is downregulated in a wide range of tumors, including cervical cancer [160]. The results presented here show that miR-143/145 is not constitutively expressed in several cervical cell lines, including tumor lines, reinforcing the hypothesis that this miRNA cluster function as a tumor suppressor. Although miR-143/145 expression is downregulated only in advanced stages of cervical cancer [125,161], no expression was observed in HPV non-tumorigenic immortalized keratinocytes. Other report showed miR-143/145 expression in normal cervical tissue but not in isolated cells from cervical intraepithelial neoplasia biopsies and cervical cancer cell lines [75], suggesting that miR-143/145 expression could be under the regulation of cellular proteins (i.e. p53), that are inhibited by HPV oncogenes [143].

The potential tumor suppressor role of the miR-143/145 cluster has been widely reported [For a review see 17]. Concurrently, the present data confirm miR-143/145 as tumor suppressors in cervical cells, with miR-145 as the main effector. In 3D spheroid cultures, both miR-143 and miR-145 decreased membrane integrity, suggesting that they induce cell death (likely by apoptosis induction), as previous reports showed for monolayer cervical cultures [163,164], with a stronger effect by miR-145 [165]. Moreover, colony growth in soft agar was inhibited only by miR-145, suggesting inhibition of proliferation. Therefore, the miR-143/145 cluster targets different and independent tumor suppressor pathways. Although some authors have reported the inhibition of proliferation by miR-143 in cervical cancer cells, they actually performed metabolic viability assays instead of proliferation assays [163,165]. The null effect in 3D proliferation by miR-143 and the relatively small effect in cell viability could explain the lack of suppressive effect on the 3D spheroid growth contrary to miR-145, which decreased both cell viability and proliferation in soft agar, thereby showing a strong effect on spheroid growth and morphology.

Cell migration was inhibited in monolayer cultures by miR-145 but not by miR-143, as previously observed in cervical cancer cell lines [164,166]. However, invasion in 3D spheroid HeLa cultures was inhibited by both miR-143 and miR-

145, further confirming that the regulatory pathways targeted by miR-143 and miR-145 are different and independent, with miR-145 as a more potent tumor suppressor [166,167]. This is in agreement with bioinformatic analyses showing miR-145, but no miR-143, as a potential prognostic predictor for cervical cancer patients [168].

The miR-143/145 cluster has been studied in several diseases and conditions, such as vascular injury, where these miRNAs modulate cytoskeletal dynamics [82]. The cytoskeletal remodeling and dynamics are crucial for processes related to cancer progression, such as cell division and migration [135,136]. Levels of pMLC, which regulates the cytoskeleton contraction and reorganization [169], were higher in cells transfected with miR-145 compared to negative control (NC) and miR-143 transfections. An increase in pMLC levels and activity are essential to induce membrane blebbing and permeabilization during apoptosis [102,170]. In addition, low pMLC levels are associated with cancer tissues and cells (including cervical cancer) compared to their normal counterparts [171]. Moreover, a deficiency in pMLC has been related to cytokinesis failure in several cancer cell lines, including HeLa [172]. An increase in pMLC can be explained by either an increase in kinase activity or by an inhibition of phosphatase activity. Since miRNAs are usually translational silencers, the effect of miR-145 on myosin phosphatase, the only one known phosphatase for myosin, was tested as its binging subunit (MYPT1) contains a putative miR-145 target site at the 3´-UTR. The validation of MYPT1 as a miR-145 target suggests a direct regulatory association between miR-145 and MYPT1, which results in the downregulation of MYPT1 at the translational level. Therefore, such association will result in the inhibition of cell viability, migration, and invasion as shown with siRNA-directed MYPT1 silencing. Previous reports have shown an increase in MYPT1 levels in several tumor cells compared to non-tumorigenic cells and an inhibition of its activity had tumor suppressive effects such as decrease in proliferation, cell-cycle arrest, chemotherapy sensitivity, reduction of multipolar mitosis and inhibition of migration by regulation of pMLC and actin assembly [99,172,173]. In addition,

other targets of miR-145 could be involved in the up-regulation of pMLC, such as PAK1, a negative regulator of MLCK [174], which has been validated as a miR-145 target with implications on invasion of bladder cancer cells [175].

In conclusion, high levels of pMLC are achieved through miR-145 silencing of MYPT1, a novel target with deep implications in the viability, migration and invasion in cervical tumor cells. Further cytoskeleton rearrangement evaluation (i.e. by immunofluorescence based on cell micropatterning) may be required to fully corroborate the MYPT1 role in cervical cancer.

Expression of mir-143/145 in Keratinocyte Differentiation

miR-143/145 expression was observed in stratified epidermis, contrary to monolayer cultures, suggesting that these miRNAs are expressed in terminal keratinocyte differentiation [118]. The function of miR-143/145 in differentiation has been largely described in several tissues [169,170], mainly through targeting pluripotency factors like KLF4, OCT4 and SOX2 [65], hence being crucial for proliferation-differentiation homeostasis. Disruption of this balance may lead to cancer progression or other diseases. Further experiments like *in situ* hybridization are needed to precisely locate expression of miR-143/145 through the different layers of the epidermis.

Although miR-143/145 expression increased during keratinocyte stratification, this expression would be dispensable because transgenic mice lacking these miRNAs were viable and fertile and did not show developmental macroscopic defects [82,178]. Nevertheless, these mice failed to heal after vascular or intestinal injury [82,141]. With this perspective, HaCaT epidermis transiently expressing miR-145 mimics or inhibitors were UVC-irradiated to create “sunburn” wounds [179] and evaluate the miR-145 expression in a skin-like healing process. In the first hours, damaged keratinocytes produce signaling molecules, mainly proinflammatory cytokines IL-1 and TNF-α, that act in an autocrine and paracrine fashion, resulting in pleiotropic effects on multiple cells [180]. These cytokines increase keratinocyte migration and proliferation and will activate fibroblasts, increasing secretion of both keratinocyte and fibroblast

growth factors. After a confluent layer of keratinocytes covers the wound, the cells will form a multi-layered stratified epithelium triggered and matured by other important signaling molecule: TGF-β [181]. Thus, the increase in miR-145 expression in epidermis after 12 h of irradiation could be associated to autocrine TGF-β activity, a well-known miR-145 inductor in skin scarring [182], thus triggering the differentiation of the migrated and proliferated keratinocytes. This is reinforced by the increase of miR-203 expression, a keratinocyte differentiation marker with high levels of expression in wounds [183].

In addition, TGF-β activates fibroblasts differentiation into myofibroblasts trough miR-145 induction [184], likely in a paracrine fashion by TGF-β, thus explaining the expression peak of miR-145 in keratinocytes and subsequently in fibroblasts. The myofibroblasts activation, characterized by α-smooth muscle actin (α-SMA) expression, is crucial for scarring because they secrete a sophisticated ECM and matrix metalloproteinases facilitating wound closure [185]. Inhibition of miR-145 in fibroblasts results in lack of activation by TGF-β, affecting migration and contraction and probably impairing wound healing [182,184]. Additionally, miR-145 inhibition in fibroblasts leads to mesenchymal-epithelial transition, thus enhancing the reprogramming efficiency to induced pluripotent stem cell [186].

In summary, the function of miR-145 is key for the skin homeostasis likely to regulation of proliferation-differentiation balance by targeting pluripotency factors and growth factors as TGF-β. This function has implications not only in wound healing, but also cancer progression where the differentiation is lost and proliferation is extended and aberrant.

This work gives a new perspectivity about the miR-145 function in tissue homeostasis, relating opposite process: cancer and differentiation. In cancer cells miR-145 is downregulated and when it is restored, miR-145 function as a strong tumor suppressor by regulating MYPT1. Therefore, miR-145 represents a potential biomarker and therapeutic miRNA for cervical and prostate cancer. Unlike cancer, miR-145 is only expressed in stratified keratinocytes and expression increase after wound, suggesting an important role of miR-145

during the keratinocyte differentiation as well as in healing process. This shows the relevance of 3D models in miRNA expression and furthermore, it may have deep implications in skin wound cares and healing scarring.

CONCLUSIONS

- miR-143/145 has tumor suppressive effects in viability, proliferation, migration and invasion in both prostate cancer and cervical cancer.
- miR-145 showed the strongest effect
- miR-143/145 do not induce apoptosis in prostate cancer. However, the results with spheroids cultures of cervical cancer cells suggest that exists an induction of cell death
- miR-145 increased pMLC levels in prostate and cervical cancer cell, producing thicker actin bundles
- MYPT1, a MLCP subunit, is targeted by miR145
- MYPT1 silencing reproduced the miR-145 effects in viability, migration and invasion, thus suggesting that miR-145 act as a tumor suppressor gene through regulation of MYPT1 (MLCP) and the subsequent modulation of pMLC.
- miR-143/145 is not expressed in monolayer differentiated keratinocytes but is in 3D stratified keratinocytes
- miR-145 expression in epidermis is responsive to UVC irradiation and subsequently fibroblasts responds also increasing miR-145

PERSPECTIVES

- Determine the kind of cell death by miR-143/145 in cervical cancer cells
- Analyze the effect of miR-145 in the cytoskeleton remodeling using immunofluorescence based on cell micropatterning
- Perform *in situ* hybridization of skin samples to analyze miR-143/145 expression
- Analyze the role of HPV genes on miR-145 expression and how affect its response to UVC irradiation in skin organotypic cultures of HPV immortalized keratinocytes in normal and UVC conditions
- Determine which are the responsible keratinocyte cytokines and growth factors, especially TGF- β, that increase the expression of miR-145 in fibroblasts
- Validate the fibroblast differentiation monitoring α-SMA expression
- Perform (burn) wound healing assay with 3D cultures or animal models null or enhanced for miR-145 expression

BIBLIOGRAPHY

[1] D.P. Bartel, MicroRNAs: target recognition and regulatory functions, Cell. 136 (2009) 215–233. doi:10.1016/j.cell.2009.01.002.

[2] R.C. Friedman, K.K. Farh, C.B. Burge, D.P. Bartel, Most mammalian mRNAs are conserved targets of microRNAs, Genome Res. 19 (2009) 92–105. doi:10.1101/gr.082701.108.

[3] A. Krek, D. Grun, M.N. Poy, R. Wolf, L. Rosenberg, E.J. Epstein, P. MacMenamin, I. da Piedade, K.C. Gunsalus, M. Stoffel, N. Rajewsky, Combinatorial microRNA target predictions, Nat Genet. 37 (2005) 495–500. doi:10.1038/ng1536.

[4] R.C. Lee, R.L. Feinbaum, V. Ambros, The C. elegans heterochronic gene lin-4 encodes small RNAs with antisense complementarity to lin-14, Cell. 75 (1993) 843–854. http://www.ncbi.nlm.nih.gov/pubmed/8252621.

[5] S. Baskerville, D.P. Bartel, Microarray profiling of microRNAs reveals frequent coexpression with neighboring miRNAs and host genes, RNA. 11 (2005) 241–247. doi:10.1261/rna.7240905.

[6] G.M. Borchert, W. Lanier, B.L. Davidson, RNA polymerase III transcribes human microRNAs, Nat Struct Mol Biol. 13 (2006) 1097–1101. doi:10.1038/nsmb1167.

[7] Y. Lee, M. Kim, J. Han, K.H. Yeom, S. Lee, S.H. Baek, V.N. Kim, MicroRNA genes are transcribed by RNA polymerase II, EMBO J. 23 (2004) 4051–4060. doi:10.1038/sj.emboj.7600385.

[8] Y. Lee, C. Ahn, J. Han, H. Choi, J. Kim, J. Yim, J. Lee, P. Provost, O. Radmark, S. Kim, V.N. Kim, The nuclear RNase III Drosha initiates microRNA processing, Nature. 425 (2003) 415–419. doi:10.1038/nature01957.

[9] J.G. Ruby, C.H. Jan, D.P. Bartel, Intronic microRNA precursors that bypass Drosha processing, Nature. 448 (2007) 83–86. doi:10.1038/nature05983.

[10] S. Nakielny, G. Dreyfuss, Transport of proteins and RNAs in and out of the nucleus, Cell. 99 (1999) 677–690. http://www.ncbi.nlm.nih.gov/pubmed/10619422.

[11] R. Yi, Y. Qin, I.G. Macara, B.R. Cullen, Exportin-5 mediates the nuclear export of pre-microRNAs and short hairpin RNAs, Genes Dev. 17 (2003) 3011–3016. doi:10.1101/gad.1158803.

[12] R.F. Ketting, S.E. Fischer, E. Bernstein, T. Sijen, G.J. Hannon, R.H. Plasterk, Dicer functions in RNA interference and in synthesis of small RNA involved in developmental timing in C. elegans, Genes Dev. 15

(2001) 2654–2659. doi:10.1101/gad.927801.

[13] R.I. Gregory, T.P. Chendrimada, N. Cooch, R. Shiekhattar, Human RISC couples microRNA biogenesis and posttranscriptional gene silencing, Cell. 123 (2005) 631–640. doi:10.1016/j.cell.2005.10.022.

[14] A. Eulalio, E. Huntzinger, E. Izaurralde, Getting to the root of miRNA-mediated gene silencing, Cell. 132 (2008) 9–14. doi:10.1016/j.cell.2007.12.024.

[15] D. V Dugas, B. Bartel, MicroRNA regulation of gene expression in plants, Curr Opin Plant Biol. 7 (2004) 512–520. doi:10.1016/j.pbi.2004.07.011.

[16] B.P. Lewis, I.H. Shih, M.W. Jones-Rhoades, D.P. Bartel, C.B. Burge, Prediction of mammalian microRNA targets, Cell. 115 (2003) 787–798. http://www.ncbi.nlm.nih.gov/pubmed/14697198.

[17] I. Behm-Ansmant, J. Rehwinkel, T. Doerks, A. Stark, P. Bork, E. Izaurralde, mRNA degradation by miRNAs and GW182 requires both CCR4:NOT deadenylase and DCP1:DCP2 decapping complexes, Genes Dev. 20 (2006) 1885–1898. doi:10.1101/gad.1424106.

[18] D.T. Humphreys, B.J. Westman, D.I. Martin, T. Preiss, MicroRNAs control translation initiation by inhibiting eukaryotic initiation factor 4E/cap and poly(A) tail function, Proc Natl Acad Sci U S A. 102 (2005) 16961–16966. doi:10.1073/pnas.0506482102.

[19] S. Nottrott, M.J. Simard, J.D. Richter, Human let-7a miRNA blocks protein production on actively translating polyribosomes, Nat Struct Mol Biol. 13 (2006) 1108–1114. doi:10.1038/nsmb1173.

[20] M.A. Andrei, D. Ingelfinger, R. Heintzmann, T. Achsel, R. Rivera-Pomar, R. Luhrmann, A role for eIF4E and eIF4E-transporter in targeting mRNPs to mammalian processing bodies, RNA. 11 (2005) 717–727. doi:10.1261/rna.2340405.

[21] A. Eulalio, J. Rehwinkel, M. Stricker, E. Huntzinger, S.F. Yang, T. Doerks, S. Dorner, P. Bork, M. Boutros, E. Izaurralde, Target-specific requirements for enhancers of decapping in miRNA-mediated gene silencing, Genes Dev. 21 (2007) 2558–2570. doi:10.1101/gad.443107.

[22] J.A. Vidigal, A. Ventura, The biological functions of miRNAs: Lessons from in vivo studies, Trends Cell Biol. 25 (2015) 137–147. doi:10.1016/j.tcb.2014.11.004.

[23] R.J. Frost, E.N. Olson, Control of glucose homeostasis and insulin sensitivity by the Let-7 family of microRNAs, Proc Natl Acad Sci U S A. 108 (2011) 21075–21080. doi:10.1073/pnas.1118922109.

[24] Y. Lu, J.M. Thomson, H.Y. Wong, S.M. Hammond, B.L. Hogan, Transgenic over-expression of the microRNA miR-17-92 cluster

promotes proliferation and inhibits differentiation of lung epithelial progenitor cells, Dev Biol. 310 (2007) 442–453. doi:10.1016/j.ydbio.2007.08.007.

[25] A.S. Yoo, I. Greenwald, LIN-12/Notch activation leads to microRNA-mediated down-regulation of Vav in C. elegans, Science (80-.). 310 (2005) 1330–1333. doi:10.1126/science.1119481.

[26] G.A. Calin, C.D. Dumitru, M. Shimizu, R. Bichi, S. Zupo, E. Noch, H. Aldler, S. Rattan, M. Keating, K. Rai, L. Rassenti, T. Kipps, M. Negrini, F. Bullrich, C.M. Croce, Frequent deletions and down-regulation of micro- RNA genes miR15 and miR16 at 13q14 in chronic lymphocytic leukemia, Proc Natl Acad Sci U S A. 99 (2002) 15524–15529. doi:10.1073/pnas.242606799.

[27] A. Lujambio, S.W. Lowe, The microcosmos of cancer, Nature. 482 (2012) 347–355. doi:10.1038/nature10888.

[28] J. Lu, G. Getz, E.A. Miska, E. Alvarez-Saavedra, J. Lamb, D. Peck, A. Sweet-Cordero, B.L. Ebert, R.H. Mak, A.A. Ferrando, J.R. Downing, T. Jacks, H.R. Horvitz, T.R. Golub, MicroRNA expression profiles classify human cancers, Nature. 435 (2005) 834–838. doi:10.1038/nature03702.

[29] H. Dvinge, A. Git, S. Graf, M. Salmon-Divon, C. Curtis, A. Sottoriva, Y. Zhao, M. Hirst, J. Armisen, E.A. Miska, S.F. Chin, E. Provenzano, G. Turashvili, A. Green, I. Ellis, S. Aparicio, C. Caldas, The shaping and functional consequences of the microRNA landscape in breast cancer, Nature. 497 (2013) 378–382. doi:10.1038/nature12108.

[30] T.M. Kim, W. Huang, R. Park, P.J. Park, M.D. Johnson, A developmental taxonomy of glioblastoma defined and maintained by MicroRNAs, Cancer Res. 71 (2011) 3387–3399. doi:10.1158/0008-5472.CAN-10-4117.

[31] G.A. Calin, C. Sevignani, C.D. Dumitru, T. Hyslop, E. Noch, S. Yendamuri, M. Shimizu, S. Rattan, F. Bullrich, M. Negrini, C.M. Croce, Human microRNA genes are frequently located at fragile sites and genomic regions involved in cancers, Proc Natl Acad Sci U S A. 101 (2004) 2999–3004. doi:10.1073/pnas.0307323101010307323101 [pii].

[32] Y. Saito, G. Liang, G. Egger, J.M. Friedman, J.C. Chuang, G.A. Coetzee, P.A. Jones, Specific activation of microRNA-127 with downregulation of the proto-oncogene BCL6 by chromatin-modifying drugs in human cancer cells, Cancer Cell. 9 (2006) 435–443. doi:S1535-6108(06)00143-7 [pii]10.1016/j.ccr.2006.04.020.

[33] C. Mayr, M.T. Hemann, D.P. Bartel, Disrupting the pairing between let-7 and Hmga2 enhances oncogenic transformation, Science (80-.). 315 (2007) 1576–1579. doi:10.1126/science.1137999.

[34] A. Veronese, R. Visone, J. Consiglio, M. Acunzo, L. Lupini, T. Kim, M. Ferracin, F. Lovat, E. Miotto, V. Balatti, L. D'Abundo, L. Gramantieri, L. Bolondi, Y. Pekarsky, D. Perrotti, M. Negrini, C.M. Croce, Mutated beta-catenin evades a microRNA-dependent regulatory loop, Proc Natl Acad Sci U S A. 108 (2011) 4840–4845. doi:10.1073/pnas.1101734108.

[35] G. Sun, J. Yan, K. Noltner, J. Feng, H. Li, D.A. Sarkis, S.S. Sommer, J.J. Rossi, SNPs in human miRNA genes affect biogenesis and function, RNA. 15 (2009) 1640–1651. doi:10.1261/rna.1560209.

[36] M.S. Kumar, R.E. Pester, C.Y. Chen, K. Lane, C. Chin, J. Lu, D.G. Kirsch, T.R. Golub, T. Jacks, Dicer1 functions as a haploinsufficient tumor suppressor, Genes Dev. 23 (2009) 2700–2704. doi:10.1101/gad.1848209.

[37] I. Lambertz, D. Nittner, P. Mestdagh, G. Denecker, J. Vandesompele, M.A. Dyer, J.C. Marine, Monoallelic but not biallelic loss of Dicer1 promotes tumorigenesis in vivo, Cell Death Differ. 17 (2010) 633–641. doi:10.1038/cdd.2009.202.

[38] S. Volinia, G.A. Calin, C.G. Liu, S. Ambs, A. Cimmino, F. Petrocca, R. Visone, M. Iorio, C. Roldo, M. Ferracin, R.L. Prueitt, N. Yanaihara, G. Lanza, A. Scarpa, A. Vecchione, M. Negrini, C.C. Harris, C.M. Croce, A microRNA expression signature of human solid tumors defines cancer gene targets, Proc Natl Acad Sci U S A. 103 (2006) 2257–2261. doi:10.1073/pnas.0510565103.

[39] W.H.O. WHO, Cancer, (2015). http://www.who.int/mediacentre/factsheets/fs297/en/.

[40] B.W.; W. Stewart C. P., Worl Cancer Report, 2014.

[41] F.X. Bosch, M.M. Manos, N. Munoz, M. Sherman, A.M. Jansen, J. Peto, M.H. Schiffman, V. Moreno, R. Kurman, K. V Shah, Prevalence of human papillomavirus in cervical cancer: a worldwide perspective. International biological study on cervical cancer (IBSCC) Study Group, J Natl Cancer Inst. 87 (1995) 796–802. http://www.ncbi.nlm.nih.gov/pubmed/7791229.

[42] L. Sherman, N. Alloul, I. Golan, M. Durst, A. Baram, Expression and splicing patterns of human papillomavirus type-16 mRNAs in pre-cancerous lesions and carcinomas of the cervix, in human keratinocytes immortalized by HPV 16, and in cell lines established from cervical cancers, Int J Cancer. 50 (1992) 356–364. http://www.ncbi.nlm.nih.gov/pubmed/1310488.

[43] M. Scheffner, B.A. Werness, J.M. Huibregtse, A.J. Levine, P.M. Howley, The E6 oncoprotein encoded by human papillomavirus types 16 and 18 promotes the degradation of p53, Cell. 63 (1990) 1129–1136. http://www.ncbi.nlm.nih.gov/pubmed/2175676.

[44] B.A. Werness, A.J. Levine, P.M. Howley, Association of human papillomavirus types 16 and 18 E6 proteins with p53, Science (80-.). 248 (1990) 76–79. http://www.ncbi.nlm.nih.gov/pubmed/2157286.

[45] A. Cottage, S. Dowen, I. Roberts, M. Pett, N. Coleman, M. Stanley, Early genetic events in HPV immortalised keratinocytes, Genes Chromosom. Cancer. 30 (2001) 72–79. http://www.ncbi.nlm.nih.gov/pubmed/11107178.

[46] G. Pecoraro, M. Lee, D. Morgan, V. Defendi, Evolution of in vitro transformation and tumorigenesis of HPV16 and HPV18 immortalized primary cervical epithelial cells, Am J Pathol. 138 (1991) 1–8. http://www.ncbi.nlm.nih.gov/pubmed/1846261.

[47] J.A. DiPaolo, C.D. Woodworth, N.C. Popescu, V. Notario, J. Doniger, Induction of human cervical squamous cell carcinoma by sequential transfection with human papillomavirus 16 DNA and viral Harvey ras, Oncogene. 4 (1989) 395–399. http://www.ncbi.nlm.nih.gov/pubmed/2541388.

[48] R. Herrero, A. Hildesheim, C. Bratti, M.E. Sherman, M. Hutchinson, J. Morales, I. Balmaceda, M.D. Greenberg, M. Alfaro, R.D. Burk, S. Wacholder, M. Plummer, M. Schiffman, Population-based study of human papillomavirus infection and cervical neoplasia in rural Costa Rica, J Natl Cancer Inst. 92 (2000) 464–474. http://www.ncbi.nlm.nih.gov/pubmed/10716964.

[49] M.A. Stanley, Human papillomavirus and cervical carcinogenesis, Best Pr. Res Clin Obs. Gynaecol. 15 (2001) 663–676. doi:10.1053/beog.2001.0213.

[50] A. Jemal, R. Siegel, J. Xu, E. Ward, Cancer statistics, 2010, CA Cancer J Clin. 60 (2010) 277–300. doi:10.3322/caac.20073.

[51] R. Siegel, E. Ward, O. Brawley, A. Jemal, Cancer statistics, 2011: the impact of eliminating socioeconomic and racial disparities on premature cancer deaths, CA Cancer J Clin. 61 (2011) 212–236. doi:10.3322/caac.20121.

[52] M.M. Shen, C. Abate-Shen, Molecular genetics of prostate cancer: new prospects for old challenges, Genes Dev. 24 (2010) 1967–2000. doi:10.1101/gad.1965810.

[53] G.J. Kelloff, R. Lieberman, V.E. Steele, C.W. Boone, R.A. Lubet, L. Kopelovich, W.A. Malone, J.A. Crowell, H.R. Higley, C.C. Sigman, Agents, biomarkers, and cohorts for chemopreventive agent development in prostate cancer, Urology. 57 (2001) 46–51. http://www.ncbi.nlm.nih.gov/pubmed/11295594.

[54] E.J. Small, Advances in prostate cancer, Curr Opin Oncol. 11 (1999) 226–235. http://www.ncbi.nlm.nih.gov/pubmed/10328599.

[55] H.I. Scher, G. Heller, Clinical states in prostate cancer: toward a dynamic model of disease progression, Urology. 55 (2000) 323–327. http://www.ncbi.nlm.nih.gov/pubmed/10699601.

[56] A.B. Barqawi, K.J. Krughoff, K. Eid, Current Challenges in Prostate Cancer Management and the Rationale behind Targeted Focal Therapy, Adv Urol. 2012 (2012) 862639. doi:10.1155/2012/862639.

[57] H. Lilja, D. Ulmert, A.J. Vickers, Prostate-specific antigen and prostate cancer: Prediction, detection and monitoring, Nat. Rev. Cancer. (2008). doi:10.1038/nrc2351.

[58] W.J. Catalona, M.A. Hudson, P.T. Scardino, J.P. Richie, F.R. Ahmann, R.C. Flanigan, J.B. deKernion, T.L. Ratliff, L.R. Kavoussi, B.L. Dalkin, et al., Selection of optimal prostate specific antigen cutoffs for early detection of prostate cancer: receiver operating characteristic curves, J Urol. 152 (1994) 2037–2042. http://www.ncbi.nlm.nih.gov/pubmed/7525995.

[59] R.K. Nam, A. Toi, L.H. Klotz, J. Trachtenberg, M.A. Jewett, S. Appu, D.A. Loblaw, L. Sugar, S.A. Narod, M.W. Kattan, Assessing individual risk for prostate cancer, J Clin Oncol. 25 (2007) 3582–3588. doi:10.1200/JCO.2007.10.6450.

[60] I.M. Thompson, D.P. Ankerst, C. Chi, P.J. Goodman, C.M. Tangen, M.S. Lucia, Z. Feng, H.L. Parnes, C.A. Coltman Jr., Assessing prostate cancer risk: results from the Prostate Cancer Prevention Trial, J Natl Cancer Inst. 98 (2006) 529–534. doi:10.1093/jnci/djj131.

[61] I.M. Thompson, D.K. Pauler, P.J. Goodman, C.M. Tangen, M.S. Lucia, H.L. Parnes, L.M. Minasian, L.G. Ford, S.M. Lippman, E.D. Crawford, J.J. Crowley, C.A. Coltman Jr., Prevalence of prostate cancer among men with a prostate-specific antigen level < or =4.0 ng per milliliter, N Engl J Med. 350 (2004) 2239–2246. doi:10.1056/NEJMoa031918.

[62] L. Bubendorf, A. Schopfer, U. Wagner, G. Sauter, H. Moch, N. Willi, T.C. Gasser, M.J. Mihatsch, Metastatic patterns of prostate cancer: an autopsy study of 1,589 patients, Hum Pathol. 31 (2000) 578–583. http://www.ncbi.nlm.nih.gov/pubmed/10836297.

[63] L. Costa, P.P. Major, Effect of bisphosphonates on pain and quality of life in patients with bone metastases, Nat Clin Pr. Oncol. 6 (2009) 163–174. doi:10.1038/ncponc1323.

[64] C. Esau, X. Kang, E. Peralta, E. Hanson, E.G. Marcusson, L. V Ravichandran, Y. Sun, S. Koo, R.J. Perera, R. Jain, N.M. Dean, S.M. Freier, C.F. Bennett, B. Lollo, R. Griffey, MicroRNA-143 regulates adipocyte differentiation, J Biol Chem. 279 (2004) 52361–52365. doi:10.1074/jbc.C400438200.

[65] R.R. Chivukula, J.T. Mendell, Abate and switch: miR-145 in stem cell

differentiation, Cell. 137 (2009) 606–608. doi:10.1016/j.cell.2009.04.059.

[66] K.R. Cordes, N.T. Sheehy, M.P. White, E.C. Berry, S.U. Morton, A.N. Muth, T.H. Lee, J.M. Miano, K.N. Ivey, D. Srivastava, miR-145 and miR-143 regulate smooth muscle cell fate and plasticity, Nature. 460 (2009) 705–710. doi:10.1038/nature08195.

[67] N. Xu, T. Papagiannakopoulos, G. Pan, J.A. Thomson, K.S. Kosik, MicroRNA-145 regulates OCT4, SOX2, and KLF4 and represses pluripotency in human embryonic stem cells, Cell. 137 (2009) 647–658. doi:10.1016/j.cell.2009.02.038.

[68] M.Z. Michael, O.C. SM, N.G. van Holst Pellekaan, G.P. Young, R.J. James, Reduced accumulation of specific microRNAs in colorectal neoplasia, Mol Cancer Res. 1 (2003) 882–891. http://www.ncbi.nlm.nih.gov/pubmed/14573789.

[69] Y. Akao, Y. Nakagawa, T. Naoe, MicroRNAs 143 and 145 are possible common onco-microRNAs in human cancers, Oncol Rep. 16 (2006) 845–850. http://www.ncbi.nlm.nih.gov/pubmed/16969504.

[70] T. Takagi, A. Iio, Y. Nakagawa, T. Naoe, N. Tanigawa, Y. Akao, Decreased expression of microRNA-143 and -145 in human gastric cancers, Oncology. 77 (2009) 12–21. doi:10.1159/000218166.

[71] Y. Akao, Y. Nakagawa, Y. Kitade, T. Kinoshita, T. Naoe, Downregulation of microRNAs-143 and -145 in B-cell malignancies, Cancer Sci. 98 (2007) 1914–1920. doi:10.1111/j.1349-7006.2007.00618.x.

[72] L. Dyrskjot, M.S. Ostenfeld, J.B. Bramsen, A.N. Silahtaroglu, P. Lamy, R. Ramanathan, N. Fristrup, J.L. Jensen, C.L. Andersen, K. Zieger, S. Kauppinen, B.P. Ulhoi, J. Kjems, M. Borre, T.F. Orntoft, Genomic profiling of microRNAs in bladder cancer: miR-129 is associated with poor outcome and promotes cell death in vitro, Cancer Res. 69 (2009) 4851–4860. doi:10.1158/0008-5472.CAN-08-4043.

[73] T. Lin, W. Dong, J. Huang, Q. Pan, X. Fan, C. Zhang, L. Huang, MicroRNA-143 as a tumor suppressor for bladder cancer, J Urol. 181 (2009) 1372–1380. doi:10.1016/j.juro.2008.10.149.

[74] H.C. Chen, G.H. Chen, Y.H. Chen, W.L. Liao, C.Y. Liu, K.P. Chang, Y.S. Chang, S.J. Chen, MicroRNA deregulation and pathway alterations in nasopharyngeal carcinoma, Br J Cancer. 100 (2009) 1002–1011. doi:10.1038/sj.bjc.6604948.

[75] X. Wang, S. Tang, S.Y. Le, R. Lu, J.S. Rader, C. Meyers, Z.M. Zheng, Aberrant expression of oncogenic and tumor-suppressive microRNAs in cervical cancer is required for cancer cell growth, PLoS One. 3 (2008) e2557. doi:10.1371/journal.pone.0002557.

[76] A.W. Tong, P. Fulgham, C. Jay, P. Chen, I. Khalil, S. Liu, N. Senzer, A.C. Eklund, J. Han, J. Nemunaitis, MicroRNA profile analysis of human prostate cancers, Cancer Gene Ther. 16 (2009) 206–216. doi:10.1038/cgt.2008.77.

[77] A. Iio, Y. Nakagawa, I. Hirata, T. Naoe, Y. Akao, Identification of non-coding RNAs embracing microRNA-143/145 cluster., Mol. Cancer. 9 (2010) 136. doi:10.1186/1476-4598-9-136.

[78] V. Gunasekharan, L.A. Laimins, Human papillomaviruses modulate microRNA 145 expression to directly control genome amplification, J Virol. 87 (2013) 6037–6043. doi:10.1128/JVI.00153-13.

[79] C. Clapé, V. Fritz, C. Henriquet, F. Apparailly, P.L. Fernandez, F. Iborra, C. Avancès, M. Villalba, S. Culline, L. Fajas, miR-143 interferes with ERK5 signaling, and abrogates prostate cancer progression in mice, PLoS One. 4 (2009). doi:10.1371/journal.pone.0007542.

[80] B. Xu, X. Niu, X. Zhang, J. Tao, D. Wu, Z. Wang, P. Li, W. Zhang, H. Wu, N. Feng, Z. Wang, L. Hua, X. Wang, MiR-143 decreases prostate cancer cells proliferation and migration and enhances their sensitivity to docetaxel through suppression of KRAS, Mol. Cell. Biochem. 350 (2011) 207–213. doi:10.1007/s11010-010-0700-6.

[81] S. Huang, W. Guo, Y. Tang, D. Ren, X. Zou, X. Peng, miR-143 and miR-145 inhibit stem cell characteristics of PC-3 prostate cancer cells, Oncol. Rep. 28 (2012) 1831–1837. doi:10.3892/or.2012.2015.

[82] M. Xin, E.M. Small, L.B. Sutherland, X. Qi, J. McAnally, C.F. Plato, J.A. Richardson, R. Bassel-Duby, E.N. Olson, MicroRNAs miR-143 and miR-145 modulate cytoskeletal dynamics and responsiveness of smooth muscle cells to injury, Genes Dev. (2009). doi:10.1101/gad.1842409.

[83] M.A. Jordan, L. Wilson, Microtubules as a target for anticancer drugs, Nat. Rev. Cancer. (2004). doi:10.1038/nrc1317.

[84] M.A. Khanfar, D.T.A. Youssef, K.A. El Sayed, Semisynthetic latrunculin derivatives as inhibitors of metastatic breast cancer: Biological evaluations, preliminary structure-activity relationship and molecular modeling studies, ChemMedChem. (2010). doi:10.1002/cmdc.200900430.

[85] L. Blanchoin, R. Boujemaa-Paterski, C. Sykes, J. Plastino, Actin dynamics, architecture, and mechanics in cell motility., Physiol. Rev. (2014). doi:10.1152/physrev.00018.2013.

[86] Y.-W. Heng, C.-G. Koh, Actin cytoskeleton dynamics and the cell division cycle, Int. J. Biochem. Cell Biol. (2010). doi:10.1016/j.biocel.2010.04.007.

[87] A.R. Bresnick, Molecular mechanisms of nonmuscle myosin-II regulation, Curr. Opin. Cell Biol. (1999). doi:10.1016/S0955-0674(99)80004-0.

[88] S. Komatsu, T. Yano, M. Shibata, R.A. Tuft, M. Ikebe, Effects of the regulatory light chain phosphorylation of myosin II on mitosis and cytokinesis of mammalian cells, J. Biol. Chem. (2000). doi:10.1074/jbc.M003019200.

[89] Y.H. Tee, T. Shemesh, V. Thiagarajan, R.F. Hariadi, K.L. Anderson, C. Page, N. Volkmann, D. Hanein, S. Sivaramakrishnan, M.M. Kozlov, A.D. Bershadsky, Cellular chirality arising from the self-organization of the actin cytoskeleton, Nat. Cell Biol. 17 (2015) 445–457. doi:10.1038/ncb3137.

[90] G. Totsukawa, Y. Yamakita, S. Yamashiro, D.J. Hartshorne, Y. Sasaki, F. Matsumura, Distinct roles of ROCK (Rho-kinase) and MLCK in spatial regulation of MLC phosphorylation for assembly of stress fibers and focal adhesions in 3T3 fibroblasts, J. Cell Biol. 150 (2000) 797–806. doi:10.1083/jcb.150.4.797.

[91] A.W. Orr, B.P. Helmke, B.R. Blackman, M.A. Schwartz, Mechanisms of mechanotransduction, Dev. Cell. (2006). doi:10.1016/j.devcel.2005.12.006.

[92] K. Clark, M. Langeslag, C.G. Figdor, F.N. van Leeuwen, Myosin II and mechanotransduction: a balancing act, Trends Cell Biol. (2007). doi:10.1016/j.tcb.2007.02.002.

[93] F. Matsumura, Regulation of myosin II during cytokinesis in higher eukaryotes, Trends Cell Biol. (2005). doi:10.1016/j.tcb.2005.05.004.

[94] F. Matsumura, D.J. Hartshorne, Myosin phosphatase target subunit: Many roles in cell function, Biochem. Biophys. Res. Commun. 369 (2008) 149–156. doi:10.1016/j.bbrc.2007.12.090.

[95] K. Kimura, M. Ito, M. Amano, K. Chihara, Y. Fukata, M. Nakafuku, B. Yamamori, J. Feng, T. Nakano, K. Okawa, A. Iwamatsu, K. Kaibuchi, Regulation of myosin phosphatase by Rho and Rho-associated kinase (Rho- kinase), Science (80-.). (1996). doi:10.1126/science.273.5272.245.

[96] A. Endo, H.K. Surks, S. Mochizuki, N. Mochizuki, M.E. Mendelsohn, Identification and characterization of zipper-interacting protein kinase as the unique vascular smooth muscle myosin phosphatase-associated kinase, J. Biol. Chem. (2004). doi:10.1074/jbc.M403676200.

[97] E. Kiss, A. Murányi, C. Csortos, P. Gergely, M. Ito, D.J. Hartshorne, F. Erdodi, Integrin-linked kinase phosphorylates the myosin phosphatase target subunit at the inhibitory site in platelet cytoskeleton, Biochem. J. (2002). doi:10.1042/BJ20011295.

[98] G. Velasco, C. Armstrong, N. Morrice, S. Frame, P. Cohen, Phosphorylation of the regulatory subunit of smooth muscle protein phosphatase 1M at Thr850 induces its dissociation from myosin, FEBS Lett. (2002). doi:10.1016/S0014-5793(02)03175-7.

[99] S. Grindrod, S. Suy, S. Fallen, M. Eto, J. Toretsky, M.L. Brown, Effects of a fluorescent Myosin light chain phosphatase inhibitor on prostate cancer cells., Front. Oncol. 1 (2011) 27. doi:10.3389/fonc.2011.00027.

[100] K. Sogawa, T. Yamada, S. Oka, K. Kawasaki, S. Mori, H. Tanaka, H. Norimatsu, Y. Cai, H. Kuwabara, H. Shima, M. Nagao, K. Matsumoto, Enhanced expression of catalytic subunit isoform PP1γ1 of protein phosphatase type 1 associated with malignancy of osteogenic tumor, Cancer Lett. (1995). doi:10.1016/0304-3835(95)90150-7.

[101] Q. Wu, R.M. Sahasrabudhe, L.Z. Luo, D.W. Lewis, S.M. Gollin, W.S. Saunders, Deficiency in myosin light-chain phosphorylation causes cytokinesis failure and multipolarity in cancer cells., Oncogene. 29 (2010) 4183–93. doi:10.1038/onc.2010.165.

[102] G.R. Wickman, L. Julian, K. Mardilovich, S. Schumacher, J. Munro, N. Rath, S. Al Zander, A. Mleczak, D. Sumpton, N. Morrice, W. V. Bienvenut, M.F. Olson, Blebs produced by actin-myosin contraction during apoptosis release damage-associated molecular pattern proteins before secondary necrosis occurs, Cell Death Differ. (2013). doi:10.1038/cdd.2013.69.

[103] J.C. Mills, N.L. Stone, J. Erhardt, R.N. Pittman, Apoptotic membrane blebbing is regulated by myosin light chain phosphorylation, J. Cell Biol. (1998). doi:10.1083/jcb.140.3.627.

[104] D.R. Croft, M.L. Coleman, S. Li, D. Robertson, T. Sullivan, C.L. Stewart, M.F. Olson, Actin-myosin-based contraction is responsible for apoptotic nuclear disintegration, J. Cell Biol. (2005). doi:10.1083/jcb.200409049.

[105] K. Mandal, I. Wang, E. Vitiello, L.A.C. Orellana, M. Balland, Cell dipole behaviour revealed by ECM sub-cellular geometry, Nat. Commun. (2014). doi:10.1038/ncomms6749.

[106] M. Thery, Micropatterning as a tool to decipher cell morphogenesis and functions, J. Cell Sci. (2010). doi:10.1242/jcs.075150.

[107] E.R. Shamir, A.J. Ewald, Three-dimensional organotypic culture: Experimental models of mammalian biology and disease, Nat. Rev. Mol. Cell Biol. (2014). doi:10.1038/nrm3873.

[108] L. Hutchinson, R. Kirk, High drug attrition rates - Where are we going wrong?, Nat. Rev. Clin. Oncol. (2011). doi:10.1038/nrclinonc.2011.34.

[109] D. Antoni, H. Burckel, E. Josset, G. Noel, Three-{Dimensional} {Cell} {Culture}: {A} {Breakthrough} in {Vivo}, Int J Mol Sci. (2015).

doi:10.3390/ijms16035517.

[110] Y. Cui, J. Han, Z. Xiao, Y. Qi, Y. Zhao, B. Chen, Y. Fang, S. Liu, X. Wu, J. Dai, Systematic Analysis of mRNA and miRNA Expression of 3D-Cultured Neural Stem Cells (NSCs) in Spaceflight, Front. Cell. Neurosci. (2018). doi:10.3389/fncel.2017.00434.

[111] S.J. Smith, M. Wilson, J.H. Ward, C. V. Rahman, A.C. Peet, D.C. Macarthur, F.R.A.J. Rose, R.G. Grundy, R. Rahman, Recapitulation of Tumor Heterogeneity and Molecular Signatures in a 3D Brain Cancer Model with Decreased Sensitivity to Histone Deacetylase Inhibition, PLoS One. (2012). doi:10.1371/journal.pone.0052335.

[112] Y. Fang, R.M. Eglen, Three-Dimensional Cell Cultures in Drug Discovery and Development, SLAS Discov. (2017). doi:10.1177/1087057117696795.

[113] E. Fennema, N. Rivron, J. Rouwkema, C. van Blitterswijk, J. De Boer, Spheroid culture as a tool for creating 3D complex tissues, Trends Biotechnol. (2013). doi:10.1016/j.tibtech.2012.12.003.

[114] M. Zanoni, F. Piccinini, C. Arienti, A. Zamagni, S. Santi, R. Polico, A. Bevilacqua, A. Tesei, 3D tumor spheroid models for in vitro therapeutic screening: A systematic approach to enhance the biological relevance of data obtained, Sci. Rep. (2016). doi:10.1038/srep19103.

[115] R. Edmondson, J.J. Broglie, A.F. Adcock, L. Yang, Three-Dimensional Cell Culture Systems and Their Applications in Drug Discovery and Cell-Based Biosensors, Assay Drug Dev. Technol. (2014). doi:10.1089/adt.2014.573.

[116] Y. Okugawa, Y. Hirai, A novel three-dimensional cell culture method to analyze epidermal cell differentiation in vitro, Methods Mol. Biol. (2014). doi:10.1007/7651-2013-45.

[117] M. Prunieras, M. Regnier, D. Woodley, Methods for cultivation of keratinocytes with an air-liquid interface, J. Invest. Dermatol. (1983). doi:10.1111/1523-1747.ep12540324.

[118] L.A. Sitailo, A. Jerome-Morais, M.F. Denning, Mcl-1 functions as major epidermal survival protein required for proper keratinocyte differentiation, J. Invest. Dermatol. (2009). doi:10.1038/jid.2008.363.

[119] N. Lebonvallet, C. Jeanmaire, L. Danoux, P. Sibille, G. Pauly, L. Misery, The evolution and use of skin explants: Potential and limitations for dermatological research, Eur. J. Dermatology. (2010). doi:10.1684/ejd.2010.1054.

[120] J.W. Oh, T.C. Hsi, C. Fernando, R. Ramos, M. V. Plikus, Organotypic skin culture, J. Invest. Dermatol. (2013). doi:10.1038/jid.2013.387.

[121] M. Rosdy, L.C. Clauss, Terminal epidermal differentiation of human

keratinocytes grown in chemically defined medium on inert filter substrates at the air-liquid interface, J. Invest. Dermatol. (1990). doi:10.1111/1523-1747.ep12555510.

[122] A. Coquette, N. Berna, A. Vandenbosch, M. Rosdy, Y. Poumay, Differential expression and release of cytokines by an in vitro reconstructed human epidermis following exposure to skin irritant and sensitizing chemicals, Toxicol. Vitr. (1999). doi:10.1016/S0887-2333(99)00076-4.

[123] A. Frankart, J. Malaisse, E. De Vuyst, F. Minner, C.L. de Rouvroit, Y. Poumay, Epidermal morphogenesis during progressive in vitro 3D reconstruction at the air-liquid interface, Exp. Dermatol. (2012). doi:10.1111/exd.12020.

[124] E. De Vuyst, C. Charlier, S. Giltaire, V. De Glas, C.L. De Rouvroit, Y. Poumay, Reconstruction of normal and pathological human epidermis on polycarbonate filter, Methods Mol. Biol. (2014). doi:10.1007/7651-2013-40.

[125] Y. Chen, C. Ma, W. Zhang, Z. Chen, L. Ma, Down regulation of miR-143 is related with tumor size, lymph node metastasis and HPV16 infection in cervical squamous cancer, Diagn. Pathol. (2014). doi:10.1186/1746-1596-9-88.

[126] V. Agarwal, G.W. Bell, J.W. Nam, D.P. Bartel, Predicting effective microRNA target sites in mammalian mRNAs, Elife. (2015). doi:10.7554/eLife.05005.

[127] M.F. Kramer, Stem-loop RT-qPCR for miRNAs, Curr. Protoc. Mol. Biol. (2011). doi:10.1002/0471142727.mb1510s95.

[128] S. TD, L. EJ, J. Jiang, A. Sarkar, L. Yang, E. TS, C. Chen, Real-time PCR quantification of precursors and mature microRNA, ScienceDirect. (2007).

[129] P. Boukamp, R.T. Petrussevska, D. Breitkreutz, J. Hornung, A. Markham, N.E. Fusenig, Normal keratinization in a spontaneously immortalized aneuploid human keratinocyte cell line, J. Cell Biol. (1988). doi:10.1083/jcb.106.3.761.

[130] L.M. Alvarez-Salas, T.E. Arpawong, J. a DiPaolo, Growth inhibition of cervical tumor cells by antisense oligodeoxynucleotides directed to the human papillomavirus type 16 E6 gene., Antisense Nucleic Acid Drug Dev. (1999). doi:10.1089/oli.1.1999.9.441.

[131] C.D. Woodworth, P.E. Bowden, J. Doniger, L. Pirisi, W. Barnes, W.D. Lancaster, J.A. DiPaolo, Characterization of Normal Human Exocervical Epithelial Cells Immortalized in Vitro by Papillomavirus Types 16 and 18 DNA, Cancer Res. (1988).

[132] J. Schindelin, I. Arganda-Carreras, E. Frise, V. Kaynig, M. Longair, T. Pietzsch, S. Preibisch, C. Rueden, S. Saalfeld, B. Schmid, J.Y. Tinevez, D.J. White, V. Hartenstein, K. Eliceiri, P. Tomancak, A. Cardona, Fiji: An open-source platform for biological-image analysis, Nat. Methods. (2012). doi:10.1038/nmeth.2019.

[133] N. Martinez-Acuna, A. Gonzalez-Torres, J.V. Tapia-Vieyra, L.M. Alvarez-Salas, MARK1 is a Novel Target for miR-125a-5p: Implications for Cell Migration in Cervical Tumor Cells., MicroRNA (Shariqah, United Arab Emirates). (2017). doi:10.2174/2211536606666171024160244.

[134] A. Pitaval, A. Christ, A. Curtet, Q. Tseng, M. Théry, Probing ciliogenesis using micropatterned substrates, Methods Enzymol. (2013). doi:10.1016/B978-0-12-397944-5.00006-7.

[135] A.J. Ridley, Rho GTPase signalling in cell migration, Curr. Opin. Cell Biol. (2015). doi:10.1016/j.ceb.2015.08.005.

[136] S. Kümper, F.K. Mardakheh, A. McCarthy, M. Yeo, G.W. Stamp, A. Paul, J. Worboys, A. Sadok, C. Jørgensen, S. Guichard, C.J. Marshall, Rho-associated kinase (ROCK) function is essential for cell cycle progression, senescence and tumorigenesis, Elife. (2016). doi:10.7554/eLife.12203.001.

[137] K. Carver, X. Ming, R.L. Juliano, Multicellular tumor spheroids as a model for assessing delivery of oligonucleotides in three dimensions, Mol. Ther. - Nucleic Acids. (2014). doi:10.1038/mtna.2014.5.

[138] A.F. Deyrieux, V.G. Wilson, In vitro culture conditions to study keratinocyte differentiation using the HaCaT cell line, Cytotechnology. (2007). doi:10.1007/s10616-007-9076-1.

[139] A.M. Lena, R. Shalom-Feuerstein, P.R. di Val Cervo, D. Aberdam, R.A. Knight, G. Melino, E. Candi, miR-203 represses “stemness” by repressing ΔNp63, Cell Death Differ. (2008). doi:10.1038/cdd.2008.69.

[140] A. Iio, Y. Nakagawa, I. Hirata, T. Naoe, Y. Akao, Identification of non-coding RNAs embracing microRNA-143/145 cluster, Mol. Cancer. (2010). doi:10.1186/1476-4598-9-136.

[141] R.R. Chivukula, G. Shi, A. Acharya, E.W. Mills, L.R. Zeitels, J.L. Anandam, A.A. Abdelnaby, G.C. Balch, J.C. Mansour, A.C. Yopp, A. Maitra, J.T. Mendell, An essential mesenchymal function for miR-143/145 in intestinal epithelial regeneration, Cell. (2014). doi:10.1016/j.cell.2014.03.055.

[142] T.A. Lehman, R. Modali, P. Boukamp, J. Stanek, W.P. Bennett, J.A. Welsh, R.A. Metcalf, M.R. Stampfer, N. Fusenig, E.M. Rogan, C.C. Harris, P53 mutations in human immortalized epithelial cell lines, Carcinogenesis. (1993). doi:10.1093/carcin/14.5.833.

[143] M. Sachdeva, S. Zhu, F. Wu, H. Wu, V. Walia, S. Kumar, R. Elble, K. Watabe, Y.-Y. Mo, p53 represses c-Myc through induction of the tumor suppressor miR-145, Proc. Natl. Acad. Sci. (2009). doi:10.1073/pnas.0808042106.

[144] R. Takasawa, H. Nakamura, T. Mori, S. Tanuma, Differential apoptotic pathways in human keratinocyte HaCaT cells exposed to UVB and UVC, Apoptosis. (2005). doi:10.1007/s10495-005-0901-8.

[145] M. Hart, E. Nolte, S. Wach, J. Szczyrba, H. Taubert, T.T. Rau, A. Hartmann, F. a Grässer, B. Wullich, Comparative microRNA profiling of prostate carcinomas with increasing tumor stage by deep sequencing., Mol. Cancer Res. 12 (2014) 250–63. doi:10.1158/1541-7786.MCR-13-0230.

[146] C. Coarfa, W. Fiskus, V.K. Eedunuri, K. Rajapakshe, C. Foley, S.A. Chew, S.S. Shah, C. Geng, J. Shou, J.S. Mohamed, B.W. O'Malley, N. Mitsiades, Comprehensive proteomic profiling identifies the androgen receptor axis and other signaling pathways as targets of microRNAs suppressed in metastatic prostate cancer, Oncogene. (2015) 1–12. doi:10.1038/onc.2015.295.

[147] K.R.M. Leite, A. Tomiyama, S.T. Reis, J.M. Sousa-Canavez, A. Sañudo, L.H. Camara-Lopes, M. Srougi, MicroRNA expression profiles in the progression of prostate cancer-from high-grade prostate intraepithelial neoplasia to metastasis, Urol. Oncol. Semin. Orig. Investig. 31 (2013) 796–801. doi:10.1016/j.urolonc.2011.07.002.

[148] X. Peng, W. Guo, T. Liu, X. Wang, X. Tu, D. Xiong, S. Chen, Y. Lai, H. Du, G. Chen, G. Liu, Y. Tang, S. Huang, X. Zou, Identification of miRs-143 and -145 that is associated with bone metastasis of prostate cancer and involved in the regulation of EMT, PLoS One. 6 (2011). doi:10.1371/journal.pone.0020341.

[149] X. Yan, X. Chen, H. Liang, T. Deng, W. Chen, S. Zhang, M. Liu, X. Gao, Y. Liu, C. Zhao, X. Wang, N. Wang, J. Li, R. Liu, K. Zen, C.-Y. Zhang, B. Liu, Y. Ba, miR-143 and miR-145 synergistically regulate ERBB3 to suppress cell proliferation and invasion in breast cancer., Mol. Cancer. 13 (2014) 220. doi:10.1186/1476-4598-13-220.

[150] S. Noguchi, Y. Yasui, J. Iwasaki, M. Kumazaki, N. Yamada, S. Naito, Y. Akao, Replacement treatment with microRNA-143 and -145 induces synergistic inhibition of the growth of human bladder cancer cells by regulating PI3K/Akt and MAPK signaling pathways, Cancer Lett. 328 (2013) 353–361. doi:10.1016/j.canlet.2012.10.017.

[151] M. Fuse, N. Nohata, S. Kojima, S. Sakamoto, T. Chiyomaru, K. Kawakami, H. Enokida, M. Nakagawa, Y. Naya, T. Ichikawa, N. Seki, Restoration of miR-145 expression suppresses cell proliferation, migration and invasion in prostate cancer by targeting FSCN1., Int. J.

Oncol. 38 (2011) 1093–101. doi:10.3892/ijo.2011.919.

[152] S. Kojima, H. Enokida, H. Yoshino, T. Itesako, T. Chiyomaru, T. Kinoshita, M. Fuse, R. Nishikawa, Y. Goto, Y. Naya, M. Nakagawa, N. Seki, The tumor-suppressive microRNA-143/145 cluster inhibits cell migration and invasion by targeting GOLM1 in prostate cancer., J. Hum. Genet. (2013) 1–10. doi:10.1038/jhg.2013.121.

[153] D.T. Burnette, L. Shao, C. Ott, A.M. Pasapera, R.S. Fischer, M.A. Baird, C. Der Loughian, H. Delanoe-Ayari, M.J. Paszek, M.W. Davidson, E. Betzig, J. Lippincott-Schwartz, A contractile and counterbalancing adhesion system controls the 3D shape of crawling cells, J. Cell Biol. 205 (2014) 83–96. doi:10.1083/jcb.201311104.

[154] H. Dweep, N. Gretz, C. Sticht, MiRWalk database for miRNA-target interactions, Methods Mol. Biol. 1182 (2014) 289–305. doi:10.1007/978-1-4939-1062-5_25.

[155] X. Wan, Q. Cheng, R. Peng, Z. Ma, Z. Chen, Y. Cao, B. Jiang, ROCK1, a novel target of miR-145, promotes glioma cell invasion, Mol. Med. Rep. 9 (2014) 1877–1882. doi:10.3892/mmr.2014.1982.

[156] P. Lei, J. Xie, L. Wang, X. Yang, Z. Dai, Y. Hu, microRNA-145 inhibits osteosarcoma cell proliferation and invasion by targeting ROCK1, Mol. Med. Rep. 10 (2014) 155–160. doi:10.3892/mmr.2014.2195.

[157] W. Ding, H. Tan, C. Zhao, X. Li, Z. Li, C. Jiang, Y. Zhang, L. Wang, MiR-145 suppresses cell proliferation and motility by inhibiting ROCK1 in hepatocellular carcinoma, Tumor Biol. (2015) 1–6. doi:10.1007/s13277-015-4462-3.

[158] M. Zheng, X. Sun, Y. Li, W. Zuo, MicroRNA-145 inhibits growth and migration of breast cancer cells through targeting oncoprotein ROCK1., Tumour Biol. (2015). doi:10.1007/s13277-015-4722-2.

[159] G. Totsukawa, Y. Wu, Y. Sasaki, D.J. Hartshorne, Y. Yamakita, S. Yamashiro, F. Matsumura, Distinct roles of MLCK and ROCK in the regulation of membrane protrusions and focal adhesion dynamics during cell migration of fibroblasts, J. Cell Biol. 164 (2004) 427–439. doi:10.1083/jcb.200306172.

[160] M.-Y. Li, X.-X. Hu, Meta-analysis of microRNA expression profiling studies in human cervical cancer., Med. Oncol. (2015). doi:10.1007/s12032-015-0510-5.

[161] Q. Wang, J. Qin, A. Chen, J. Zhou, J. Liu, J. Cheng, J. Qiu, J. Zhang, Downregulation of microRNA-145 is associated with aggressive progression and poor prognosis in human cervical cancer, Tumor Biol. (2015). doi:10.1007/s13277-014-3009-3.

[162] A. V. Das, R.M. Pillai, Implications of miR cluster 143/145 as universal

anti-oncomiRs and their dysregulation during tumorigenesis, Cancer Cell Int. (2015). doi:10.1186/s12935-015-0247-4.

[163] F. Zheng, J. Zhang, S. Luo, J. Yi, P. Wang, Q. Zheng, Y. Wen, miR-143 is associated with proliferation and apoptosis involving ERK5 in heLa cells, Oncol. Lett. (2016). doi:10.3892/ol.2016.5016.

[164] S. Yan, X. Li, Q. Jin, J. Yuan, MicroRNA-145 sensitizes cervical cancer cells to low-dose irradiation by downregulating OCT4 expression, Exp. Ther. Med. (2016). doi:10.3892/etm.2016.3731.

[165] L. Anton, A. DeVine, L.J. Sierra, A.G. Brown, M.A. Elovitz, MIR-143 and miR-145 disrupt the cervical epithelial barrier through dysregulation of cell adhesion, apoptosis and proliferation, Sci. Rep. (2017). doi:10.1038/s41598-017-03217-7.

[166] A. Sathyanarayanan, K.S. Chandrasekaran, D. Karunagaran, microRNA-145 modulates epithelial-mesenchymal transition and suppresses proliferation, migration and invasion by targeting SIP1 in human cervical cancer cells, Cell. Oncol. (2017). doi:10.1007/s13402-016-0307-3.

[167] P. Dong, Y. Xiong, S.J.B. Hanley, J. Yue, H. Watari, Musashi-2, a novel oncoprotein promoting cervical cancer cell growth and invasion, is negatively regulated by p53-induced miR-143 and miR-107 activation, J. Exp. Clin. Cancer Res. (2017). doi:10.1186/s13046-017-0617-y.

[168] B. Liang, Y. Li, T. Wang, A three miRNAs signature predicts survival in cervical cancer using bioinformatics analysis, Sci. Rep. (2017). doi:10.1038/s41598-017-06032-2.

[169] M. Eto, J.A. Kirkbride, D.L. Brautigan, Assembly of MYPT1 with protein phosphatase-1 in fibroblasts redirects localization and reorganizes the actin cytoskeleton, Cell Motil. Cytoskeleton. (2005). doi:10.1002/cm.20088.

[170] M.L. Coleman, E.A. Sahai, M. Yeo, M. Bosch, A. Dewar, M.F. Olson, Membrane blebbing during apoptosis results from caspase-mediated activation of ROCK I, Nat. Cell Biol. (2001). doi:10.1038/35070009.

[171] H.J. Yu, L.A. Serebryannyy, M. Fry, M. Greene, O. Chernaya, W.Y. Hu, T.L. Chew, N. Mahmud, S.S. Kadkol, S. Glover, G. Prins, Z. Strakova, P. De Lanerolle, Tumor stiffness is unrelated to myosin light chain phosphorylation in cancer cells, PLoS One. (2013). doi:10.1371/journal.pone.0079776.

[172] Q. Wu, R.M. Sahasrabudhe, L.Z. Luo, D.W. Lewis, S.M. Gollin, W.S. Saunders, Deficiency in myosin light-chain phosphorylation causes cytokinesis failure and multipolarity in cancer cells, Oncogene. (2010). doi:10.1038/onc.2010.165.

[173] D. Xia, J.T. Stull, K.E. Kamm, Myosin phosphatase targeting subunit 1 affects cell migration by regulating myosin phosphorylation and actin assembly, Exp. Cell Res. (2005). doi:10.1016/j.yexcr.2004.11.025.

[174] L.C. Sanders, Inhibition of Myosin Light Chain Kinase by p21-Activated Kinase, Science (80-.). (1999). doi:10.1126/science.283.5410.2083.

[175] B. Kou, Y. Gao, C. Du, Q. Shi, S. Xu, C.Q. Wang, X. Wang, D. He, P. Guo, MiR-145 inhibits invasion of bladder cancer cells by targeting PAK1, Urol. Oncol. Semin. Orig. Investig. (2014). doi:10.1016/j.urolonc.2014.01.003.

[176] L. Elia, M. Quintavalle, J. Zhang, R. Contu, L. Cossu, M.V.G. Latronico, K.L. Peterson, C. Indolfi, D. Catalucci, J. Chen, S.A. Courtneidge, G. Condorelli, The knockout of miR-143 and -145 alters smooth muscle cell maintenance and vascular homeostasis in mice: Correlates with human disease, Cell Death Differ. (2009). doi:10.1038/cdd.2009.153.

[177] H. Liu, H. Lin, L. Zhang, Q. Sun, G. Yuan, L. Zhang, S. Chen, Z. Chen, MiR-145 and miR-143 regulate odontoblast differentiation through targeting Klf4 and Osx genes in a feedback loop, J. Biol. Chem. (2013). doi:10.1074/jbc.M112.433730.

[178] T. Boettger, N. Beetz, S. Kostin, J. Schneider, M. Krüger, L. Hein, T. Braun, Acquisition of the contractile phenotype by murine arterial smooth muscle cells depends on the Mir143/145 gene cluster, J. Clin. Invest. (2009). doi:10.1172/JCI38864.

[179] A. Forsyth, C.W. Ide, H. Mosiley, Acute sunburn due to accidental irradiation with UVC, Contact Dermatitis. (1991). doi:10.1111/j.1600-0536.1991.tb01674.x.

[180] I. Pastar, O. Stojadinovic, N.C. Yin, H. Ramirez, A.G. Nusbaum, A. Sawaya, S.B. Patel, L. Khalid, R.R. Isseroff, M. Tomic-Canic, Epithelialization in Wound Healing: A Comprehensive Review, Adv. Wound Care. (2014). doi:10.1089/wound.2013.0473.

[181] C.K. Jiang, M. Tomic-Canic, D.J. Lucas, M. Simon, M. Blumenberg, TGFβ promotes the basal phenotype of epidermal keratinocytes: Transcriptional induction of k#5 and k#14 keratin genes, Growth Factors. (1995). doi:10.3109/08977199509028955.

[182] C. Gras, D. Ratuszny, C. Hadamitzky, H. Zhang, R. Blasczyk, C. Figueiredo, miR-145 Contributes to Hypertrophic Scarring of the Skin by Inducing Myofibroblast Activity., Mol. Med. (2015). doi:10.2119/molmed.2014.00172.

[183] I. Pastar, A.A. Khan, O. Stojadinovic, E.A. Lebrun, M.C. Medina, H. Brem, R.S. Kirsner, J.J. Jimenez, C. Leslie, M. Tomic-Canic, Induction of specific microRNAs inhibits cutaneous wound healing, J Biol Chem. (2012). doi:10.1074/jbc.M112.382135.

[184] Y.S. Wang, S.H. Li, J. Guo, A. Mihic, J. Wu, L. Sun, K. Davis, R.D. Weisel, R.K. Li, Role of miR-145 in cardiac myofibroblast differentiation, J. Mol. Cell. Cardiol. (2014). doi:10.1016/j.yjmcc.2013.08.007.

[185] I.A. Darby, B. Laverdet, F. Bonté, A. Desmoulière, Fibroblasts and myofibroblasts in wound healing, Clin. Cosmet. Investig. Dermatol. (2014). doi:10.2147/CCID.S50046.

[186] T. Barta, L. Peskova, J. Collin, D. Montaner, I. Neganova, L. Armstrong, M. Lako, Brief Report: Inhibition of miR-145 Enhances Reprogramming of Human Dermal Fibroblasts to Induced Pluripotent Stem Cells, Stem Cells. (2016). doi:10.1002/stem.2220.

ANNEXE I

Biochemical and Biophysical Research Communications 507 (2018) 348–354

Contents lists available at ScienceDirect

Biochemical and Biophysical Research Communications

journal homepage: www.elsevier.com/locate/ybbrc

MYPT1 is targeted by miR-145 inhibiting viability, migration and invasion in 2D and 3D HeLa cultures

Alejandro González-Torres [a], Evelyn Gabriela Bañuelos-Villegas [a], Natalia Martínez-Acuña [a], Eric Sulpice [b], Xavier Gidrol [b], Luis Marat Alvarez-Salas [a, *]

[a] Laboratorio de Terapia Génica, Departamento de Genética y Biología Molecular, Centro de Investigación y de Estudios Avanzados del I.P.N., Av. I.P.N. 2508, Ciudad de México, 07360, Mexico

[b] University of Grenoble Alpes, CEA, INSERM, BIG-BGE U1038, 38000, Grenoble, France

ARTICLE INFO

Article history:
Received 25 October 2018
Accepted 6 November 2018
Available online 14 November 2018

Keywords:
Cervical cancer
Myosin phosphatase
miRNA
miR-145
MYPT1

ABSTRACT

The miR-143/145 cluster is down-regulated in cervical tumor cells suggesting a role in tumorigenesis including cytoskeleton remodeling, a key event for tumor progression. The aim of the present work was to determine the role of miR-143/145 in the modulation of the myosin regulator phospho-myosin light chain (pMLC). HeLa monolayer and tridimensional cultures were transfected with miR-143 or miR-145 mimics inhibiting cell viability, proliferation, migration and invasion, mainly through miR-145. MiR-145 transfection increased pMLC levels by targeting the MYPT1 subunit of the regulatory myosin phosphatase. MYPT1 knockdown by siRNAs reproduced miR-145 effects suggesting miR-145 as a tumor suppressor through MYPT1 targeting, leading to a subsequent increase of pMLC levels with implications for cervical cell viability, migration and invasion.

1. Introduction

MicroRNAs (miRNAs) are small non-coding RNAs which post-transcriptionally regulate the expression of mRNAs containing complementary sequences [1]. Disruption of miRNA function has been widely reported in cancer, including cervical cancer [2]. Furthermore, high-risk human papillomavirus (HPV), a major risk factor for cervical cancer [3], can modulate expression of host miRNAs to control the viral life cycle [4].

The miR-143/145 cluster is a bicistronic transcript located at chromosome 5q33.1 [5]. Both miR-143 and miR-145 have been reported as the main down-regulated miRNAs in cervical cancer tumors [6]. In addition, these miRNAs are important for remodeling the actomyosin cytoskeleton [7], which comprises globular actin and the molecular motor myosin that is actively reorganized during several processes such as cell division, apoptosis and cell motility [8]. Phosphorylation of the myosin light chain (pMLC) at Ser19 regulates both myosin motor activity and filament assembly [9]. The mechanical forces driven by myosin activity play a key role in the regulation of cell proliferation, apoptosis, adhesion and migration [10]. Phosphorylation of MLC is dynamically coordinated by two groups of enzymes: one consists of several protein kinases (including MLCK and ROCK) and the other represented by the myosin phosphatase (MP) [11]. MP contains three subunits: the type 1 protein phosphatase catalytic subunit (PP1), the myosin phosphatase target subunit (MYPT1) and a small subunit of unknown function [12]. MP is upregulated in prostate, breast and bone tumors [13,14]. Moreover, pMLC levels are low in cancer cell lines compared to no-tumorigenic cells due to an overexpression of MP resulting in cytokinesis failures [15].

In the present work, actomyosin regulation by miR-143/145 was investigated in HeLa cells, focusing on the pMLC levels.

2. Materials and methods

2.1. Plasmids and oligonucleotides

All oligodeoxynucleotides were purchased from T4 oligo® (Irapuato, Mexico). The sequences for hsa-miR-143-3p primers were based on previous reports [16]. All RT-qPCR primer sequences were listed in Table 1.

The miR-145 wild-type target sequence in *ppp1r12a* (MYPT1) transcript (5′-CTCGAGGACCATAATTGGCAGTCACTGGAAGCGGCCGC-3′) was predicted using the TargetScan.org software [17] and a triple

* Corresponding author.
E-mail address: lalvarez@cinvestav.mx (L.M. Alvarez-Salas).

https://doi.org/10.1016/j.bbrc.2018.11.039
0006-291X/

Table 1
Primers used for miR-143, miR-145, PPP1R12A and U6 RT-qPCR.

Primer	Sequence
miR-143-3p RT	5′GTCGTATCCAGTGCGTGTCGTGGAGTCGGCAATTGCACTGGATACGACTGAGCTA3′
miR-143-3p Forward	5′AGTGCGTGTCGTGGAGT3′
miR-143-3p Reverse	5′GCCTGAGATGAAGCACTGT3′
miR-145-5p RT	5′GTCGTATCCAGTGCAGGGTCCGAGGTATTCGCACTGGATACGACAGGGAT3′
miR-145-5p Forward	5′ACACGCAGTCCAGTTTTCCCAG3′
miR-145-5p Reverse	5′GTGCAGGGTCCGAGG3′
snRNA U6 RT	5′AAAATATGGAACGCTTCACGAATTTG3′
snRNA U6 Forward	5′CTCGCTTCGGCAGCACATATACT3′
snRNA U6 Reverse	5′ACGCTTCACGAATTTGCGTGTC3′
PPP1R12A Forward	5′GAGAGGGGATGAAGATGGCG3′
PPP1R12A Reverse	5′TTCACCTTGGTCTTCTGGCG3′

mutant at the seed sequence was designed as a control (5′-CTCGAGGACCATAATTGGCAGTCACGTCAAGCGGCCGC-3′). Both sequences were cloned into the dual-reporter psiCHECK2 vector (Promega, Madison, WI).

The synthetic miR-143-3p/145-5p mimics and the scrambled miRNA negative control (NC) were purchased from Ambion® (Thermo Fisher Scientific Inc., Waltham, MA). MYPT1 and Allstars-Negative Control siRNAs were purchased from Santa Cruz Biotechnology (Dallas, TX) and QIAGEN (Venio, The Netherlands), respectively.

2.2. RT-qPCR assays

The relative quantification of miRNAs was made by two-step RT-qPCR. Briefly, small RNA (<200 nucleotides) was purified from monolayer cultures using the Quick-RNA™ miniprep kit (Zymo Research, Irvine, CA). Retro-transcription was made using Invitrogen™ SuperScript III (Thermo Fisher Scientific) and the quantification was performed with MAXIMA SYBR Green Master Mix (Thermo Fisher Scientific) in a Rotor Gene-3000 (Corbett Research, Australia). RNA from foreskins was used as positive control for miR-143/145. The U6 snRNA (RNU6-1) was used as reference control. Relative gene quantification was estimated by the $^{\Delta\Delta}$CT [18]. The end-point PCR products were analyzed by native PAGE 8%.

2.3. Cell culture

The cervical cancer cell lines HeLa (ATCC® CCL-2™), SiHa (ATCC® HTB-35™), CaSki (ATCC® CRL-1550™) and C-33A (ATCC® HTB-31™) were grown in GIBCO™ DMEM medium (Thermo Fischer Scientific) supplemented with 5% GIBCO™ fetal bovine serum (FBS) (Thermo Fisher Scientific), 1% streptomycin/penicillin (GE Healthcare, Piscataway NJ) and 10 μg/mL Gentamicin (Thermo Fisher Scientific). The spontaneously immortalized keratinocytes HaCaT [19], HPV16-immortalized keratinocytes HKc16E6/E7-II [20] and Cx16.2 [21] were cultured in GIBCO™ keratinocyte serum-free medium (Thermo Fisher Scientific), as described. All the cultures were routinely checked for mycoplasma contamination and maintained in a humidified atmosphere at 5% CO_2 and 37 °C.

RNAi transfection was performed using Invitrogen™ Lipofectamine RNAiMAX reagent (Thermo Fisher Scientific) following the manufacturer instructions, using miRNA mimics or siRNAs at 60 nM final concentration.

2.4. 3D spheroid culture

Three hundred transfected cells per well were seeded in 96-well Corning® U-bottom ultra-low attachment plates (Corning Inc., Corning, NY) and incubated for 7 days. Spheroids were photographed with a Zeiss Axiovert 25 inverted Microscope (Carl Zeiss GA, Oberkochen, Germany) at 10X magnification. Spheroid size was calculated with the FIJI software (Image J) [22]. Cell viability was determined three days after transfection by adding 100 mM SYTOX Green (Thermo Fisher Scientific) and 1 μg/mL Hoechst 33342 (Merck KGaA, Darmstadt Germany) and further 24 h incubation. Live cells fluorescence was calculated as a subtraction of SYTOX Green (impermeable) from Hoechst (permeable) fluorescence staining intensities using a Zeiss Axiovert 25 inverted microscope (Carl Zeiss) with epifluorescence at 10X magnification and FIJI software.

2.5. Soft agar colony formation assays

Transfected cells (1.25×10^3) were embedded in 0.35% agarose on a 0.5% agar base. The cultures were maintained for 12 days with media change every three days. Five colonies per assay were randomly photographed with an inverted microscope (Carl Zeiss) and the size (area) was determined using FIJI software.

2.6. Migration assays

Migration assays were performed essentially as described [23]. Briefly, 1.5×10^4 transfected cells were seeded into the upper chamber of Corning® non-coated polycarbonate Transwell™ inserts (0.8 μm pore) (Corning) and starved 16 h in basal media before addition of supplemented media with 10% FBS to the lower chambers. After 48 h, non-migrating cells were removed from the upper chamber using cotton swabs. Cells were fixed with cold methanol (−20 °C) and stained with 2% crystal violet for 30 min before densitometric analysis with ImageStudio™ Software (Li-Cor Biosciences, Lincoln, NE).

2.7. Invasion assays

Spheroid cultures were transfected and grown for four days as described above, before addition of 100 μL of Matrigel Matrix (Corning) and allowed to solidify by 30 min at 37 °C and later overlaid with DMEM medium. The Matrigel embedded spheroids were maintained for 48 h and the invasion rate was estimated by measuring the area between the spheroid edge and the leading edge of invasive cells using an inverted microscope (Zeiss) and FIJI software.

2.8. Immunoblotting

Protein extracts from HeLa cells transfected with 200 nM miRNA mimics were prepared in RIPA buffer (50 mM Tris-HCl, pH 7.4, 150 mM NaCl, 0.1% SDS, 0.5% Sodium deoxycholate, 1% NP-40, 1 mM AEBSF) supplemented with cOmplete™ protease cocktail inhibitor (Roche, Basel, Switzerland), 1 mM PMSF, 2 mM Na_3VO_4,

and 20 mM β-glycerophosphate. A total of 30 μg of protein were resolved on SDS-polyacrylamide 4–8% gels and transferred onto PVDF membranes (Merck-Millipore, Billerica, MA). Membranes were blocked with 5% BSA or 10% non-fat dry milk for 1 h and incubated with primary antibody against phospho-Myosin Light Chain 2 (Ser19) (#3671, Cell Signaling Technology, Danvers, MA) and MYPT1 (SC-514261, Santa Cruz Biotechnology) overnight at 4 °C. Membranes were incubated with anti-rabbit horseradish peroxidase-conjugated secondary antibodies (Santa Cruz Biotechnology) and Luminata™ HRP substrates (Merck-Millipore) before quantification using a C-Digit Scanner (Li-COR Biosciences). A β-Actin antibody (SC-1616, Santa Cruz Biotechnology) was used as loading control.

2.9. Luciferase reporter assay

Cells (2.7×10^4) were co-transfected with 20 nM miRNA mimics and 20 ng dual-luciferase reporter using Invitrogen™ Lipofectamine™ RNAiMAX reagent (Thermo Fisher Scientific). After 48 h, *Renilla* and Firefly luciferase activities were determined with the Dual-Luciferase Reporter Assay System (Promega) following the manufacturer's instructions, in a Glomax® Multi JR Luminometer (Promega). Luciferase activity was calculated as *Renilla* luciferase (hRluc) activity divided by firefly luciferase (hluc+) activity.

2.10. Statistical analysis

Statistical analyses were performed with the GraphPad Prism 5 software (GraphPad Software, San Diego, CA). A *t*-test was used for comparison of two groups and one-way ANOVA with Tukey post-hoc tests when comparing three or more experimental groups. Statistical significance was considered at $p < 0.05$ (indicated with *). Results were expressed as a bar graph of the mean with standard deviation of at least three different experiments or as a boxplot with whiskers and maximum range (1.5 interquartile) from at least three technical replicates from three different experiments.

3. Results and discusion

3.1. The miR-143/145 cluster is not expressed in cervical cancer cell lines and immortalized keratinocytes

As a first approach to further elucidate the role of the miR-143/145 cluster in cervical cancer, miR-143 and miR-145 expression was analyzed by end-point RT-PCR in monolayer cultures of the cervical cancer cell lines HeLa (HPV18+), CaSki (HPV16+), SiHa (HPV16+) and C-33A (HPV−) and the non-tumorigenic immortal keratinocytes HaCaT (HPV−), CX16.2 (HPV16+) and HKc16E6/E7-II (HPV16+); normal foreskin RNA served as positive control for miR-143/145 expression. The RNU6-1 was used as internal control. No expression of either miR-143 or miR-145 was detected in any of the cell lines tested although both miRNAs were expressed in the positive control, suggesting that the miR-143/145 cluster is not constitutively expressed in the cell lines used in this study (Fig. 1A), reinforcing the hypothesis that this miRNA cluster functions as a tumor suppressor. Although miR-143/145 expression has been reported as downregulated in advanced cervical tumors [16], no expression was observed in HPV non-tumorigenic immortalized keratinocytes similar to isolated cells from cervical precancerous biopsies [24]. This suggests that miR-143/145 expression may be regulated by other cellular factors (i.e. p53), that are inhibited by HPV oncogenes [25].

3.2. Ectopic miR-143/145 expression decreases viability in spheroid cultures, impairs colony formation and inhibits cell migration and invasion

Expression of miR-143/145 was restored in HeLa cells by transfection with miRNA mimics to test their function in 3D spheroids [26], a cell culture technique that provides a more physiological model to mimic *in vivo* tumor conditions. A scrambled miRNA mimic was used as negative control (NC). Both miRNA mimics showed efficient transfection although miR-143 was detected with 5-fold higher intensity than miR-145 (Supplementary 1A). Transfection with miR-145 mimic severely affected spheroid size (35% smaller than NC) and morphology suggested cell death. In contrast, transfection with the miR-143 mimic produced no statistically significant effect (Fig. 1B, Supplementary 1B).

To evaluate cell death, viability assays based on membrane integrity were performed with SYTOX Green/Hoechst 33342 on HeLa spheroid cultures transfected with miRNA mimics. Both miR-143 and miR-145 produced a significant decrease in viability (30 and 60% less than NC, respectively) further suggesting that the miR-143/145 cluster expression may induce cell death with miR-145 producing the strongest effect (Fig. 1C, Supplementary 1C). The observed cell death may be likely to apoptosis induction, as previous reports showed for monolayer cervical cultures [27,28].

In addition to cell death, inhibition of proliferation can also affect 3D growth. Soft agar colony formation assays were performed to further explore the ability of miR143/145-transfected single cells to proliferate and form anchorage-independent colonies relative to the NC. Only HeLa cells transfected with the miR-145 mimic showed a significant reduction of 60% in colony size compared with the NC. No morphological difference was noticed in these assays as the mechanical restraint produced by soft agar restricts colony shape. Transfection of the miR-143 mimic did not produce a statistically significant effect on colony size (Fig. 1D, Supplementary 1D). The null effect in 3D proliferation by miR-143 and the relatively small effect in cell viability could explain the lack of suppressive effect on the 3D spheroid growth contrary to miR-145, which decreased both cell viability and proliferation in soft agar, thereby showing a strong effect on spheroid growth and morphology. These results suggest that although both miR-143 and miR-145 affect cell viability on 3D cultures, they follow different regulatory pathways with miR-145 producing a stronger inhibition.

The effect of miR-143 and miR-145 on cell migration was analyzed by transwell migration assays. Hela cells transfected with the miR-145 mimic exhibited a significant inhibition of 35% on cell migration relative to the NC, while transfection with the miR-143 mimic showed no significant effect (Fig. 1E, Supplementary 1E). Invasion assays using HeLa spheroids transfected with either miR-143 or miR-145 mimics presented a significant decrease (>50%) on invasion area compared to the NC, suggesting that the miR-143/145 cluster may play a role in the control of cell migration and invasion (Fig. 1F, Supplementary 1F). The differential effects by miR-143/145 in cell migration and invasion, confirm that the regulatory pathways targeted by miR-143 and miR-145 are different and independent, with miR-145 as a more potent tumor suppressor [29,30]. This is in agreement with bioinformatic analyses showing miR-145, but no miR-143, as a potential prognostic predictor for cervical cancer patients [31].

3.3. miR-145 increases pMLC levels by direct target of MYPT1

It has been reported that miR-143/145 can regulate cytoskeleton dynamics during muscle injury [7]. Since the actomyosin cytoskeleton activity is crucial for cell division and migration [32] and thus to tumor progression and invasion, the observed inhibitory

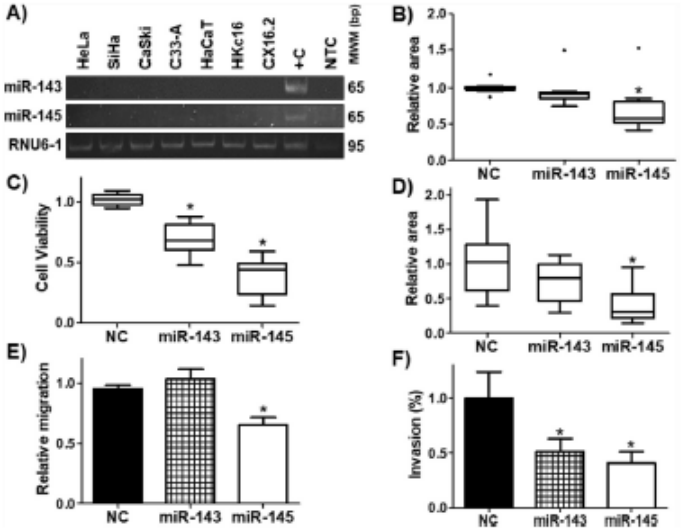

Fig. 1. Effects of restoration of miR-143/145 in 3D growth, viability, colony formation, migration and invasion in HeLa cells. The endogenous levels of miR-143/145 were determined by end-point RT-PCR using RNA from cervical cancer cell lines and immortalized keratinocytes. Foreskin RNA was used as positive control (+C) and small nuclear U6 RNA (RNU6-1) was used as reference gene. NTC, non-template control; bp, base pairs; MWM, molecular weight marker (A). HeLa spheroids transfected with a negative control (NC), miR-143 or miR-145 mimics were analyzed for spheroid size (B), cell viability (C), soft agar colony formation (D), cell migration (E) and invasion (F). The graphs represent the quartiles distribution or the mean and standard deviation of three independent experiments (* – $p < 0.05$).

effects of miR-143/145 on cell viability, migration and invasion were analyzed through the phosphorylation of Myosin Light Chain (pMLC), a key post-translational modification for actomyosin contractile activity and cytoskeletal reorganization [33]. The levels of pMLC on Ser19 were determined by immunoblotting from HeLa cells transfected with either miR-143 or miR-145 mimics. Transfection of miR-145 produced a significant 2-fold increase of pMLC levels compared to the NC. On the contrary, no significant difference was observed between miR-143 transfected cells and the NC (Fig. 2A). An increase in pMLC levels and activity are indispensable to induce membrane blebbing and permeabilization during apoptosis [34,35]. In addition, low pMLC levels are associated with cancer tissues and cells (including cervical cancer) compared to their normal counterparts [36]. Moreover, a deficiency in pMLC has been related to cytokinesis failure in several cancer cell lines, including HeLa [15]. The increased pMLC response to miR-145 would be explained due to the silencing of a negative regulator (i.e. a phosphatase or a kinase inhibitor).

To elucidate the role of miR-145 on pMLC up-regulation, a TargetScan search for miR-145 target sequences (http://www.targetscan.org/vert_71/) was performed to select transcripts involved in MLC phosphorylation. The MYPT1 transcript, a subunit of the phosphatase involved in the negative regulation of MLC, contains a potential miR-145 target site within the 3'-UTR. Dual-luciferase reporters containing the wild-type or an inactive miR-145 mutant target site in MYPT1 were co-transfected in HeLa monolayer cultures with NC or miR-145 mimics (Fig. 2B). Co-transfection with miR-145 produced a significant inhibition of 30% in luciferase activity in the reporter containing the wild-type target sequence compared with the NC, suggesting a direct regulation of MYPT1 by miR-145 (Fig. 2C). This inhibition was completely abolished by mutation of the miR-145 target sequence (Fig. 2C), confirming the seed sequence specificity of this inhibition. Moreover, transfection of the miR-145 mimic downregulated MYPT1 protein levels relative to the NC (Fig. 3B), although it did not affect the MYPT1 mRNA content (Fig. 3A), suggesting that miR-145 may mediate MYPT1 translational repression but not RNA degradation.

3.4. MYPT1 knockdown increases pMLC levels and reduces viability, cell migration and invasion

Further support for the miR-145 suppressive effects through MYPT1 downregulation was obtained by reproducing MYPT1 silencing by siRNAs. HeLa cells transfected with a MYPT1-specific siRNA (siMYPT1) significantly decreased 80% MYPT1 protein levels relative to cells transfected with a scrambled siRNA negative control (siControl) (Fig. 3C). Moreover, as with miR-145, cells transfected with siMYPT increased 2.4-fold pMLC levels relative to siControl, thus confirming the regulatory pathway miR-145-MYPT-pMLC (Fig. 3D). Evaluation of the cell response to MYPT1 silencing by siRNAs produced similar results to those observed for miR-145. Transfection of siMYPT (but not siControl) significantly decreased spheroid viability (Fig. 4A, Supplementary 2A) and inhibited cell migration (Fig. 4B, supplementary 2B) and invasion (Fig. 4C, Supplementary 2C). Therefore, downregulation of MYPT1 by miR-145 increased pMLC levels negatively affect cell viability/migration/invasion, suggesting a regulatory role on pMLC levels of miR-145 by directly targeting of MYPT1. Previous reports have shown an increase in MYPT1 levels in several tumor cells compared to non-tumorigenic cells and inhibition of its activity had tumor suppressor effects such as decrease in proliferation, cell-cycle arrest, chemotherapy sensitivity, reduction of multipolar mitosis and inhibition of migration by regulating pMLC and actin assembly

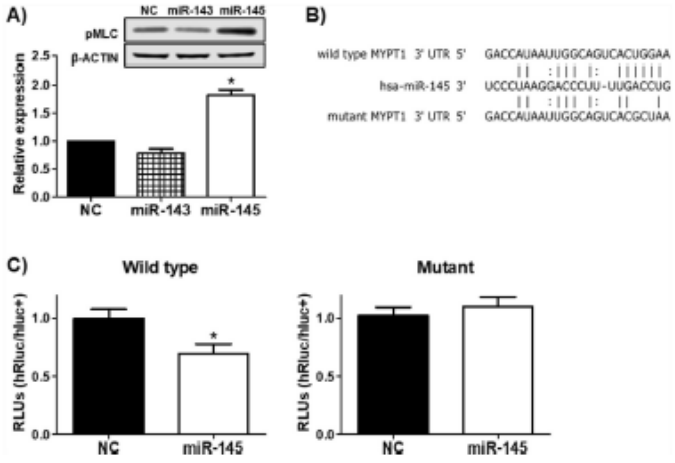

Fig. 2. Myosin phosphatase target subunit 1 (MYPT1) is targeted by miR-145. A) Densitometric analysis of pMLC immunoblots of Hela cells transfected with NC, miR-143 or miR-145 mimics. A representative immunoblot for pMLC is shown (inset). B) Sequence alignment of the miR-145 target sequence in MYPT1 (wild type MYPT1 3'-UTR), miR-145 (hsa-miR-145) and a mutant target site (mutant MYPT1 3'-UTR). Vertical lines indicate perfect WC matches and dotted lines indicate atypical base pairing. C) Hela cells were co-transfected with NC or miR-145 mimics and a dual-Luciferase expression vector containing either the wild type or mutant miR-145 sites in MYPT1. RLUs, Relative Lights Units. The graphs show the mean and standard deviation of three independent experiments (* – $p < 0.05$).

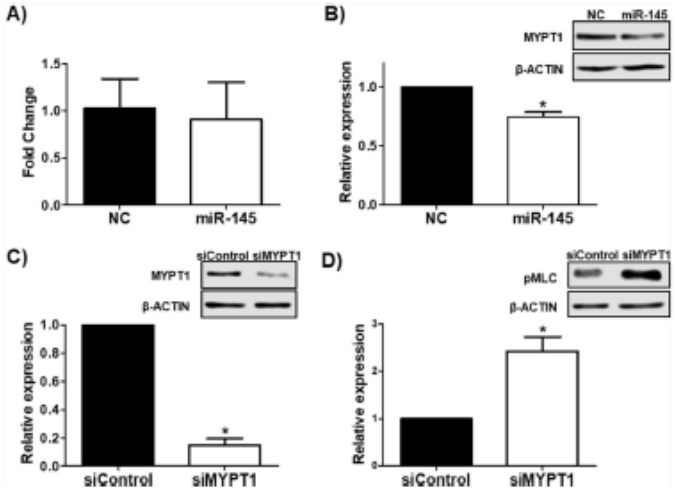

Fig. 3. MYPT1 silencing increases pMLC expression. Transfection of miR-145 decreases MYPT1 protein levels but not mRNA levels. MYPT1 expression levels in HeLa cells transfected with the NC or miR-145 mimic, were determined by RT-qPCR for mRNA (A) and immunoblotting for protein (B). Silencing of MYPT1 increases pMLC expression. Hela cells were transfected with either a siRNA scrambled negative control (siControl) or a MYPT1-specific siRNA (siMYPT1). The levels of MYPT1 (C) or pMLC (B) were determined by immunoblotting. The insets show representative immunoblots for each protein, respectively. The graphs denote the mean and standard deviation of three independent experiments (* – $p < 0.05$).

[15,37,38]. In addition, other targets of miR-145 could be involved in the up-regulation of pMLC, such as PAK1, a negative regulator of MLCK [39], which has been validated as a miR-145 target with implications on invasion of bladder cancer cells [40].

In conclusion, high levels of pMLC are achieved through miR-145 silencing of MYPT1, a novel target with deep implications in the viability, migration and invasion capacities of cervical tumor cells. Further cytoskeleton rearrangement evaluation (i.e. by immunofluorescence based on cell micropatterning) may be required to fully corroborate the MYPT1 role in cervical cancer.

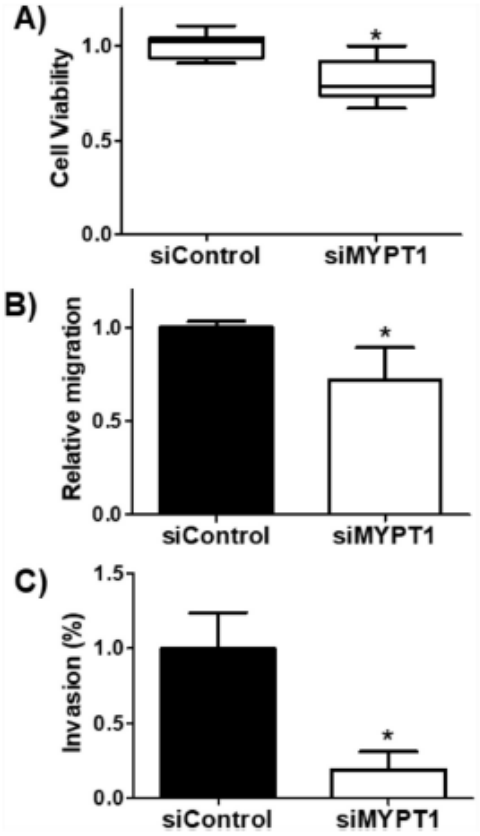

Fig. 4. The siRNA-mediated silencing of MYPT1 reproduces miR-145 effects. HeLa spheroids were transfected with siControl or siMYPT1 siRNAs and analyzed for viability (A), cell migration (B) and invasion (C). The graphs represent the quartiles distribution or the mean and standard deviation of three independent experiments (* – $p < 0.05$).

Conflict of interest

The authors declare that all the work is original and that there is not conflict of interest.

Acknowledgments

We thank Stephanie Combe and J. Virginia Tapia-Vieyra for technical support and José Arellano-Galindo M.D. for the isolated neonatal foreskin RNA. This research did not receive any specific grant from funding science in the public, commercial, or not-for-profit sectors.

Appendix A. Supplementary data

Supplementary data to this article can be found online at https://doi.org/10.1016/j.bbrc.2018.11.039.

References

[1] A.E. Pasquinelli, MicroRNAs and their targets: recognition, regulation and an emerging reciprocal relationship, Nat. Rev. Genet. (2012), https://doi.org/10.1038/nrg3162.
[2] Y. Peng, C.M. Croce, The role of MicroRNAs in human cancer, Signal Transduct. Target. Ther. (2016), https://doi.org/10.1038/sigtrans.2015.4.
[3] F.X. Bosch, M.M. Manos, N. Muñoz, M. Sherman, A.M. Jansen, J. Peto, M.H. Schiffman, V. Moreno, R. Kurman, K.V. Shah, Prevalence of human papillomavirus in cervical cancer: a worldwide perspective. International biological study on cervical cancer (IBSCC) Study Group, J. Natl. Cancer Inst. (Bethesda) 87 (1995) 796–802. http://www.ncbi.nlm.nih.gov/pubmed/7791229.
[4] V. Gunasekharan, L.A. Laimins, Human papillomaviruses modulate microRNA 145 expression to directly control genome amplification, J. Virol. 87 (2013) 6037–6043, https://doi.org/10.1128/JVI.00153-13.
[5] A. Iio, Y. Nakagawa, I. Hirata, T. Naoe, Y. Akao, Identification of non-coding RNAs embracing microRNA-143/145 cluster, Mol. Canc. (2010), https://doi.org/10.1186/1476-4598-9-136.
[6] M.-Y. Li, X.-X. Hu, Meta-analysis of microRNA expression profiling studies in human cervical cancer, Med. Oncol. (2015), https://doi.org/10.1007/s12032-015-0510-5.
[7] M. Xin, E.M. Small, L.B. Sutherland, X. Qi, J. McAnally, C.F. Plato, J.A. Richardson, R. Bassel-Duby, E.N. Olson, MicroRNAs miR-143 and miR-145 modulate cytoskeletal dynamics and responsiveness of smooth muscle cells to injury, Genes Dev. (2009), https://doi.org/10.1101/gad.1842409.
[8] L. Blanchoin, R. Boujemaa-Paterski, C. Sykes, J. Plastino, Actin dynamics, architecture, and mechanics in cell motility, Physiol. Rev. (2014), https://doi.org/10.1152/physrev.00018.2013.
[9] Y.H. Tee, T. Shemesh, V. Thiagarajan, R.F. Hariadi, K.L. Anderson, C. Page, N. Volkmann, D. Hanein, S. Sivaramakrishnan, M.M. Kozlov, A.D. Bershadsky, Cellular chirality arising from the self-organization of the actin cytoskeleton, Nat. Cell Biol. 17 (2015) 445–457, https://doi.org/10.1038/ncb3137.
[10] K. Clark, M. Langeslag, C.G. Figdor, F.N. van Leeuwen, Myosin II and mechanotransduction: a balancing act, Trends Cell Biol. (2007), https://doi.org/10.1016/j.tcb.2007.02.002.
[11] F. Matsumura, Regulation of myosin II during cytokinesis in higher eukaryotes, Trends Cell Biol. (2005), https://doi.org/10.1016/j.tcb.2005.05.004.
[12] F. Matsumura, D.J. Hartshorne, Myosin phosphatase target subunit: many roles in cell function, Biochem. Biophys. Res. Commun. 369 (2008) 149–156, https://doi.org/10.1016/j.bbrc.2007.12.090.
[13] S. Grindrod, S. Suy, S. Fallen, M. Eto, J. Toretsky, M.L. Brown, Effects of a fluorescent Myosin light chain phosphatase inhibitor on prostate cancer cells, Front. Oncol. (2011), https://doi.org/10.3389/fonc.2011.00027.
[14] K. Sogawa, T. Yamada, S. Oka, K. Kawasaki, S. Mori, H. Tanaka, H. Norimatsu, Y. Cai, H. Kuwabara, H. Shima, M. Nagao, K. Matsumoto, Enhanced expression of catalytic subunit isoform PP1γ1 of protein phosphatase type 1 associated with malignancy of osteogenic tumor, Cancer Lett. (1995), https://doi.org/10.1016/0304-3835(95)80150-7.
[15] Q. Wu, R.M. Sahasrabudhe, L.Z. Luo, D.W. Lewis, S.M. Gollin, W.S. Saunders, Deficiency in myosin light-chain phosphorylation causes cytokinesis failure and multipolarity in cancer cells, Oncogene (2010), https://doi.org/10.1038/onc.2010.165.
[16] Y. Chen, C. Ma, W. Zhang, Z. Chen, L. Ma, Down regulation of miR-143 is related with tumor size, lymph node metastasis and HPV16 infection in cervical squamous cancer, Diagn. Pathol. (2014), https://doi.org/10.1186/1746-1596-9-88.
[17] V. Agarwal, G.W. Bell, J.W. Nam, D.P. Bartel, Predicting effective microRNA target sites in mammalian mRNAs, Elife (2015), https://doi.org/10.7554/eLife.05005.
[18] S. TD, L. EJ, J. Jiang, A. Sarkar, L. Yang, E. TS, C. Chen, Real-time PCR Quantification of Precursors and Mature MicroRNA, ScienceDirect, 2007.
[19] P. Boukamp, R.T. Petrussevska, D. Breitkreutz, J. Hornung, A. Markham, N.E. Fusenig, Normal keratinization in a spontaneously immortalized aneuploid human keratinocyte cell line, J. Cell Biol. (1988), https://doi.org/10.1083/jcb.106.3.761.
[20] L.M. Alvarez-Salas, T.E. Arpawong, J.A. DiPaolo, Growth inhibition of cervical tumor cells by antisense oligodeoxynucleotides directed to the human papillomavirus type 16 E6 gene, Antisense Nucleic Acid Drug Dev. (1999), https://doi.org/10.1089/oli.1.1999.9.441.
[21] C.D. Woodworth, P.E. Bowden, J. Doniger, L. Pirisi, W. Barnes, W.D. Lancaster, J.A. DiPaolo, Characterization of normal human exocervical epithelial cells immortalized in vitro by papillomavirus types 16 and 18 DNA, Cancer Res. 48 (1988) 4620–4628.
[22] J. Schindelin, I. Arganda-Carreras, E. Frise, V. Kaynig, M. Longair, T. Pietzsch, S. Preibisch, C. Rueden, S. Saalfeld, B. Schmid, J.Y. Tinevez, D.J. White, V. Hartenstein, K. Eliceiri, P. Tomancak, A. Cardona, Fiji: an open-source platform for biological-image analysis, Nat. Methods (2012), https://doi.org/10.1038/nmeth.2019.
[23] N. Martinez-Acuna, A. Gonzalez-Torres, J.V. Tapia-Vieyra, L.M. Alvarez-Salas, MARK1 is a novel target for mir-125a-5p: implications for cell migration in cervical tumor cells, MicroRNA (2017), https://doi.org/10.2174/2211536606666171024160244.
[24] X. Wang, S. Tang, S.Y. Le, R. Lu, J.S. Rader, C. Meyers, Z.M. Zheng, Aberrant

ANNEXE II

Send Orders for Reprints to reprints@benthamscience.ae

MicroRNA, 2018, 7, 54-61

RESEARCH ARTICLE

MARK1 is a Novel Target for miR-125a-5p: Implications for Cell Migration in Cervical Tumor Cells

Martínez-Acuña Natalia, González-Torres Alejandro, Tapia-Vieyra Juana Virginia and Luis Marat Alvarez-Salas*

Laboratorio de Terapia Génica, Departamento de Genética y Biología Molecular, Centro de Investigación y de Estudios Avanzados del I.P.N., Ciudad de México, México

ARTICLE HISTORY

Received: May 12, 2017
Revised: September 15, 2017
Accepted: October 04, 2017

DOI:
10.2174/2211536606666171024160244

Abstract: ***Background***: Aberrant miRNA expression is associated with the development of several diseases including cervical cancer. Dysregulation of miR-125a-5p is present in a plethora of tumors, but its role in cervical cancer is not well understood.

Objective: The aim was to analyze the expression profile of miR-125a-5p in tumor and immortal cell lines with further target prediction, validation and function analysis.

Methods: MiR-125a-5p expression was determined by real-time RT-PCR from nine cervical cell lines. *In silico* tools were used to find target transcripts with an miR-125-5p complementary site within the 3´UTR region. Further target selection was based on gene ontology annotation and ΔG analysis. Target validation was performed by transfection of synthetic miR-125a-5p mimics and luciferase assays. Functional evaluation of miR-125a-5p on migration was performed by transwell migration assays.

Results: Differential miR-125a-5p expression was observed between immortal and tumor cells regardless of the human papillomavirus (HPV) content. Thermodynamic and ontological analyses showed Microtubule-Affinity-Regulating Kinase1 (MARK1) as a putative target for miR-125a-5p. An inverse correlation was observed among miR-125a-5p expression and MARK1 protein levels in tumor but not in immortal cells. Luciferase assays showed direct miR-125a-5p regulation over MARK1 through recognition of a predicted target site within the 3'-UTR. HeLa and C-33A cervical tumor cells enhanced migration after transfection with miR-125a-5p mimics and stimulation of cell migration was reproduced by siRNA-mediated inhibition of MARK1.

Conclusion: The results showed MARK1 as a novel functional target for miR-125a-5p with implications on cell migration of tumor cervical cancer cells.

Keywords: Cell migration, cervical cancer, MARK1, microRNAs, miR-125a-5p, tumor.

1. INTRODUCTION

MicroRNAs (miRNAs) are small non-coding RNAs that regulate gene expression at the post-transcriptional level and are critical to many fundamental biological processes [1, 2]. MiRNA dysregulation plays a significant role in the onset and progression of several tumor types [3, 4]. Moreover, miRNA expression patterns appear spatially and temporally controlled and may reveal particular conditions present in normal and tumor cells, allowing the use of miRNAs as specific cancer biomarkers and therapeutical targets [5, 6].

Cervical cancer has been associated with high-risk human papillomavirus (HPV) infection [7]. Nevertheless, over 90% HPV infections are spontaneously cleared in immunocompetent subjects, and only a fraction of infected women develop cervical cancer. Thus, additional factors are likely to contribute to cervical malignant progression [8]. Genomic data from cervical tumors and cell lines indicate that aberrant miRNA function may be involved in malignant transformation of HPV-infected cells [9].

MiR-125a-5p belongs to a highly conserved miRNA family which is dysregulated in a variety of carcinomas and other diseases [10]. MiR-125a-5p is located at chromosome 19q13 and transcribed as a polycistronic transcript [11]. Biological processes associated with miR-125a-5p function include cell metabolism [12], hematopoiesis [11], vasoconstriction [13] and virus-host interaction [14]. In cancer, miR-

*Address correspondence to this author at the Laboratorio de Terapia Génica, Departamento de Genética y Biología Molecular, Centro de Investigación y de Estudios Avanzados del I.P.N., Av. I.P.N. 2508, Ciudad de México 07360, México; Tel/Fax: +52-55-5747-3800;
E-mail: lalvarez@cinvestav.mx.

2211-5374/18 $58.00+.00

125a-5p has been reported as both oncogene and tumor suppressor depending on the cellular context. Ectopic miR-125a-5p expression can inhibit proliferation and metastasis of hepatocellular carcinoma, and significantly hinders the malignant phenotype by repressing MMP11 and VEGF-A [15]. Also, miR-125a-5p targets E2F3 constraining proliferation, migration and invasion in gastric cancer cells [16] and regulates angiogenesis through VEGF-A targeting [17]. In contrast, miR-125a-5p enhances the invasive potential of urothelial carcinomas [18], appears upregulated in basal cell skin carcinoma [19], promotes proliferative and anti-apoptotic phenotype in malignant B cells [20] and enhances cell migration and invasion in non-small cell lung tumors [21].

In cervical cancer, no significant difference in miR-125a-5p expression was observed between early stage invasive squamous cell carcinoma (ISCC) and normal cervical tissue [22]. However, miR-125a-5p expression appeared downregulated in cervical tumors compared against paired non-tumor samples [23]. Recently, miR-125a-5p downregulation in cervical cancer patients has been proposed as a part of a non-responder miRNA profile [24]. No significant association with HPV infection was established in any of these reports.

In the present report, the miR-125a-5p function in cervical cells was evaluated in a panel of immortal and tumor cell lines. MiR-125a-5p expression levels were determined by RT-qPCR, showing high expression only in tumor cells. No association with HPV infection was observed, suggesting that alterations in miR-125a-5p expression are independent of viral gene expression. Bioinformatics analysis allowed the selection of potential miR-125a-5p targets involved in cellular processes such as apoptosis, cell death, cell proliferation and cell migration. Steady-state miR-125a-5p expression showed an inverse correlation to the target MARK1 protein (Microtubule-affinity-regulating kinase1) in cervical tumor cell lines. MARK1 participates in the establishment of cell polarity, intracellular signal transduction, microtubule cytoskeleton organization, and migration process [25, 26]. Furthermore, MARK1 was validated as an miR-125a-5p target through a predicted binding site located within the 3'-UTR mediating traduccional repression instead RNA degradation. Transfection with an miR-125a-5p mimic, promoted migration in tumor lines and siRNA-induced silencing of MARK1 reproduced the effect. Therefore, miR-125a-5p is proposed as a regulator of MARK1 expression in cervical tumor cells suggesting a potential role of this miRNA in cervical cancer progression.

2. MATERIALS AND METHODS

2.1. Plasmids and Oligonucleotides

All oligodeoxynucleotides were purchased from T4 oligo™ (ADN Sintético S.A.P.I. de C.V., Mexico). The pMIR-Luc-MARK1wt and pMIR-Luc-MARK1mt constructs contain wild-type (5'-CTAGTCCAAATTTACAGGTTCAG GGA-3') or mutant (5'-CTAGTCCAAATTTACAGGTaC tGcGA-3') [27] miR-125a-5p binding sites within the MARK1 3'-UTR cloned into the Ambion® pMIR-REPORT™ luciferase reporter vector, respectively (Life Technologies™ Corp., Grand Island NY). The synthetic pre-miR-125a-5p mimic and the scrambled miRNA control were purchased from Life Technologies.

2.2. Cell Culture

Tumor cell lines HeLa (ATCC® CCL-2™), SiHa (ATCC® HTB-35™), QGU [28], CaSki (ATCC® CRL-1550™) and C-33A (ATCC® HTB-31™) were cultured in GIBCO® DMEM medium (Life Technologies) supplemented with 5% fetal bovine serum (FBS) (PAA Laboratories GmbH, Germany). The HPV16-immortalized cell lines HKc16E6/E7-II [29], Cx16.2 [30] and the tumor-derived CXT.1 cell line [31] were cultured in GIBCO® keratinocyte serum-free medium (K-SFM) (Life Technologies). The immortal HaCaT keratinocytes [32] were grown in GIBCO® DMEM/F12 1:1 medium (Life Technologies) supplemented with 5% FBS (PAA Laboratories). All cell lines were maintained in 100 IU/mL penicillin and 100 µg/mL streptomycin (PAA Laboratories) in 5% CO_2 at 37°C.

2.3. RT-qPCR Analysis

Relative levels of miR-125a-5p were determined by RT-qPCR, as described [33]. Briefly, small RNA (<200 nt) was isolated from subconfluent (80-90%) cultures and stored at -70°C. Steady-state miRNA levels were quantified by the stem-loop RT-qPCR method [34] using Ambion® miR-125a-5p RT primer set (Life Technologies) in a Rotor Gene™ 3000 (Corbett Research Pty Ltd., Australia). The 5S rRNA was used as endogenous reference. Relative gene quantification was calculated by the ΔCT method in arbitrary units relative to 100 [35]. For MARK1 analysis we used the primer set 5'-ACTTAATGGGGTTCGCTTCAA-3' and 5'-TCTACATGGGGAGATTCACAGG-3'. β-actin was used as reference gene and was amplified using the primer set 5'-TCATTCCAAATATGAGATGCGTTGT-3' and 5'-TGCA TTACATAATTTACACGAAAGC-3'.

2.4. Immunoblotting

Total protein extracts from 80% confluent cultures were resolved in denaturing SDS-polyacrylamide gels and electrotransferred onto PVDF membranes (Merck Millipore, Billerica MA). For MAP2 analysis, protein extracts were prepared from transfected cells using 1% SDS lysis followed by sonication (3 pulses of 20 seconds and 80% amplitude) in a GEX 130 PB ultrasonic processor (Cole-Parmer Instrument Co., Vernon Hills, IL). Blotted membranes were blocked and incubated with primary antibodies against MARK1 (sc-130815), MAP2 (sc-20172) or the internal control β-actin (sc-1616) and a horseradish peroxidase (HRP)-conjugated secondary antibody (Santa Cruz Biotechnology™ Inc., Santa Cruz CA). Protein expression was assessed using Luminata™ kits (Merck Millipore) and analyzed in a C-Digit™ scanner (LI-COR Biotechnology, Lincoln NE).

2.5. Knockdown of Endogenous MARK1

Cultured cells ($2x10^5$) were transfected with increasing doses of synthetic pre-miRNAs or siRNAs against MARK1 mRNA using Lipofectamine® 2000 (Life Technologies), as described [33].

2.6. Luciferase Reporter Assay

Cells ($1x10^5$) were co-transfected with 200 ng luciferase reporter, 50ng pGST-GFP (as transfection efficiency control) and 10 nM synthetic pre-miRNAs, using Lipofectamine® RNAiMAX (Life Technologies). After 24 hrs, cells were lysed using the Bright-Glo™ luciferase assay system (Promega Corp., Madison WI) following the manufacturer's instructions. Light intensities were quantified with a Glo-max® Multi JR luminometer (Promega).

2.7. Cell Migration Assays

Migration assays were performed essentially as described [33]. Briefly, $2x10^5$ transfected cells were seeded into the upper chambers of non-coated polycarbonate Transwell® inserts (8.0 µm pore) (Corning Inc., Corning NY) and starved 16 hrs in basal DMEM before addition of DMEM supplemented with 5% FBS to the lower chambers and incubated for further 48 hrs. Non-migrating cells were removed from the upper chamber using cotton swabs. Cells were fixed with cold methanol (-20°C) and stained with 2% crystal violet solution for 15 min. Membranes were removed from the chambers and analyzed by densitometry.

2.8. miRNA Target Prediction and Statistical Analysis

Target sites for miR-125a-5p were predicted using microRNA.org (http://www.microrna.org), TargetScan (http://www.targetscan.org) and miRWalk (http://www.umm.uni-heidelberg.de/apps/zmf/mirwalk) routines. For functional annotation, we used GOEAST application (http://omicslab.genetics.ac.cn/GOEAST). The estimation of ΔG was performed using the RNAfold routine from the Vienna RNA Package (http://www.tbi.univie.ac.at/RNA/RNAfold.html) taking 70 nucleotides (nt) upstream and downstream from the predicted target site. Statistical significance was assessed using the Student's t test with a significance at least of $P<0.05$ indicated with *.

3. RESULTS

3.1. Expression of miR-125a-5p is Associated with the Tumor Phenotype in Cervical Cell Lines

To determine the miR-125a-5p expression profile in cervical cells, RT-qPCR analyses were performed using small RNA fractions from nine cervical cell lines. The HPV16-immortalized cell lines (HKc16E6/E7-II, Cx16.2 and CXT.1), and the HPV-free cell lines HaCaT and C-33A, showed the lowest levels of miR-125a-5p expression. On the other hand, the HPV-positive HeLa, QGU, CaSki and SiHa tumor cells showed significantly higher miR-125a-5p levels (Fig. **1A**). No correlation between miR-125a-5p and HPV content was observed under the experimental setting. Overall, miR-125a-5p showed low expression levels in the HPV-positive immortal cell line set (HKc16E6/E7-II, Cx16.2 and CXT.1) and miR-125a-5p expression was generally higher and disperse in the HPV-positive tumor cell set (HeLa, CaSki, QGU and SiHa) (Fig. **1B**).

3.2. MARK1 is a Direct Target of miR-125a-5p

To investigate the mechanisms associated with the miR-125a-5p function in cervical cells, three bioinformatics programs (miRanda, TargetScan and miRWalk) were used to identify 2395 potential target mRNAs. Gene ontology annotation was used to narrow the data list to 385 target genes involved in cellular processes relevant to the malignant phenotype such as apoptosis, cell death, cell proliferation, cell cycle, migration, and invasion. Target accessibility to miR-125a-5p was evaluated through predicted binding site location within the 3'UTR and the thermodynamic properties (ΔG (Kcal/mol)) of neighboring sequences [36]. ΔG values of validated targets were taken as a reference for final target selection (Table **1**). MARK1 was selected as possible target regulated by miR-125a-5p in cervical cells because the lack of reports on its role in cervical cancer and the biological relevance based on known functions [26].

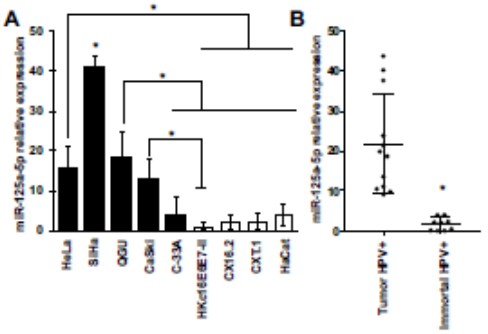

Fig. (1). Expression profile of miR-125a-5p in several cervical cancer cell lines. **A**) The small RNA fractions (<200 nt) from tumor (black bars) and immortal (white bars) cervical cell lines were analyzed by RT-qPCR for miR-125a-5p content and normalized against 5S RNA. **B**) Relative expression of miR-125a-5p in HPV-positive cell lines. MiR-125a-5p expression levels from each cell line were normalized against 5S RNA and grouped by tumor or immortal phenotype. The plots show the mean and standard deviation from three independent experiments.

For target validation, the expression profile of MARK1 was evaluated by immunoblotting (Fig. **2A**) and correlated with the miR-125a-5p levels found in each cell line through Pearson correlation analysis grouped by immortal or tumor phenotype. A significant inverse correlation value was found in tumor cervical cell lines between miR-125a-5p expression and MARK1 ($r=-0.9217$, $P=0.0260$) (Fig. **2B**, left panel).

No significant correlation was found between the levels of miR-125a-5p and MARK1 expression on immortal cells (Fig. **2B**, right panel). As MARK1 represented a new potential target for miR-125a-5p, we focused on the functional interaction between MARK1 and miR-125a-5p. The validated miR-125a-5p targets VEGF and Bcl-2 were also analyzed showing a similar inverse correlation only in tumor cells (Supplementary Fig. **R1**).

Because the miR-125a-5p expression is relatively low in C-33A cells (Fig. **1**), we used a gain-of-function approach to investigate the effect of miR-125a-5p on the endogenous MARK1 protein levels by transfecting a synthetic miR-125a-5p mimic (pre-miR-125a-5p). A scrambled synthetic miRNA (miR C-) was used as negative control. Transfection of pre-

Table 1. Predicted ΔG of the 5' and 3' sequences (70 nt) flanking potential and validated miR-125a-5p binding sites.

GENE	5' end (kcal/mol)	3' end (kcal/mol)	Relative 3'-UTR Position[d]
LIN28[a]	-19.18	-7.50	728
ERBB2[b]	-18.44	-28.20	20
ERBB3[b]	-4.10	-11.87	3
VEGF[c]	-8.48	-10.70	4
MMP11[c]	-14.90	-20.89	1
MARK1	-12.00	-11.80	6
MARK2	-20.60	-27.50	421
MARK4	-25.10	-17.30	2114

a) Reference [40].
b) Reference [30].
c) Reference [25].
d) The 3'-UTR position site is relative to the termination codon.

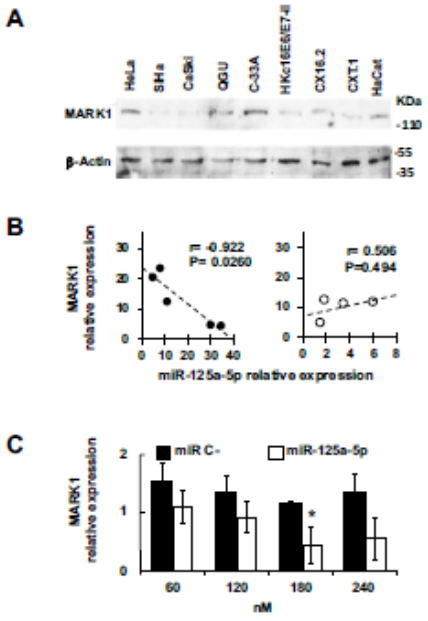

Fig. (2). MARK1 protein expression inverse correlated with miR-125a-5p levels. **A)** MARK1 and β-actin immunoblottings from total protein extracts of cervical cell lines. **B**). Correlation plots of MARK1 vs. miR-125a-5p expression. A Pearson correlation analysis was used to estimate the correlation factor (r) between the predicted target and miR-125a-5p for tumor (left panel) or immortal (right panel) phenotype. **C**) MARK1 immunoblotting of total protein extracts from cells transfected with pre-miR-125a-5p. C33-A cells were transfected with increasing amounts of a synthetic pre-miR-125a-5p mimic or a scrambled miRNA negative control (miR C-). β-actin was used as an input control.

miR-125a-5p caused down-regulation of the endogenous MARK1 protein levels significantly at 180μM compared to the controls, suggesting that miR-125a-5p may regulate expression of the endogenous MARK1 protein and thus representing a new target for miR-125a-5p (Fig. **2C**).

Targeting of MARK1 by miR-125a-5p was validated by cloning the predicted MARK1 miR-125a-5p target site into the pmiR-LUC vector (pmiR-LUC-MARK1wt), and co-transfected in HeLa and C-33A with a scrambled control (miR C-) or the pre-miR-125a-5p mimic cells (Fig. 3A). Significant reduction of luciferase activity was observed first in HeLa cells co-transfected with pmiR-LUC-MARK1wt and pre-miR-125a-5p, but not in cells co-transfected with the scrambled control (Fig. 3B, left panel). The effect of miR-125a-5p on luciferase activity was abolished when the predicted target site was mutated, thus confirming the functional interaction between miR-125a-5p and MARK1. (Fig. 3B, right panel). A similar effect was observed in C-33A cells, were co-transfection with pMIR-Luc-MARK1wt and miR-125a-5p induce a significant downregulation of luciferase activity (Fig. 3C, left panel) but recovered in cells transfected with pMIR-Luc-MARK1mt (Fig. 3C, right panel), indicating that functional interaction with miR-125a-5p occurs in both cell lines.

3.3. MiR-125a-5p Targeting Does Not Alter MARK1 mRNA Levels

To evaluate if direct targeting of MARK1 by miR-125a-5p is attributable to miRNA-induced mRNA degradation, we transfected HeLa and C-33A cells with miR-125a-5p and the miR negative control (miR C-). Transfected cells were evaluated for MARK1 mRNA levels by qRT-PCR. Results showed that transfection with miR-125a-5p does not significantly modify MARK1 transcript levels in any of the tested cell lines, suggesting a translational-repression process which not involves mRNA decay (Fig. 4).

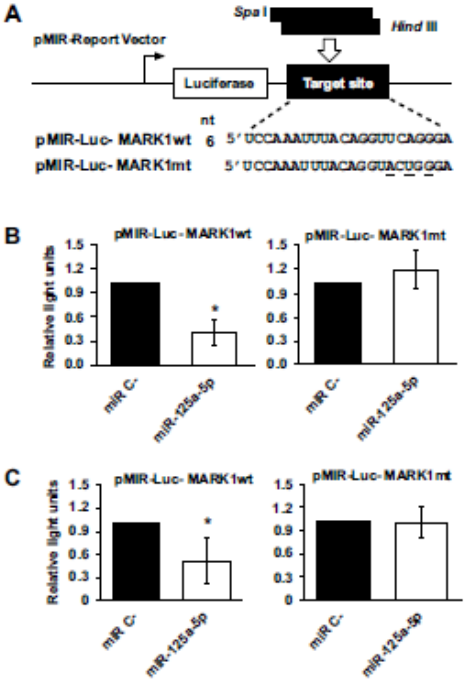

Fig. (3). Direct targeting of MARK1 by miR-125a-5p in cervical carcinoma cells. **A)** Layout of luciferase reporter constructs. Double–stranded oligonucleotides containing a predicted miR-125a-5p site within MARK1 3'-UTR (pMIR-Luc-MARK1wt), or a negative control containing three mutated positions (underlined) abolishing miR-125a-5p hybridization (pMIR-Luc-MARK1mt). Nucleotide positions from the MARK1 3'-UTR are indicated. HeLa **B)** and C-33A **C)** cells were co-transfected with the pmiR-Luc-MARK1wt or pmiR-Luc-MARK1mt reporters, plus the transfection efficiency control pGST-GFP and the miR-125a-5p mimic (miR-125a-5p) or the negative scrambled miRNA control (miR C-). The plots represent the mean and standard deviation of the corrected luciferase activity after 24 hrs.

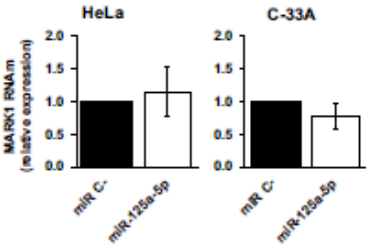

Fig. (4). MARK1 targeting by miR-125a-5p does not induce mRNA decay. HeLa and C-33A cells were transfected with 60nM miR-126a-5p mimic or miR C- scrambled control. MARK1 mRNA levels were evaluated by qRT-PCR from total RNA extracts 24 hrs post-transfection. Expression of MARK1 was normalized against β-actin. Graph shows the mean and standard deviation from three independent experiments.

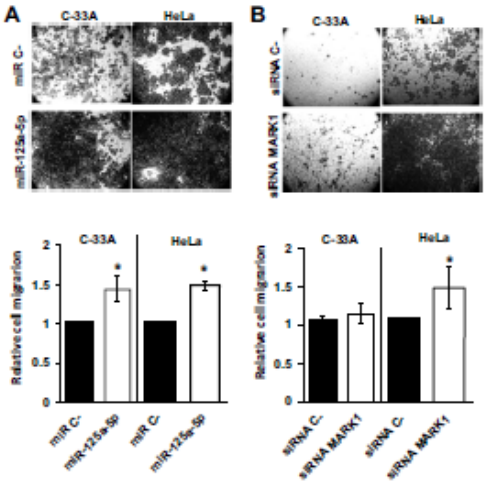

Fig. (5). Effect of miR-125a-5p on cell migration in cervical carcinoma cells. **A)** Upper Panel, C-33A and HeLa cells were transfected with the miR-125a-5p synthetic mimic (miR-125a-5p) or the scrambled miRNA control (miR C-) and seeded into transwell chambers 24 hrs post-transfection. Transfected cells were starved for overnight and stimulated with 5% FBS. Migrating cells across the membrane were stained and microphotographed at 100X. Lower Panel, stained membranes were removed from the chambers and quantified by densitometry. The plots represent the mean and standard deviation of the fold change in migrating cells compared to the non-stimulated control. **B)** MARK1 downregulation by siRNAs stimulates migration. Upper Panel, C-33A and HeLa cells were transfected with a siRNA directed against MARK1 mRNA (siRNA-MARK1) or a scrambled siRNA negative control (siRNA C-). Migrating cells across the membranes were stained and microphotographed at 100X. Lower Panel, the plots show the mean and standard deviation of the densitometry from stained membranes compared to non-stimulated controls from three independent experiments.

3.4. Transfection of miR-125a-5p Promotes Cell Migration by Downregulating MARK1 in Cervical Tumor Cells

The effect of miR-125a-5p expression on the migration of cervical tumor cells was analyzed in C-33A and HeLa cells transfected with pre-miR-125a-5p and seeded on transwell migration chambers. Cell migration was significantly enhanced in pre-miR-12a-5b-transfected cells compared to miR C- control (Fig. **5A**), suggesting that MARK1 downregulation by miR-125a-5p is associated with migration in cervical tumor cells. To discern whether the effect on cell migration was attributable to MARK1 regulation, we treated C-33A and HeLa cells with a MARK1-specific siRNA and evaluated the effect on cell migration. MARK1 siRNA caused significant enhancement of migration in HeLa cells and a slight increase in migration in C-33A cells (Fig. **5B**). The observed differences in MARK1 silencing between C-33A and HeLa cells can be attributed to contextual differences or mutations at the 3′UTR target site. Nevertheless, these results confirm a role for MARK1 in cervical cell migration.

As shown in Fig. (3), miR-125a-5p can down-regulate MARK1 by direct targeting in both Hela and C-33A cells but the effect on migration process was mainly observed in HeLa cells (Fig. 5). Previous reports have shown that MARK1 can mediate migration through the direct phosphorylation of MAPs, altering microtubule dynamics [26]. To further clarify the function of miR125a-5p/MARK1 interaction in cell migration, the levels of MAP2 protein (a functional target of MARK1 expressed in epithelial tumor cells and related to cell motility [37]) were analyzed by immunoblotting in miR-125a-5p-transfected HeLa and C-33A cells. A short 70 Kd form of MAP2, referred as MAP2c [38], was observed only in C-33A cells suggesting a differential microtubule dynamics regulation between both cell lines.

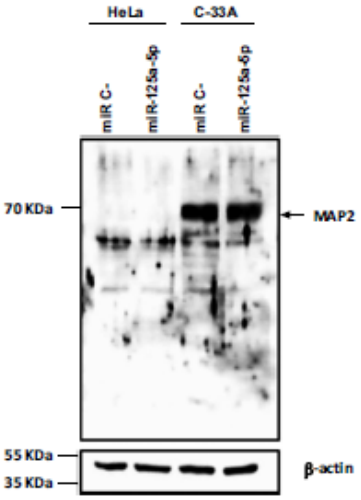

Fig. (6). Differential MAP2 levels in HeLa and C-33A cells. Total protein extracts from HeLa and C-33A cells transfected with miR-125a-5p transfection were analyzed by immunoblotting using an anti-MAP-2 antibody. β-actin was used as load control. A 70 Kd band corresponding to MAP2 protein is indicated.

4. DISCUSSION

In the present study, miR-125a-5p and its novel target MARK1 are suggested as potential factors for cervical cancer progression. MiR-125a-5p showed differential expression among a panel of cervical cell lines and MARK1 was identified as a direct target for miR-125a-5p regulation with functional relevance on cell migration. Additionally, miR-125a-5p overexpression and the subsequent MARK1 downregulation stimulated cell migration in cervical tumor lines, further suggesting a potential role for miR-125a-5p in cervical cancer tumorigenesis.

The relationship between miR-125a-5p and cervical cancer has been previously explored with no clear conclusion about its functional role. In the present approach, an inverse correlation was established between endogenous miR-125a-5p levels and MARK1 expression in tumor but not in immortal cells. This phenomenon was also observed in SKBR3 cells (a mammary tumor-derived cell line), where miR-125a-5p had a significant inhibitory effect on growth and migration but only a marginal effect in non-transformed cells, also suggesting that a tumor or immortal phenotype is relevant for the expression and function of miR-125a-5p [39].

Functionally, miR-125a-5p has been previously characterized as a possible tumor suppressor gene in cervical cancer, inhibiting cell proliferation and invasion in cultured cells, while suppressing cell cycle and reducing tumor growth and metastasis *in vivo*. Moreover, miR-125a-5p regulated these events by directly binding and downregulating STAT3 mRNA [40, 41]. In another report, lentivirus-mediated miR-125a-5p upregulation inhibited *in vitro* cancer proliferation and migration and *in vivo* cervical carcinoma transplantation. ABL2 was shown as a direct regulatory target of miR-125a-5p [23]. The results presented here indicate that miR-125a-5p enhances migration in cervical tumor cells through MARK1 downregulation suggesting a possible role as an oncogene. Expression of miR-125a-5p impaired cell migration in breast cancer cells by targeting ERBB2-ERBB3 and HuR [42], ABL2 in cervical cancer [23] and Gab2 in glioma cells [43]. However, miR-125a-5p overexpression increased migration in non-small cell lung SPC-A-1 cells and silencing caused a decrease in cell migration [21]. Therefore, the miR-125a-5p function in cell migration appears to be associated with a wide spectrum of targets relying on a particular cell context and/or physiological state.

There are four MARK proteins (MARK1/2/3/4) in humans, with several roles in the establishment and maintenance of cell polarity and the regulation of microtubule dynamics, both phenomena implied in the control of cell movement in cancer and development. Excluding MARK3, virtually the entire MARK family can be regulated by miR-125a-5p although the thermodynamic properties of the adjacent sequences may not be as favorable as those present in MARK1 (Table 1). MARK1 activity can modulate cell migration by altering microtubule dynamics *via* MAP phosphorylation and by non-canonical pathways as the promotion of *Wnt* activation [44] and LKB1 signaling [45]. Microtubule dynamics is essentially regulated by MAPs that in turn are regulated by MARK1. MAPs in non-phosphorylated form bind to the microtubule lattice, where they can stabilize/destabilize microtubules through dephosphorylation/phosphorylation cycles managed by MARK proteins. Moreover, dysregulation of this mechanism has been related to the malignant phenotype in tumor cells where MAP2 overexpression can induce mitotic defects, growth inhibition and metastatic predisposition in melanoma-derived cells [46, 47] and promotes cell migration on invasive oral carcinoma cells [37]. This MAP2 gain of function in epithelial cells can induce a global stabilization of the microtubule network [48, 49] and confer neurite-like protrusions to enhance migration [50, 51]. Here, a differential effect of MARK1 downregulation was observed between two cervical cancer cell lines.

Response to migratory stimuli may be influenced by MAP expression profile and MAP isoforms. The present results showed that migration is not enhanced in C-33A despite regulation over MARK1 but it is in HeLa cells (Fig. 6). Additionally, MAP2c is highly expressed in C-33A cells but no in HeLa cells which may explain the lack of effect on

migration observed in C-33A compared to HeLa cells. In oral cancer cells (Ca-22 cells), overexpression of MAP2c caused bundling on microtubules, but marginally stimulate migration [37]. Thus, C-33A can be resistant to migratory stimuli despite regulation of MARK1 by miR-125a-5p. In the case of HeLa cells, microtubule dynamics may be further regulated by MAP4, other target of MARK1. Moreover, migration can be stimulated by non-canonical pathways dependent on MARK1 as phosphorylation of *Wnt* components or LBK signaling. Putting together, MAP2c overexpression may confer a resistant context to migration process. Participation of another forms of MAP, as MAP4 needs to be evaluated for a complete understanding of migration regulation in HeLa cells.

Microtubule stabilization may confer sensibility to paclitaxel treatment [41, 52]. Further studies will be required to clarify the precise mechanism by which miR-125a-5p participate in cell migration in cervical cancer. Nevertheless, the evidence provided here suggesting miR-125a-5p regulation of cell migration in cervical tumor cells through the targeting of MARK1 offers a novel view of cervical carcinogenesis and establish a novel target for potential therapies.

CONCLUSION

Here, miR-125a-5p and its novel target MARK1 were described as potential factors for cervical cancer progression. MiR-125a-5p showed differential expression among a panel of cervical cell lines. In particular, miR-125a-5p was significantly overexpressed in tumor HPV-positive cell lines in comparison to immortal HPV-positive cell lines. MARK1 was identified as a direct target for miR-125a-5p regulation with functional relevance on cell migration. Overexpression of miR-125a-5p and the subsequent MARK1 downregulation promoted cell migration in HeLa cell line, suggesting a potential role for miR-125a-5p in cervical cancer tumorigenesis.

ETHICS APPROVAL AND CONSENT TO PARTICIPATE

Not applicable.

HUMAN AND ANIMAL RIGHTS

No Animals/Humans were used for studies that are base of this research.

CONSENT FOR PUBLICATION

Not applicable.

CONFLICT OF INTEREST

The authors declare no conflict of interest, financial or otherwise.

ACKNOWLEDGEMENTS

Martínez-Acuña N. designed and performed experiments, analyzed data and wrote the manuscript; González-Torres A. performed experiments, cell culture and revised manuscript; Tapia-Vieyra J.V. managed cell culture and revised manuscript and Alvarez-Salas L.M. conceived the principal strategies, supervised and funded the project, analyzed results, wrote the paper and performed final revision of the manuscript.

This work was supported by CONACyT (Grant CB-2012-176281). We thank to Maria Guadalupe Aguilar-González M.Sc. for automated sequencing service and Sergio Israel Rangel-Guerrero M.Sc. for critical discussion.

SUPPLEMENTARY MATERIAL

Supplementary material is available on the publisher's web site along with the published article.

REFERENCES

[1] Bartel DP. MicroRNAs: target recognition and regulatory functions. Cell 2009; 136: 215-33.
[2] Pasquinelli AE. MicroRNAs and their targets: recognition, regulation and an emerging reciprocal relationship. Nat Rev Genet 2012; 13: 271-82.
[3] Hwang HW, Mendell JT. MicroRNAs in cell proliferation, cell death, and tumorigenesis. Br J Cancer 2006; 94: 776-80.
[4] Calin GA, Croce CM. MicroRNA signatures in human cancers. Nat Rev Cancer 2006; 6: 857-66.
[5] Yu Z, Baserga R, Chen L, Wang C, Lisanti MP, Pestell RG. microRNA, cell cycle, and human breast cancer. Am J Pathol 2010; 176: 1058-64.
[6] Boeri M, Verric C, Conte D, *et al*. MicroRNA signatures in tissues and plasma predict development and prognosis of computed tomography detected lung cancer. Proc Natl Acad Sci U S A 2011; 108: 3713-8.
[7] Hellner K, Munger K. Human papilloma viruses as therapeutic targets in human cancer. J Clin Oncol 2011; 29: 1785-94.
[8] Nobbenhuis MA, Helmerhorst TJ, van den Brule AJ, *et al*. Cytological regression and clearance of high-risk human papillomavirus in women with an abnormal cervical smear. Lancet 2001; 358: 1782-3.
[9] Reshmi G, Pillai MR. Beyond HPV: oncomirs as new players in cervical cancer. FEBS Lett 2008; 582: 4113-6.
[10] Sun YM, Lin KY, Chen YQ. Diverse functions of miR-125 family in different cell contexts. J Hematol Oncol 2013; 6: 6-14.
[11] Gerrits A, Walasek MA, Olthof S, *et al*. Genetic screen identifies microRNA cluster 99b/let-7e/125a as a regulator of primitive hematopoietic cells. Blood 2012; 119: 377-87.
[12] Herrera BM, Lockstone HE, Taylor JM, *et al*. MicroRNA-125a is over-expressed in insulin target tissues in a spontaneous rat model of type 2 diabetes. BMC Med Genomics 2009; 18: 54-64.
[13] Li D, Yang P, Xiong Q, *et al*. MicroRNA-125a/b-5p inhibits endothelin-1 expression in vascular endothelial cells. J Hypertens 2010; 28: 1646-54.
[14] Potenza N, Papa U, Mosca N, Zerbini F, Nobile V, Russo A. Human microRNA hsa-miR-125a-5p interferes with expression of hepatitis B virus surface antigen. Nucleic Acids Res 2011; 39: 5157-63.
[15] Bi Q, Tang S, Xia L, *et al*. Ectopic expression of MiR-125a inhibits the proliferation and metastasis of hepatocellular carcinoma by targeting MMP11 and VEGF. PLoS ONE 2012; 7: e40169-e40179.
[16] Xu Y, Huang Z, Liu Y. Reduced miR-125a-5p expression is associated with gastric carcinogenesis through the targeting of E2F3. Mol Med Rep 2014; 10: 2601-8.
[17] Dai J, Wang J, Yang L, Xiao Y, Ruan Q. miR-125a regulates angiogenesis of gastric cancer by targeting vascular endothelial growth factor A. Int J Oncol 2015; 47: 1801-10.
[18] Ratert N, Meyer HA, Jung M, *et al*. Reference miRNAs for miRNAome analysis of urothelial carcinomas. PLoS ONE 2012; 7: e39309-e39318.
[19] Sand M, Skrygan M, Georgas D, *et al*. Microarray analysis of microRNA expression in cutaneous squamous cell carcinoma. J Dermatol Sci 2012; 68: 119-26.
[20] Kim SW, Ramasamy K, Bouamar H, Lin AP, Jiang D, Aguiar RC. MicroRNAs miR-125a and miR-125b constitutively activate the NF-kappaB pathway by targeting the tumor necrosis factor alpha-induced protein 3 (TNFAIP3, A20). Proc Natl Acad Sci U S A 2012; 109: 7865-70.

[21] Jiang L, Huang Q, Zhang S, *et al*. Hsa-miR-125a-3p and hsa-miR-125a-5p are downregulated in non-small cell lung cancer and have inverse effects on invasion and migration of lung cancer cells. BMC Cancer 2010; 10: 318-30.

[22] Lee JW, Choi CH, Choi JJ, *et al*. Altered MicroRNA expression in cervical carcinomas. Clin Cancer Res 2008; 14: 2535-42.

[23] Qin X, Wan Y, Wang S, Xue M. MicroRNA-125a-5p modulates human cervical carcinoma proliferation and migration by targeting ABL2. Drug Des Devel Ther 2015; 10: 71-9.

[24] Pedroza-Torres A, Fernandez-Retana J, Peralta-Zaragoza O, *et al*. A microRNA expression signature for clinical response in locally advanced cervical cancer. Gynecol Oncol 2016; 142: 557-65.

[25] Matenia D, Mandelkow EM. The tau of MARK: a polarized view of the cytoskeleton. Trends Biochem Sci 2009; 34: 332-42.

[26] McDonald JA. Canonical and noncanonical roles of Par-1/MARK kinases in cell migration. Int Rev Cell Mol Biol 2014; 312: 169-99.

[27] Nishida N, Mimori K, Fabbri M, *et al*. MicroRNA-125a-5p is an independent prognostic factor in gastric cancer, and inhibits the proliferation of human gastric cancer cells in combination with trastuzumab. Clin Cancer Res 2011; 17: 2725-33.

[28] Shirasawa H, Tomita Y, Sekiya S, Takamizawa H, Simizu B. Integration and transcription of human papillomavirus type 16 and 18 sequences in cell lines derived from cervical carcinomas. J GenVirol 1987; 68: 583-91.

[29] Alvarez-Salas LM, Arpawong TE, DiPaolo JA. Growth inhibition of cervical tumor cells by antisense oligodeoxynucleotides directed to the human papillomavirus type 16 E6 gene. Antisense Nucleic Acid Drug Dev 1999; 9: 441-50.

[30] Woodworth CD, Bowden PE, Doniger J, *et al*. Characterization of normal human exocervical epithelial cells immortalized *in vitro* by papillomavirus types 16 and 18 DNA. Cancer Res 1988; 48: 4620-8.

[31] Woodworth CD, McMullin E, Iglesias M, Plowman GD. Interleukin 1 alpha and tumor necrosis factor alpha stimulate autocrine amphiregulin expression and proliferation of human papillomavirus-immortalized and carcinoma-derived cervical epithelial cells. Proc Natl Acad Sci U S A 1995; 92: 2840-4.

[32] Boukamp P, Petrussevska RT, Breitkreutz D, Hornung J, Markham A, Fusenig NE. Normal keratinization in a spontaneously immortalized aneuploid human keratinocyte cell line. J Cell Biol 1988; 106: 761-71.

[33] Lopez JA, Alvarez-Salas LM. Differential effects of miR-34c-3p and miR-34c-5p on SiHa cells proliferation apoptosis, migration and invasion. Biochem Biophys Res Commun 2011; 409: 513-9.

[34] Chen C, Ridzon DA, Broomer AJ, *et al*. Real-time quantification of microRNAs by stem-loop RT-PCR. Nucleic Acids Res 2005; 33: e179-e187.

[35] Schmittgen TD, Lee EJ, Jiang J, *et al*. Real-time PCR quantification of precursor and mature microRNA. Methods 2008; 44: 31-8.

[36] Kuhn DE, Martin MM, Feldman DS, Terry AV, Jr., Nuovo GJ, Elton TS. Experimental validation of miRNA targets. Methods 2008; 44: 47-54.

[37] Liu SY, Chen YT, Tseng MY, *et al*. Involvement of microtubule-associated protein 2 (MAP2) in oral cancer cell motility: a novel biological function of MAP2 in non-neuronal cells. Biochem Biophys Res Commun 2008; 366: 520-5.

[38] Garner CC, Matus A. Different forms of microtubule-associated protein 2 are encoded by separate mRNA transcripts. J Cell Biol 1988; 106: 779-83.

[39] Scott GK, Goga A, Bhaumik D, Berger CE, Sullivan CS, Benz CC. Coordinate suppression of ERBB2 and ERBB3 by enforced expression of micro-RNA miR-125a or miR-125b. J Biol Chem 2007; 282: 1479-86.

[40] Fan Z, Cui H, Xu X, *et al*. MiR-125a suppresses tumor growth, invasion and metastasis in cervical cancer by targeting STAT3. Oncotarget 2015; 6: 25266-80.

[41] Fan Z, Cui H, Yu H, *et al*. MiR-125a promotes paclitaxel sensitivity in cervical cancer through altering STAT3 expression. Oncogenesis 2016; 5: e197-e205.

[42] Guo X, Wu Y, Hartley RS. MicroRNA-125a represses cell growth by targeting HuR in breast cancer. RNA Biol 2009; 6: 575-83.

[43] Sun L, Zhang B, Liu Y, Shi L, Li H, Lu S. MiR125a-5p acting as a novel Gab2 suppressor inhibits invasion of glioma. Mol Carcinog 2016; 55: 40-51.

[44] Wallingford JB, Habas R. The developmental biology of Dishevelled: an enigmatic protein governing cell fate and cell polarity. Development 2005; 132: 4421-36.

[45] Goodwin JM, Svensson RU, Lou HJ, Winslow MM, Turk BE, Shaw RJ. An AMPK-independent signaling pathway downstream of the LKB1 tumor suppressor controls Snail1 and metastatic potential. Mol Cell 2014; 55: 436-50.

[46] Fang D, Hallman J, Sangha N, *et al*. Expression of microtubule-associated protein 2 in benign and malignant melanocytes: Implications for differentiation and progression of cutaneous melanoma. Am J Pathol 2001; 158: 2107-15.

[47] Soltani MH, Pichardo R, Song Z, *et al*. Microtubule-associated protein 2, a marker of neuronal differentiation, induces mitotic defects, inhibits growth of melanoma cells, and predicts metastatic potential of cutaneous melanoma. Am J Pathol 2005; 166: 1841-50.

[48] Witte H, Bradke F. The role of the cytoskeleton during neuronal polarization. Curr Opin Neurobiol 2008; 18: 479-87.

[49] Hammond JW, Huang CF, Kaech S, Jacobson C, Banker G, Verhey KJ. Posttranslational modifications of tubulin and the polarized transport of kinesin-1 in neurons. Mol Biol Cell 2010; 21: 572-83.

[50] Gundersen GG, Bulinski JC. Selective stabilization of microtubules oriented toward the direction of cell migration. Proc Natl Acad Sci U S A 1988; 85: 5946-50.

[51] Bulinski JC, Gundersen GG. Stabilization of post-translational modification of microtubules during cellular morphogenesis. Bioessays 1991; 13: 285-93.

[52] Ahmed AA, Mills AD, Ibrahim AE, *et al*. The extracellular matrix protein TGFBI induces microtubule stabilization and sensitizes ovarian cancers to paclitaxel. Cancer Cell 2007; 12: 514-27.